



University of
Stavanger

Faculty of Science and Technology

MASTER'S THESIS

Study program/ Specialization: Master of Science in Petroleum Engineering Specialization- Natural Gas Engineering	Spring semester, 2016 Open / Restricted access
Writer: Kanchana Srisan (Writer's signature)
Faculty supervisor: Prof. Rune Wiggo Time Co-supervisor : Sr. Eng. Herimonja Andrianifaliana Rabenjafimanantsoa	
Thesis title: Experimental Investigation of Mixing and Separation Mechanisms of Oil-Water System	
Credits (ECTS): 30	
Key words: Water-oil mixtures Emulsion Rheology Interfacial tension Separation	Pages: 88 Stavanger, 15.06.2016 Date/year

© COPYRIGHT 2016
BY
KANCHANA SRISAN
RUNE WIGGO TIME

ABSTRACT

The behaviour of oil-water mixtures/emulsions is of great importance for a variety of industries and sciences. Specially in oil and gas industry, it can be encountered at different stages while drilling, production, storage, transportation and processing of crude oil. The purpose of this thesis is to improve the understanding of oil-water mixtures/emulsions through laboratory experiments. Two mineral oils Bayol 35 and Exxsol D60 and tap water were used as the test materials. Oil - water samples were prepared with varying proportion of oil and water ranging from 5% to 95%. The mixing experiments were conducted in two modes; Hand shaking and mechanical mixing. Under the mechanical mixing mode, the oil-water mixtures were prepared at different mixing speeds (400rpm, 1000rpm, and 1600rpm) and mixing times (1minute and 5minutes). The separation phenomena was studied as a function of the type of oil, mixing duration, mixing speed and adding of colouring agent (Sudan blue and Uranine). The rheology, surface/interfacial tension and density of the oil water mixtures were examined for better understanding of the influence of physical properties on oil-water mixing and separation phenomena. Microscopic pictures were taken to study the separation phenomena, droplet sizes and their distribution.

The results showed that Exxsol D60 oil-water mixtures produce smaller water droplets in oil than Bayol 35 oil-water mixtures, but still Exxsol D60 separates faster explaining that the less viscosity of Exxsol D60 oil phase has a major influence over the droplet size in separation process. Longer mixing time and higher mixing speed lead to higher stability of the emulsions. This is due to the increased energy transferred for the break-up process which eventually lead to small droplets and more stable emulsions. Adding colouring agents modified the interfacial tension so that Sudan blue increased it and Uranine decreased the interfacial tension. This resulted that Sudan blue added oil-water mixtures gave bigger droplets and achieved faster separation in comparison to the Uranine added oil-water mixtures. Pure mineral oil showed Newtonian behaviour while it behaved non-Newtonian for oil-water mixtures.

It was a significant observation to see that always the water droplets were bigger than the oil droplets in all the oil-water mixtures regardless of the type of oil, composition or method of preparation. Further investigations to be carried out to make sure whether this is a phenomena related to the physical properties of oil, physico-chemical properties of oil-water emulsions such as Gibbs free energy or thermodynamics of emulsion formation and break down.

THIS PAGE IS INTENTIONALLY LEFT BLANK

ACKNOWLEDGEMENT

Firstly, I would like to thank my supervisor Prof. Rune Wiggo Time and Sr. Eng. Herimonja Andrianifaliana Rabenjafimanantsoa for giving me an opportunity to work with him on this interesting project. Their support, guidance, patience and encouragement has been instrumental in making of this thesis. My utmost thanks goes to PhD student Kshanthi Perera and Nikita Potokin for helping me out in all the laboratory experiments and giving constant feedback on my thesis.

I would also like to thank my friends Dhruvit and Bikram for giving suggestions and providing valuable comments on my thesis. I also wish to thank rest of the faculty members from Department of Petroleum Engineering for their supports and contributions to my academic achievements.

Special thanks are due to my husband Rune Austdal and family for their constant moral support and encouragement throughout my thesis. Without your support, I wouldn't have made it so far.

Finally, I would like to express my sincere gratitude to University of Stavanger for letting me a part of this impressive organization.

THIS PAGE IS INTENTIONALLY LEFT BLANK

TABLE OF CONTENTS

ABSTRACT	ii
ACKNOWLEDGEMENT	iv
TABLE OF CONTENTS	vi
LIST OF FIGURES	viii
LIST OF TABLES	x
NOMENCLATURE	xi
CHAPTER 1 INTRODUCTION	1
1.1 Motivation	1
1.2 Objective	3
1.3 Outline of the thesis.....	4
CHAPTER 2 THEORETICAL BACKGROUND	5
2.1 Fundamentals of Emulsions	5
2.2 Characteristics of Emulsions	7
2.3 Oil Composition	8
2.4 Morphology of Emulsion	10
2.5 Phase Inversion	11
2.6 Droplet size and droplet-size distribution	13
2.7 Emulsion Stability	16
2.7.1 Ostwald Ripening	16
2.7.2 Sedimentation or Creaming	17
2.7.3 Coalescence	18
2.7.4 Flocculation	18
2.8 Factors Determining Emulsion Stability	20
2.9 Emulsion Rheology	21
2.9.1 Viscosity of Emulsions	23
CHAPTER 3 EXPERIMENTS	25
3.1 Materials.....	25
3.2 Preparation of Oil-Water Mixture	26
3.3 Evaluation of the separation of oil-water mixtures	27
3.3 Microscopy Analysis of water-oil mixtures/emulsions.....	29
3.4 Rheology	30
3.5 Surface and interfacial tension	32

3.5.1 Du Noüy Ring Method	32
3.6 Density	33
3.7 Selecting the better phase identification agent	34
CHAPTER 4 RESULTS AND DISCUSSION.....	35
4.1 Physical properties of materials measured at 20 °C	35
4.2 Oil-water mixtures.....	36
4.2.1 Mixing by manual shaking	36
4.2.2 Mixing by Silverson L4RT-A mixer	39
4.3 Microscopy.....	44
4.3.1 Droplet sizes	46
4.3.2 Separation Phenomena	47
4.3.3 Effect of stirring speed	50
4.3.4 Effect of mixing times	52
4.4 Rheology	52
4.4.1 Viscosity test.....	52
4.4.3 Effects of stirring speed on viscosity.....	56
4.4.4 Effects of Temperature on viscosity	57
4.5 Surface and interfacial tension	59
4.5.1 Effect of phase Ratios.....	60
4.6 Density	62
4.7 Selecting the better phase identification additive.....	64
4.8 Important observations.....	68
CHAPTER 5 CONCLUSIONS.....	70
REFERENCES.....	72
APPENDIX A	75
APPENDIX B	81
APPENDIX C	84

LIST OF FIGURES

Figure 2.1 Types of Emulsions (Abdel-Raouf, 2012).....	6
Figure 2.2 Composition of crude oil (Abdel-Raouf, 2012)	9
Figure 2.3 Schematic of SARA fractionation of oil (Fateev, 2014).	10
Figure 2.4 Morphologies of different type of emulsions (Alwadani, 2010).....	11
Figure 2.5 Schematic of Inversion Process for Water-Oil Flow (Alwadani, 2010).	12
Figure 2.6 Droplet size distribution of petroleum emulsions (Petrowiki, 2015)	14
Figure 2.7 Drop size distributions commonly found in emulsions (Alwadani, 2010).....	15
Figure 2.8 Destabilizing mechanisms in emulsions (Alwadani, 2010)	16
Figure 2.9 Emulsions with high internal volume fraction (Langevin et al., 2004).....	18
Figure 2.10 Classification of Non-Newtonian fluids (Chhabra, 2010).....	23
Figure 2.11 viscosities of tight emulsions at 125°F at different water cuts	24
Figure 3.1 Silverson L4RT-A mixer	27
Figure 3.2 Light microscope Ziess Stemi DV4	30
Figure 3.3 Silverson L4RT-A mixer and the Light microscope Ziess Stemi DV4.....	30
Figure 3.4 Anton Paar MCR 302 rheometer (Concentric cylinder systems).....	31
Figure 3.5 C-LTD 70/PIV rheometer (Measuring cylinder D:32mm; L:16.5mm, black anodized).....	31
Figure 3.6 a) Picture of the tensiometer type 8451,KRUSS b) Sketch of tensiometer.....	33
Figure 3.7 Anton Paar DMA 4500 densitometer	34
Figure 4.1 (I) Bayol 35_S2 (80-20 % water-oil mixture) with Sudan blue and (II) without Sudan blue.....	37
Figure 4.2 (I) Bayol 35_S6 (20-80 % water-oil mixture) with Sudan blue and (II) without Sudan blue.....	37
Figure 4.3 Illustrated separation times of w-o (Bayol 35) with mixing by hands shanking....	38
Figure 4.4 Oil-water mixture's pictures after mixing (Bayol 35 with Sudan blue).....	39
Figure 4.5 Comparison of separation time between mineral oil samples prepared at mixing speed 1600 rpm and mixing time 5 mins.	42
Figure 4.6 Comparison of oil-water mixtures prepared of Bayol 35 with stirring speed at 400 rpm.	43
Figure 4.7 Comparison of oil-water mixtures prepared of Exxsol D60 with stirring speed at 400 rpm.	43

Figure 4.8 Comparison of three difference stirring speeds of Bayol 35 with mixing time for 1 minute.	44
Figure 4.9 Comparison of three difference stirring speeds of exxsol D60 with mixing time for 1 minute.	44
Figure 4.10 Microscope images for water-Bayol 35 mixtures with stirring speed 1600 rpm, mixing for 5 minutes. (a) S1,95% of water cut (b) S2,80% of water cut (c) S3,60% of water cut (d)S4,50% of water cut (e) S5,40% of water cut.	46
Figure 4.11 Microscope view of S3 (60-40 % w-o) at T = 0 minute.....	48
Figure 4.12 Microscope view of S3 (60-40 % w-o) at T = 1 minute.....	48
Figure 4.13 Microscope view of S3 (60-40 % w-o) at T = 2 minutes.	49
Figure 4.14 Microscope view of S3 (60-40 % w-o) at T = 5 minutes.	49
Figure 4.15 Microscope view of S3 (60-40 % w-o) at T = 30 minutes.	50
Figure 4.16 Droplet size distribution at (a) and (b) 50-50 % water-oil mixture of Bayol 35 mixing for 5 mins.....	51
Figure 4.17 Droplet size distribution at (a) and (b) 60-40 % w-o mixture of Bayol 35	52
Figure 4.18 Viscosity measurement of water.	53
Figure 4.19 Viscosity measurement of Bayol 35 (a) and Exxsol D60 (b).....	54
Figure 4.20 The behavior of oil-water mixtures for Bayol 35 at different phase ratio.....	55
Figure 4.21 The behavior of oil-water mixtures for Exxsol D60 at different phase ratio.	56
Figure 4.22 Comparison of viscosity for samples containing Exxsol D60 with different stirring speeds,(a) Exxsol D60 (50-50% w-o) and (b) Exxsol D60 (20-80% w-o).	57
Figure 4.23 (a) Effects of viscosity at varied temperature in 50-50 % w-o and (b) 20-80 % w-o.....	58
Figure 4.24 Shear rate vs shear stress for oil samples with dye at room temperature.	58
Figure 4.25 Shear rate vs shear stress for high viscous Marcol 82 at room temperature.	59
Figure 4.26 Surface and interface tensions measurements for varying volume fraction of oil at 20 °C.....	62
Figure 4.27 Density measurements of two oils.....	63
Figure 4.28 Comparing the effect of Sudan blue and Uranine dye in Bayol 35 sample.	65
Figure 4.29 Comparing the effect of Sudan blue and Uranine dye in Exxsol D60 sample.	66
Figure 4.30 Sample 3 (60-40% w-o) with Sudan blue (Exxsol D60).....	67
Figure 4.31 Sample 3 (60-40% w-o) with Sudan blue (Bayol 35)	67
Figure 4.32 Illustrated water/oil droplets in different phases for two oils.....	69

LIST OF TABLES

Table 3.1 Physical Properties of materials measured at 20°C.....	25
Table 3.2 Properties of mineral oils.....	26
Table 3.3 Compositions of water-oil samples.....	28
Table 4.1 Physical properties of materials measured at 20 °C.....	35
Table 4.2 Illustrated separation times of w-o mixtures/emulsions (Bayol 35).....	38
Table 4.3 Oil-water mixtures/emulsions resulted by mixing with Silverson L4RT-A mixer. 39	
Table 4.4 Interfacial mixing layer separation time for water-oil mixtures/emulsions.....	40
Table 4.5 The droplet size distribution for S1-S5 w-o mixtures measurement.	47
Table 4.6 Preparation of oil-water mixtures.	60
Table 4.7 Typical surface and interface tensions of liquids at 20 °C.....	60
Table 4.8 Preparation of oil-water mixtures.	61
Table 4.9 Typical surface and interface tensions of various liquid mixtures at 20 °C.....	61
Table 4.10 Preparation of oil-water mixtures.	63
Table 4.11 The results from the density test.	64
Table 4.12 Surface and interfacial tension for sample 3 with Sudan blue and Uranine	66

NOMENCLATURE

W/O	Water-in-oil
O/W	Oil-in-water
O/W/O	Oil-in-water-in-oil
W/O/W	Water-in-oil-water
W-O	Water-oil mixtures
HLB	Hydrophilic-lipophilic Balance
SARA	Saturate, Aromatic, Resin and Asphaltene
DSD	Droplet Size Distribution
IFT	Interfacial Tension

CHAPTER 1

INTRODUCTION

Emulsion is an important part of the oil and gas industry and can be encountered at different stages while drilling, production, storage, transportation and processing of crude oil. Efforts are put in to produce crude oil alone but it is generally commingled with water. This water or the formation water causes problems and influence the production. It also usually increases the unit cost of production. The produced water must be separated from the oil, treated and disposed of properly because the crude oil as selling product must not have more than 1% of water and sediments. The presence of water is also unwanted because of its contents of inorganic salts, which could provoke corrosion and obstruction damages to the refining and transport installations.

Produced water can be in the form “free water” which will settle out rapidly, or in the form of an emulsion. A regular oilfield emulsion is a dispersion of water droplets in oil. Emulsions are generally difficult to treat and may cause several operational problems in wet-crude handling facilities and gas/oil separating plants. They can also lead to high-pressure drops in flow lines, and cause an increase in demulsifier use. The problem is usually at its worst during the winter because of lower surface temperatures.

1.1 Motivation

As per the oil and gas industry experts, most of the easily developed oil and gas resources have been already found. Most of the new source of energy may be located in the deepwater oil

fields such as these in Gulf of Mexico, Norwegian Continental Shelf and other frontier area. Development of these resources is much more challenging and costlier. Focus of the companies have shifted from near-shore, shallow waters to oil and gas resources in water depths of 1000 feet and beyond.

In addition to the environmental considerations in deep water productions, there are many technical challenges which remain to be solved. These operations are very complex, risky and costly environment and often require significant amounts of time between initial exploration and first production. Therefore, it is very important for deepwater crude oil producers to search for any opportunity that can contribute to save the cost of processing this oil. Significant attempts need to be made in finding new solutions and innovative technology to develop new fields more economically, especially during the downturn of the industry.

Another area of importance with respect to oil-water mixing and emulsions is in drilling and drilling fluids. Drilling fluids can be highly complex multiphase system which are broadly classified into two types: 1. Oil based as oil in continuous phase and 2. Water based with water as continuous phase. With respect to well control, it is important to know the emulsion characteristics of the drilling fluid and how it will behave in the presence of formation water or reservoir fluid influx. In the presence of oil-based mud, the influx from the reservoir can dissolve in the fluid at high pressure and temperature condition which leaves very less time for kick detection. Emulsions are also used in cement slurries to fill annular space between the borehole and the casing. This prevents the migration of such fluids in the annulus, and protects the casing from corrosion.

The study of this project is also important for the evolving Managed Pressure Drilling (MPD) Technology. As per IADC, MPD can be defined as an adaptive drilling process used to precisely control the annular pressure profile throughout the wellbore. The objectives are to ascertain the downhole pressure environment limits and to manage the annular hydraulic pressure profile accordingly. MPD is intended to avoid continuous influx of formation fluids to the surface. Alternatively, MPD is drilling overbalanced while maintaining near constant or correct bottomhole pressure using a combination of mud density, equivalent circulating density, and backpressure. To sustain this, pressure balance is maintained in a closed system. With increasing demand for Managed Pressure Drilling to mitigate drilling challenges and to drill by accurately controlling bottomhole pressure, the proper selection of drilling fluid in terms of oil-water mixture/emulsion stability is important. The results of this thesis will help

in selecting the better synthetic oil from Bayol 35 and Exxsol D60 for MPD applications. Moreover, more informed decision can be made in terms of choosing the colour agent for the oil-water mixture.

This thesis focuses on the study of water-oil mixtures/emulsions and separation through laboratory experiments and analysis of the data obtained. It is also an attempt to reduce significant cost associated with oil-water mixtures and separation which is encountered at different stages of exploration and production of crude oil.

1.2 Objective

The objective on the broader scale of this work is to improve the understanding of oil-water mixtures/emulsion and separation process. The thesis also aims at verifying the theoretical concepts related to oil-water mixtures and emulsions through laboratory experiments. These concepts involve study of the size of water and oil droplets in the mixture, separation speed of droplets and effect of additives (colour agent) with different viscosities on the mixture.

The various tasks of the project can be classified into:

1. To study the effect of oil-water proportions, effect of stirring speed, effect of mixing time on oil-water mixture/ emulsion.
2. To investigate the effect of density, viscosity on mixture by using two different types of base oil (Bayol 35 and Exxsol D60).
3. To analyse the interfacial or surface tension between two phase of oil and water and also in case of pure oil and water alone.
4. To categorize the mixtures with different proportions as per their fluid behaviour into Newtonian or non-Newtonian type.
5. To analyse the droplet size and droplet size distribution using Microscopic images.
6. To investigate the effect of additives (dyes) such as Sudan Blue and Uranine on the oil-water mixture/emulsion.
7. To study the separation time of the mixture in different oil-water ratio and also in the presence or absence of additives.

1.3 Outline of the thesis

The project aims at improving the understanding of oil-water mixtures/emulsions and separations by carrying out laboratory experiments and analysis of data generated.

Chapter 2 of this thesis presents the fundamentals and theoretical concepts related to oil-water emulsions and separation. It also focuses on how stability of emulsion can be maximized and the mechanism involved in demulsifications. It also gives brief introduction to different fluid behaviours based on rheology and shear viscosity.

Chapter 3 focuses on the laboratory experimental procedures used in this thesis. It also describes the physical properties of materials used and gives the methodology used for mixing of oil-water samples, preparation of emulsion and separation.

Chapter 4 shows the results obtained through laboratory experiments. The effect of different oil-water proportions, stirring speed, mixing time, droplet size is analysed and discussed in detail. The description of fluid behaviour based on rheology and shear viscosity is also given. Moreover, how the presence of an additive influence the mixture or emulsion is studied. Finally, the analysis of separation with or without additive is made and important observations are drawn towards the end of chapter 4.

Conclusion of the thesis and future work that needs to be carried out are listed in chapter 5. This has been followed by the list of references involved in the making of this thesis. Appendix A gives the additional rheometer data that are used in plotting some of the results in chapter 4.

CHAPTER 2

THEORETICAL

BACKGROUND

2.1 Fundamentals of Emulsions

Emulsion is an important part of the oil and gas industry and can be encountered at different stages while drilling, production, storage, transportation and processing of crude oil. Emulsions are defined as colloidal dispersions that consist of two immiscible liquids. One liquid is dispersed as droplets into a volume of another liquid. These droplets are referred to as the dispersed or an internal phase while the surrounding liquid is referred as continuous or external phase. Drop size typically ranges from 1 μm to 100 μm . In this range, drops are generally large enough to settle under gravity influence. The stability of emulsion is given by the presence of stabilizing agents at the interfaces that may delay the spontaneous tendency of the liquids to separate. Such agents are most commonly molecules with polar and non-polar chemical groups in their structure usually referred to as surfactants or finely divided solids.

Emulsions are thermodynamically unstable systems because as the oil and water form two continuous phases while they separate, their decay results in decrease in free energy. Thus, the characteristics of emulsion changes over period of time. Most of the petroleum emulsions that are encountered in practice contain oil, water and emulsifying agents and exist in a metastable state that has high potential barrier to prevent coalescence of the particles.

Depending upon the nature of the dispersed phase, the emulsions can be classified into different types. The classic type of emulsion involves two immiscible liquids, water and oil. These emulsions are classified as O/W emulsion or oil droplets in water and W/O emulsion or water droplets in oil.

1. Oil-in-water emulsions (O/W): The emulsion in which oil is present as the dispersed phase and water as the dispersion medium (continuous phase).
2. Water-in-oil emulsion (W/O): The emulsion in which water forms the dispersed phase, and the oil acts as the dispersion medium is called a water-in-oil emulsion.

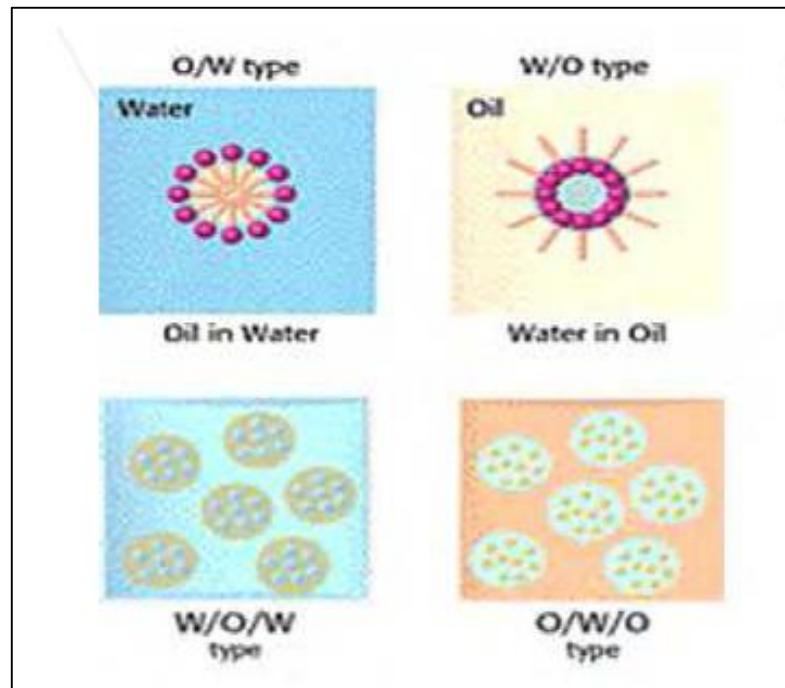


Figure 2.1 Types of Emulsions (Abdel-Raouf, 2012)

Recently, there has been development of new type of emulsions and they are called as:

1. Oil-in-water-in-oil (O/W/O)
2. Water-in-oil-water (W/O/W)

These are called multiple emulsions. In W/O/W type emulsion, water is dispersed within oil droplets of O/W emulsion, as shown in Figure 2.1. Similarly, for O/W/O type emulsion, oil is dispersed within water droplets of W/O emulsion. More complicated multiple emulsions are also possible.

The process of emulsion formation is called Emulsification. These can be formed using devices such as turbine blender, an ultrasonicator, or by passing the two phases flow through a membrane or by using a static mixer. The chemical reactions or the nucleation of one phase in another can also cause emulsification mainly due to reduction in temperature.

The emulsion satisfies following criteria (Abdel-Raouf, 2012):

1. Emulsions show all the characteristic properties of colloidal solution such as Brownian movement, Tyndall effect, electrophoresis etc.
2. These are coagulated by the addition of electrolytes containing polyvalent metal ions indicating the negative charge on the globules.
3. The size of the dispersed particles in emulsions is larger than those in the sols. It ranges from 1000 Å to 10,000 Å. However, the size is smaller than the particles in suspensions.
4. Emulsions can be converted into two separate liquids by heating, centrifuging, freezing etc. This process is also known as demulsification.

2.2 Characteristics of Emulsions

Emulsions can be characterized based on its appearance and type, texture, mixing properties, and inversion. In a true emulsion:

1. either the drop size must be small enough that forces from thermal collisions with molecules of the continuous phase produce Brownian motion that prevents settling
2. the characteristics of the interfacial surfaces must be modified by surfactants, suspended solids or
3. another semi-soluble material that renders the surface free energy low enough to preclude its acting as a driving force for coalescence (Petrowiki, 2015)

An emulsion's characteristics change over a period of time of formation. Aged emulsions can have different characteristics compared to fresh samples. This is mainly because oil contains many types of adsorbable materials whose effects can be seen over a period of time. The characteristics of emulsion also change when liquid is subjected to changes in the temperature, pressure and degree of agitation.

Depending on the droplet sizes and the difference in refractive indices between phases, emulsions can have vast range of appearance (Schramm, 2006). For example, an O/W micro-emulsion of crude oil and water may be transparent.

Emulsions can also be characterized based on their texture. O/W emulsions feel like “watery or creamy” while W/O emulsions feel “oily or greasy”. These feelings reflect the texture of external phase. However, with increase in emulsion viscosity it becomes difficult to distinguish between emulsion types.

2.3 Oil Composition

A good understanding of petroleum emulsions and its behavior is necessary for controlling within all stages of petroleum activities in the field, hydrocarbon transportation and refinery. Many studies have been done over the last years but many questions still have to be solved in emulsion behavior. The major complexity comes from the oil composition, especially from the surface-active molecules contained in the crude. These molecules cover a spread range of chemical structures, molecular weight and HLB (Hydrophilic-lipophilic-balance) values; they can interact between each other and/or reorganize at the water/oil interface (Alwadani, 2010).

Emulsions can also be stabilized by other species if they adsorb at the oil-water interface and prevent drop growth and phase separation into the original phases. Post adsorption, the surfaces become visco-elastic and this layers provide stability. Asphaltenes present in crude oil act as a natural emulsifier along with other components which are surface active such as resins, fatty acids, etc. However, they cannot alone produce emulsion stability but they can associate to asphaltenes and affect emulsion stability. Naphthenic and other naturally occurring fatty acids also do not stabilize emulsions alone while waxes co-adsorb at the interface and enhance the stability. The composition of crude oil is shown in Figure 2.2 (Abdel-Raouf, 2012).

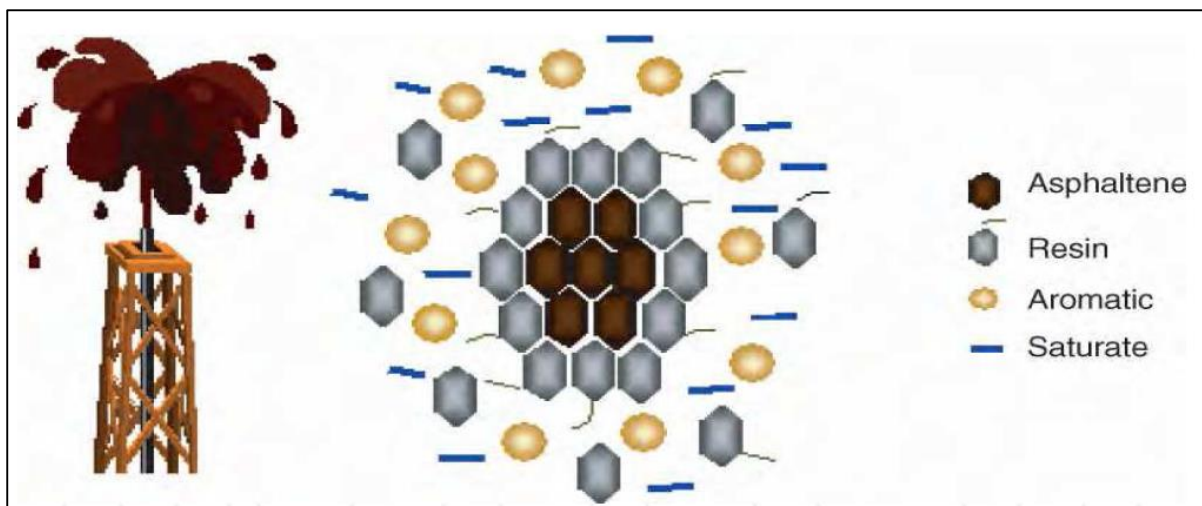


Figure 2.2 Composition of crude oil (Abdel-Raouf, 2012)

These components can be separated by simple technique known as SARA analysis (Saturated, Aromatic, Resin and Asphaltenes). Figure 2.3 shows the SARA analysis process. Particles such as silica, clay, iron oxides, etc., can be present in crude oils. These particles are hydrophilic, but can become hydrophobic due to long term exposure to the crude in the absence of water. Emulsions formed with particles and asphaltenes combined are generally much more stable than those by asphaltenes alone provided that enough asphaltenes are present: all the adsorption sites soon the particle surface need to be saturated by asphaltenes (Abdel-Raouf, 2012).

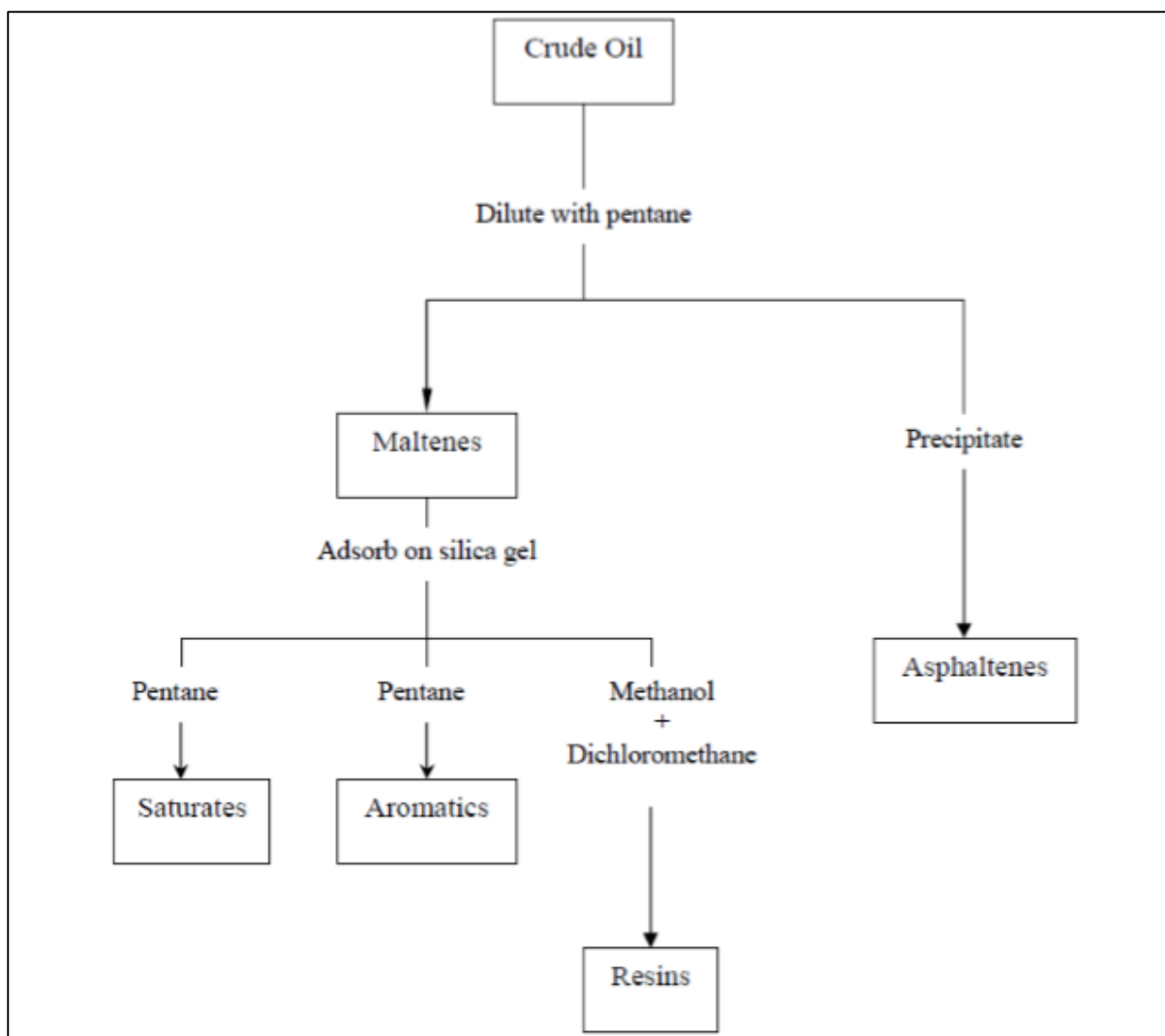


Figure 2.3 Schematic of SARA fractionation of oil (Fateev, 2014).

2.4 Morphology of Emulsion

The morphology of emulsion means its presence as either W/O, O/W or multiple emulsions. It is the most basic characteristic of an emulsion, and there are usually some qualitative procedures that can be used to distinguish emulsion type. These are based on the observation of a physical phenomenon that depends on the prevailing polarity in the continuous phase. The morphologies of some different type of emulsions are shown in Figure 2.4 (Alwadani, 2010).

Contacting a drop of the emulsion with water or oil and observing whether the external phase is miscible or not with it is one of the simple methods that can be used to distinguish between simple and multiple emulsions. However, results from this type of test are sometimes unclear and do not allow to differentiate between them. The electrical conductivity measurements can

also be used to determine the type of emulsion. The aqueous phase in an emulsion usually contains electrolytes and in most cases non-polar liquids exhibit very low electrical conductivity. Therefore, the conductivity of emulsion is very high when the aqueous phase is continuous and very low when the oil is the continuous phase. Moreover, the optical microscopy method can also be used to discern between simple and multiple emulsions because of the difference between the water and oil phase under microscopy observation (Alwadani, 2010).

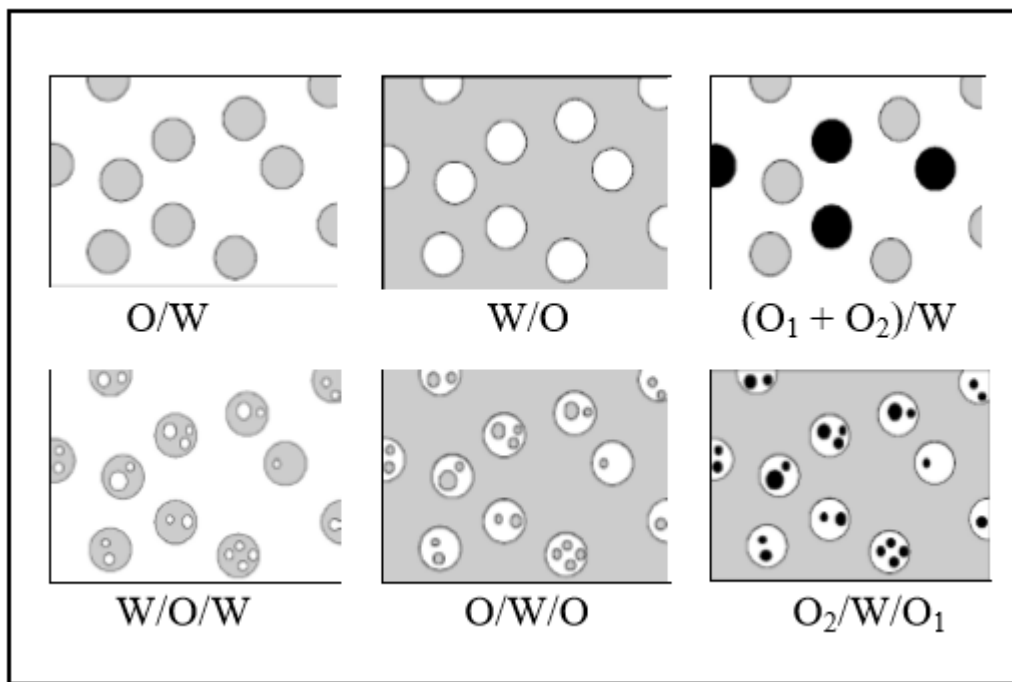


Figure 2.4 Morphologies of different type of emulsions (Alwadani, 2010).

2.5 Phase Inversion

Phase inversion refers to the state of dispersed flow when the continuous and dispersed phase spontaneously invert. This phenomenon takes place at phase inversion point. For example, in water-oil system, water droplets dispersed in oil becomes oil droplets dispersed in water, or vice versa. Phase inversion in emulsion can be one of two types: *transitional inversion* and *catastrophic inversion*. The former is induced by changing factors, such as temperature or salinity, which affect the affinity of surfactant towards the two phases. Changing the *Hydrophile-Lipophile Balance* (HLB) of an emulsion, which depends on the nature and concentration of emulsifying agents, can lead to inversion (Alwadani, 2010).

The *catastrophic inversion* is induced by increasing the volume fraction of the dispersed phase. This inversion usually occurs when the internal volume fraction exceeds some specific value, usually close to the limit of critical close packing, 0.64 for random packing and 0.74 for ordered packing (the maximum possible packing of monodisperse spheres has volume fraction of) for spheres with identical size. Above this limit, droplets are compressed against each other and the interfaces are deformed causing the emulsion to adopt a foam-like structure (Alwadani, 2010).

As shown in Figure 2.5, the dispersed droplets become more concentrated with the increase in volume of the dispersed phase. This leads to coalescing and entrapment of the initial continuous phase into droplets which causes phase inversion.

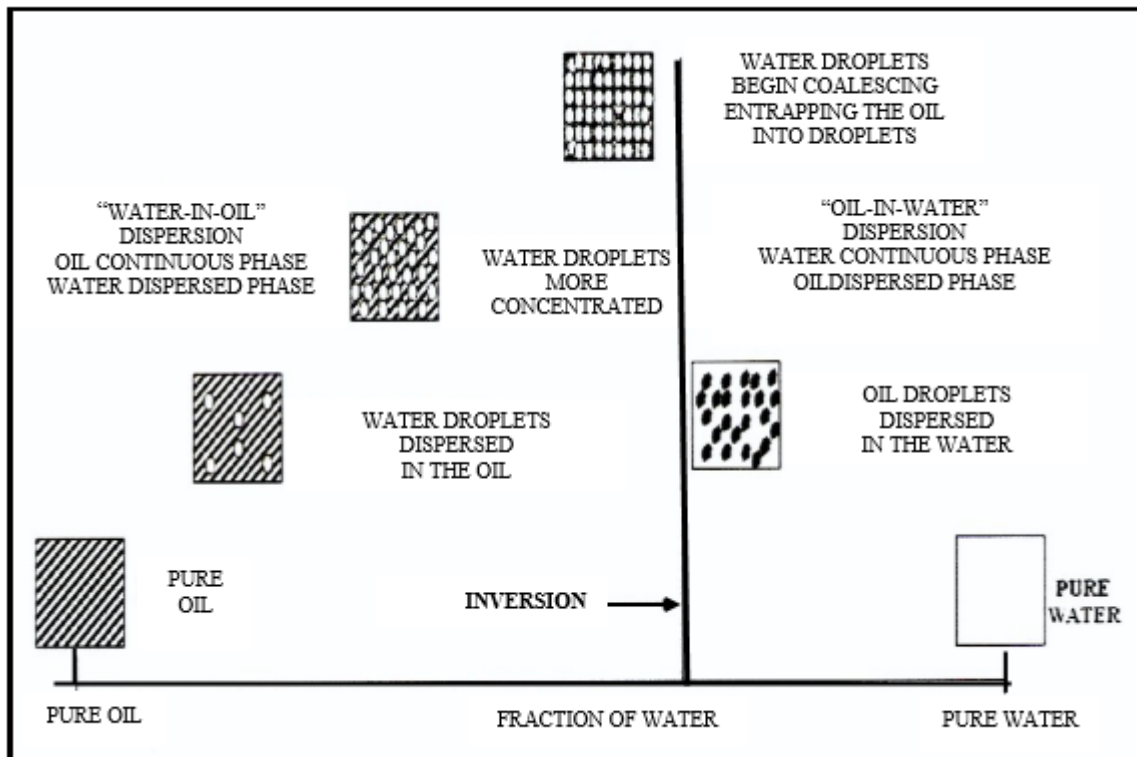


Figure 2.5 Schematic of Inversion Process for Water-Oil Flow (Alwadani, 2010).

The phase inversion point is defined as the critical volume fraction of the dispersed phase over which this phase becomes the continuous phase after small changes have been made to the physical properties of system (density, viscosity, chemical composition, interfacial tension), the geometry factors of a vessel (agitation speed, material type, wettability effect), phase ratio,

energy changes (temperature), the presence of surfactants (decrease interfacial tension) (Cabanillas, 2013). All those parameters are regarded as influence factors on phase inversion and ambivalence range (Fateev, 2014). Ambivalence range is defined as a range of volume fraction a phase above which that phase is always continuous and below which it is dispersed. In the ambivalent range, either one of the two phases can be the dispersed phase. It has been marked that the percentage maximal dispersed phase fraction can be higher 74% and even reach 90% (Pal et al., 1986, Brauner and Ullmann, 2002).

Several other factors affect phase inversion process including the nature and concentration of the emulsifiers and physical influence such as temperature or the application of mechanical shear. The emulsification protocol characteristics which indicate the way the emulsion is made or modified or how the formulation or composition are changed as a function of time or space, can also be considered to be among the factors that phase inversion depends on (Alwadani, 2010).

2.6 Droplet size and droplet-size distribution

Produced oilfield emulsions generally have droplet diameters that exceed 0.1 μm and may be larger than 100 μm . Emulsions normally have a droplet size range that can be represented by a distribution function. Figure 2.6 shows the drop-size distributions of typical petroleum emulsions. The droplet-size distribution in an emulsion depends on several factors including the:

- Interfacial tension (IFT)
- Shear
- Nature and amount of emulsifying agents
- Presence of solids
- Bulk properties of oil and water

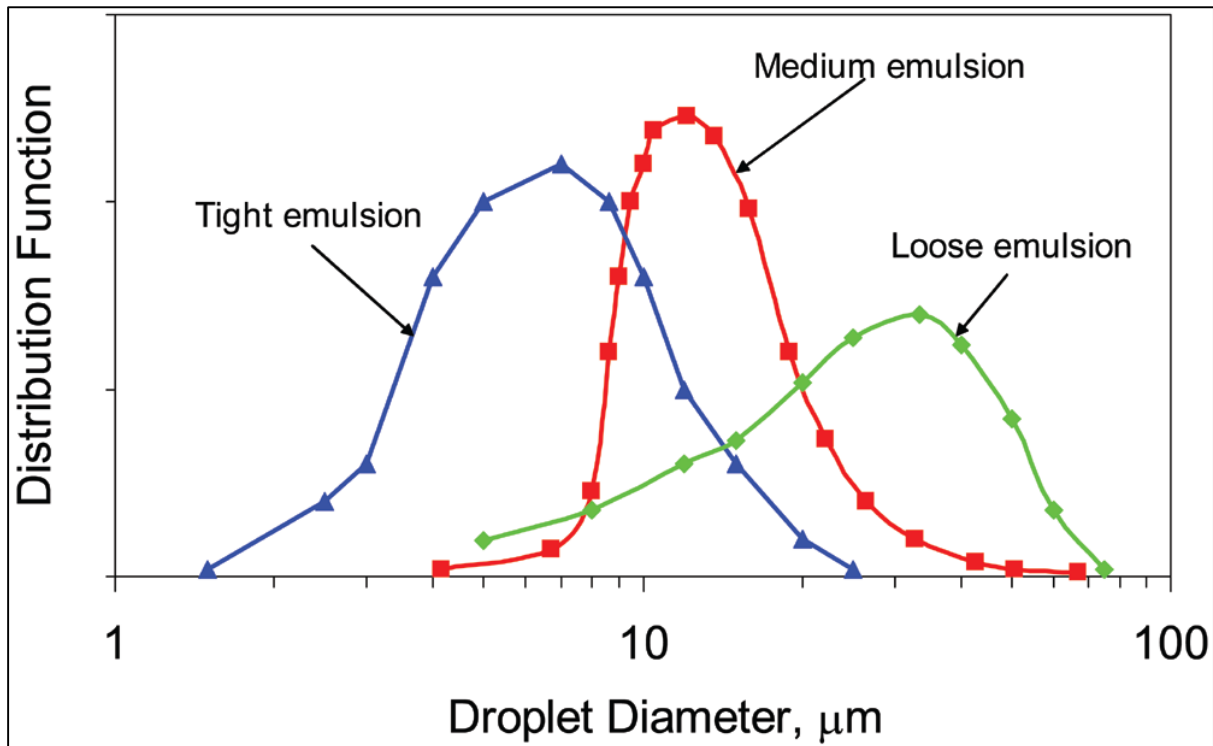


Figure 2.6 Droplet size distribution of petroleum emulsions (Petrowiki, 2015)

Droplet-size distribution in an emulsion determines, to a certain extent, the stability of the emulsion and should be taken into consideration in the selection of optimum treatment protocols. As a rule of thumb, the smaller the average size of the dispersed water droplets, the tighter the emulsion and, therefore, the longer the residence time required in a separator, which implies larger separating plant equipment sizes (Petrowiki, 2015).

Characterizing an emulsion in term of a given droplet size is very common. The emulsion structure is usually characterized by its drop size statistical distribution. This is important in a number of respects: knowledge of size distribution provides information on the efficiency of emulsification process, and the monitoring of any changes in the size distribution as the emulsion ages gives information on the stability of the system.

The droplet-size distribution for oilfield emulsions is determined by the following methods (Petrowiki, 2015).

- Microscopy and image analysis. For example, the emulsion photomicrographs can be digitized and the number of different-sized particles measured with image analysis software.
- By the use of electrical properties such as conductivity and dielectric constants.

- By the use of scattering techniques such as light scattering, neutron scattering, and X-ray scattering. These techniques cover droplet sizes from 0.4 nm to more than 100 μm.
- Physical separation including chromatographic techniques, sedimentation techniques, and field-flow fractionation.

A probability distribution function can be used to describe the droplet-size distribution. The number of drops are usually large enough to describe with continuous mathematical expression in the form of a lognormal distribution is given as (Alwadani, 2010).

$$P(a) = \frac{1}{2a\sigma\sqrt{2\pi}} \exp\left(-\frac{(\ln 2a - \ln d_0)^2}{2\sigma^2}\right) \quad 2.1$$

Here, a is the droplet radius, d_0 represents the diameter median and σ is the geometric standard deviation of the distribution or the measure of the width of the size distribution.

Figure 2.7 shows the drop size distributions that are commonly found in emulsions.

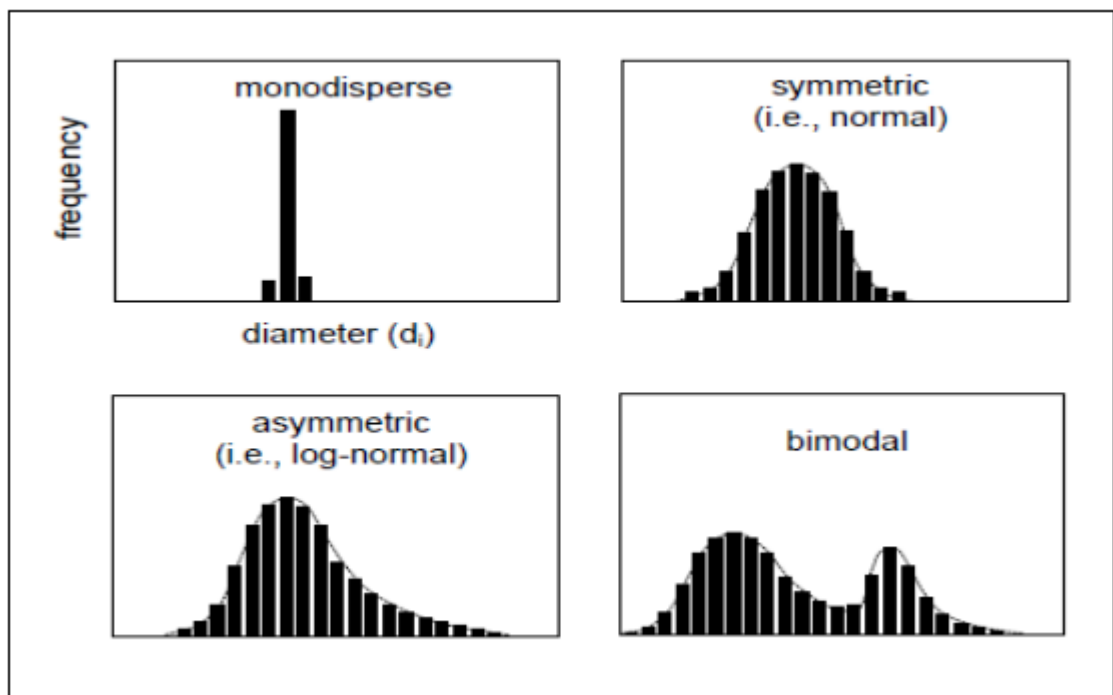


Figure 2.7 Drop size distributions commonly found in emulsions (Alwadani, 2010).

2.7 Emulsion Stability

This section is based on (Langevin et al., 2004) “Crude Oil Emulsion Properties and their Application to Heavy Oil Transportation”.

Emulsions are thermodynamically unstable systems because as the oil and water form two continuous phases while they separate, their decay results in decrease in free energy. Thus, the characteristics of emulsion changes over period of time. Most of the petroleum emulsions that are encountered in practice contain oil, water and emulsifying agents and exist in a metastable state that has high potential barrier to prevent coalescence of the particles.

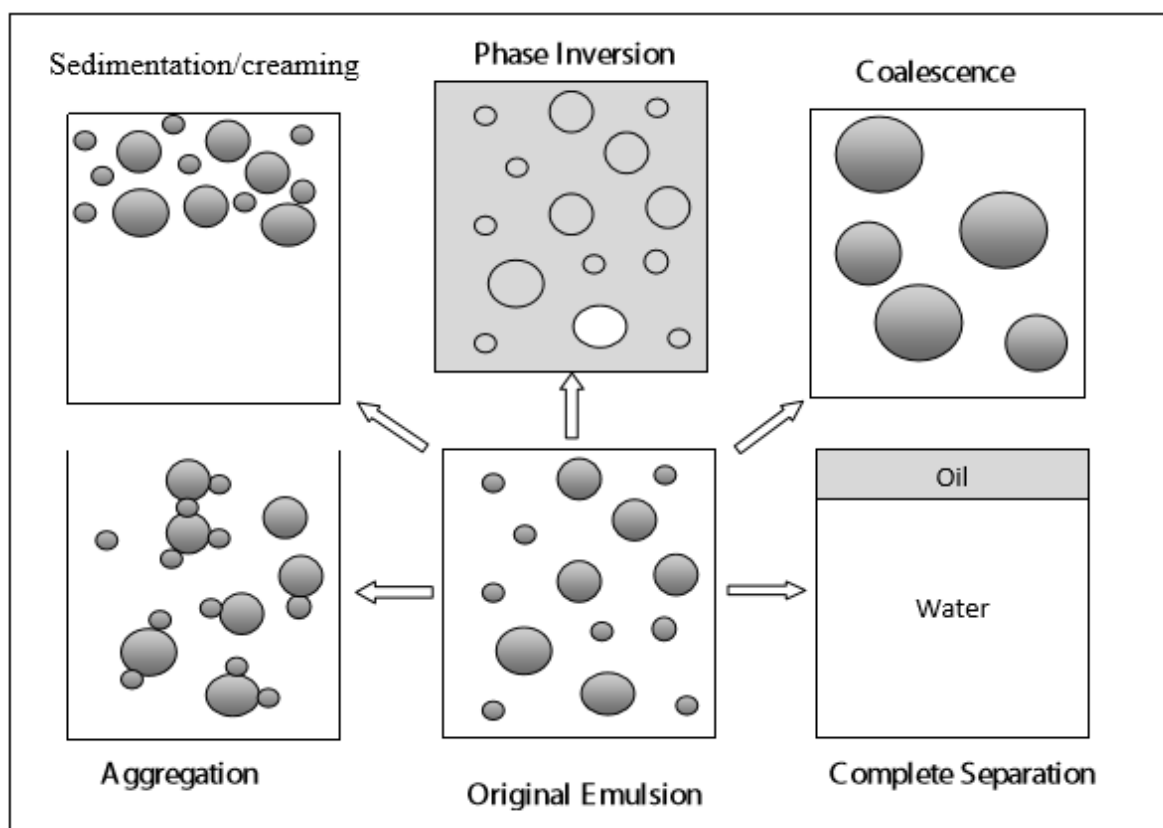


Figure 2.8 Destabilizing mechanisms in emulsions (Alwadani, 2010)

There are several mechanisms leading to emulsion destabilization which are described briefly below and in Figure 2.8:

2.7.1 Ostwald Ripening

Ostwald ripening is the drop growth process occurring when the dispersed phase has a finite solubility into the continuous phase and can migrate between drops of different sizes.

(Langevin et al., 2004) in his paper presented the formula for the corresponding time variation of drop radius:

$$R(t) = \left(\frac{8\gamma D c_{eq} v_m^2}{9kT} \right)^{1/3} t^{1/3} \quad 2.2$$

Where

c_{eq} – the equilibrium concentration of the molecules of the dispersed phase in the continuous one,

D – diffusion coefficient,

v_m – molecular volume.

The growth is faster at large drop volume fractions making exchanges between drops easier. In the case of heavy crude oil, the solubilities of oil in water or of water in oil are low, and this process is likely to be very slow.

2.7.2 Sedimentation or Creaming

Emulsions with small drops ($R < 1 \mu\text{m}$) are insensitive to sedimentation or creaming, Brownian motion dominating the effect of gravity; but when drop sizes are larger than a few microns, they sediment or rise (“cream”). For dilute dispersions, the sedimentation velocity of a drop of radius R and density ρ_i in a fluid of density ρ and viscosity η is (if $\rho_i > \rho$):

$$V = \frac{2R^2(\rho_i - \rho)g}{9\eta} \quad 2.3$$

Where g is the acceleration of gravity. If $\rho_i > \rho$, the drop rises, and the velocity is given by the same expression, provided the sign of the density difference is changed. The drop volume fraction ϕ increases with time, either in the bottom or at the top of the emulsion sample, where drops concentrate locally. When $\phi \sim 60\%$ in this region, drops are no longer spherical, they distort into polyhedral, the flattened regions between them being liquid films as in foams (these are the so called “cream emulsions”) (Figure 2.9)



Figure 2.9 Emulsions with high internal volume fraction (Langevin et al., 2004)

The drop volume fraction continues to increase, although much more slowly than predicted by Equation (2.3). The liquid then flows through the interstitial spaces between drops. With time, the films separating the drops thin and eventually break. This process is accelerated when flocculation occurs, simply because flocs have larger sizes.

2.7.3 Coalescence

Coalescence is when two or more droplets fuse together to form a single larger droplet, reducing the total surface area. In contrast to aggregation, in coalescence process droplets lose their integrity and become a part of a new unit. It is an irreversible process and for large drops approaching each other, the interfaces interact and begin to deform. A plane parallel thin film is formed and the stability of an emulsion system, therefore, depends on the rate of coalescence and it is obvious that the properties of this film will determine the stability of the emulsion.

2.7.4 Flocculation

Flocculation is aggregation of droplets, when two or more droplets clump together without coalescence occurring. Important point of flocculation is that all droplets save their own integ-

rity with no change in the total surface area. Flocculation of emulsions may occur under conditions when the van der Waals attractive energy exceeds the repulsive energy and can be weak or strong, depending on the strength of inter-drop forces.

The major driving force for flocculation can be: (Abdel-Raouf, 2012).

1. Body forces, such as gravity and centrifugation causing creaming or sedimentation, depending on whether the mass density of the drops is smaller or greater than that of the continuous phase.
2. Brownian forces or
3. Thermo-capillary migration (temperature gradients) may dominate the gravitational body force for very small droplets, less than 1 μm .

Apart from this, there are several other factors that influence and speed up the emulsion breaking, they are listed as:

1. **Temperature** – Increase in temperature weakens the interfacial film on the water droplets because of expansion and coalescence. It also weakens the interfacial tension while increasing the mobility and settling rate of water droplet. This leads to increase in droplet collision and coalescence. Thus, heating accelerates separation process and helps to break emulsion.
2. **Agitation or shear** – High speed agitation and shear causes vigorous mixing of oil and water and leads to smaller droplet sizes which are more stable. Reduction in agitation or shear reduces emulsion stability.
3. **Residence or retention time** - Separation efficiency can be improved by increasing the residence or retention time which reduces water content in crude oil. The separation equipment is however expensive.
4. **Solids removal** – Fine solids tend to stabilize emulsions, more so if the solids are both water and oil wetted. Oil wetted solids stabilize water-in-oil emulsions. Solids can be removed by dispersing them into the oil, or they can be water wetted and be removed with water.
5. **Control of emulsifying agents** – It is necessary to control emulsifying agents as they are important to have a stable emulsion. This can be done by careful selection of chemical injected during production. For example, corrosion protection, surfactants and

dispersant for control of organic and non-organic deposits control, and polymers and blocking agents for water production control (Kokal, 2005).

2.8 Factors Determining Emulsion Stability

There exist several factors that determine Emulsion Stability, i.e., the rate at which the droplets of a macro emulsion coalesce to form larger droplets, and eventually break the emulsion. These factors can be listed as physical nature of interfacial film, electrical or steric barrier on the droplets, continuous phase viscosity, droplet size distribution, phase volume ratio, and temperature.

1. **Surface and Interfacial Tension** – For interfacial or surface tension to exist, two phases needs to be present. Interfacial tension is defined as the force that holds the surface of a particular phase together while Surface tension is a contractive tendency of the surface of a liquid that allows it to resist an external force. Mathematically, surface or interfacial tension can be written in the form of force per unit length or energy per unit area.

$$\sigma = \frac{E}{A} = \frac{F}{L} \quad (2.4)$$

Where,

σ = surface-/interfacial tension [N/m]

E = energy [J or Nm]

A = area [m²]

F = force [N]

L = length of liquid surface that is deforming [m]

Low interfacial tension or low interfacial free energy makes it easier to maintain large interfacial area.

2. **Interfacial films** - These films arise from the absorption of high molecular weight polar molecules that are interfacial active. Interfacial films that form around the water droplets at the oil-water interface stabilize the emulsions by reducing interfacial tension

and increasing the interfacial viscosity. Strong interfacial film act as a barrier – it makes hard for the droplets to coalescence.

3. **Existence of an electrical or steric barrier** – In O/W emulsions, the presence of a charge on the droplets carry an electrical barrier for the approach of two particles. This is a significant factor for emulsion stability. However, in W/O emulsions, there is very little charge on the dispersed particles. Presence of steric repulsions prevents the act of collisions and aggregations and then coalescence.
4. **Emulsion rheology and shear viscosity** - An increase in the continuous phase viscosity μ reduces the droplets collision frequency and their coalescence rate. Emulsions are more stable in concentrated form than when diluted because the external phase viscosity is increased as the suspended particles number increases. Also, high bulk viscosity reduces the rate of creaming and aggregation.
5. **Droplet size distribution** – Smaller droplet size favours emulsion stability. Since large particles have less interfacial surface per unit volume than small droplets. An emulsion with a fairly uniform size distribution is more stable than one having a wider size distribution with the same average particle size.
6. **Phase volume ratio** – Small volume of the dispersed phase reduces the frequency of collision and aggregation. Increase in volume of dispersed phase increases instability in the emulsion system.
7. **Temperature** – Increase in temperature accelerates the separation process and thus helps to break the emulsion. Heating weakens the interfacial film and tension between the two phases. It also reduces the viscosity of oil and increase droplets collisions and favours coalescence.

2.9 Emulsion Rheology

Rheology in general can be defined as the study of the deformation and flow of materials under influence of applied shear stress. In other words, rheology is the study of large deformation produced by shear forces which causes many materials to flow. Rheometry is the measuring technology used to determine rheological data. The importance here lays in the measuring systems, instruments, and test and analysis methods. Liquids and solids can be investigated using rotational and oscillatory rheometers. Rotational test is preformed to characterize viscous

behaviour, and the oscillatory test are performed to evaluate viscoelastic behaviour (Mezger, 2006).

Depending on the rheological properties, fluids can be divided into two types:

- **Newtonian fluids**: shows a linear relation between the applied shear stress, τ , and the shear rate, $\dot{\gamma}$. The viscosity is therefore independent on the shear rate. The shear stress mathematically, is written as:

$$\tau = \frac{F}{A} = \mu \cdot \dot{\gamma}$$

Where, μ is the fluid viscosity. In this thesis, for example, tap water is used as a Newtonian fluid.

- **Non-Newtonian fluid**: Most commonly, the viscosity (the measure of a fluid's ability to resist gradual deformation by shear or tensile stresses) of non-Newtonian fluids is dependent on shear rate or shear rate history. Some non-Newtonian fluids with shear-independent viscosity, however, still exhibit normal stress-differences or other non-Newtonian behavior. In a non-Newtonian fluid, the relation between the shear stress and the shear rate is different and can even be time-dependent (Time Dependent Viscosity). Therefore, a constant coefficient of viscosity cannot be defined (Tropea et al., 2007).

The shear rate dependency of apparent viscosity (η) categorizes non-Newtonian fluid into several types (Figure 2.10):

a. Power Law Fluids

- Pseudoplastic – η (viscosity) decreases as shear rate increases (shear rate thinning)
- Dilatant – η (viscosity) increases as shear rate increases (shear rate thickening)

b. Bingham Plastic

- η depends on a critical shear stress (τ_0) and then becomes constant

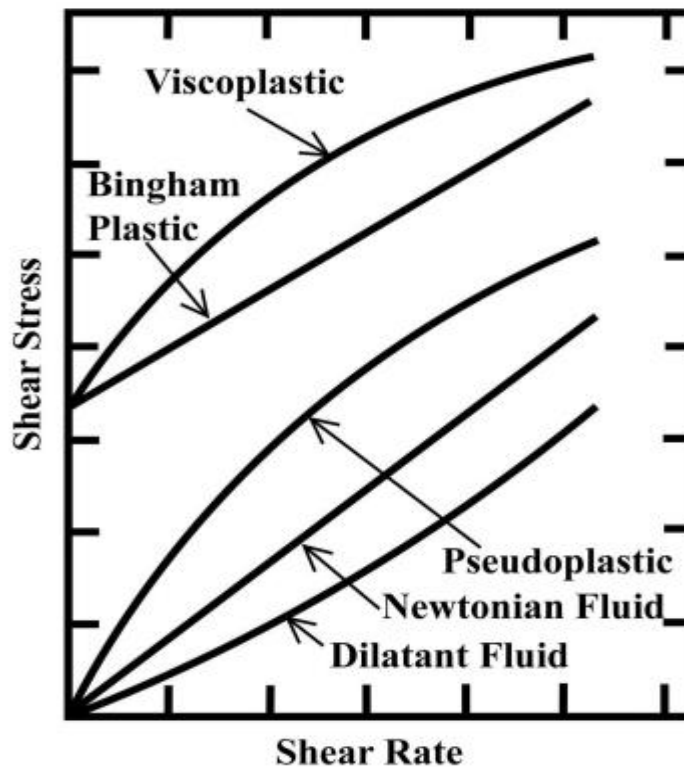


Figure 2.10 Classification of Non-Newtonian fluids (Chhabra, 2010).

2.9.1 Viscosity of Emulsions

Due to droplet crowding and structural viscosity, the viscosity of an emulsion can be substantially greater than the viscosity of either the oil or the water because emulsions show non-Newtonian behaviour. At a certain volume fraction of the water phase (water cut), oilfield emulsions behave as shear-thinning or pseudoplastic fluids (i.e., as shear rate increases, viscosity decreases). Figure 2.11 shows the viscosities of tight emulsions at 125°F at different water cuts. The constant values of viscosity for all shear rates, or a slope of zero, indicate that the emulsions exhibit Newtonian behavior up to a water content of 40%. At water cuts greater than 40%, the slope of the curves deviates from zero, which indicates non-Newtonian behavior. The non-Newtonian behavior is pseudoplastic or shear-thinning behavior. The very high viscosities achieved as the water cut increases up to 80% (compared with viscosities of oil approximately 20 cp and water <1 cp). At approximately 80% water cut, an interesting phenomenon is observed. Up to a water cut of 80%, the emulsion is a water-in-oil emulsion; at 80%, the emulsion "inverts" to an oil-in-water emulsion, and the water, which was the dispersed phase, now becomes the continuous phase. In this particular case, multiple emulsions

(water-in-oil-in-water) were observed up to very high water concentrations (>95%) (Petrowiki, 2015).

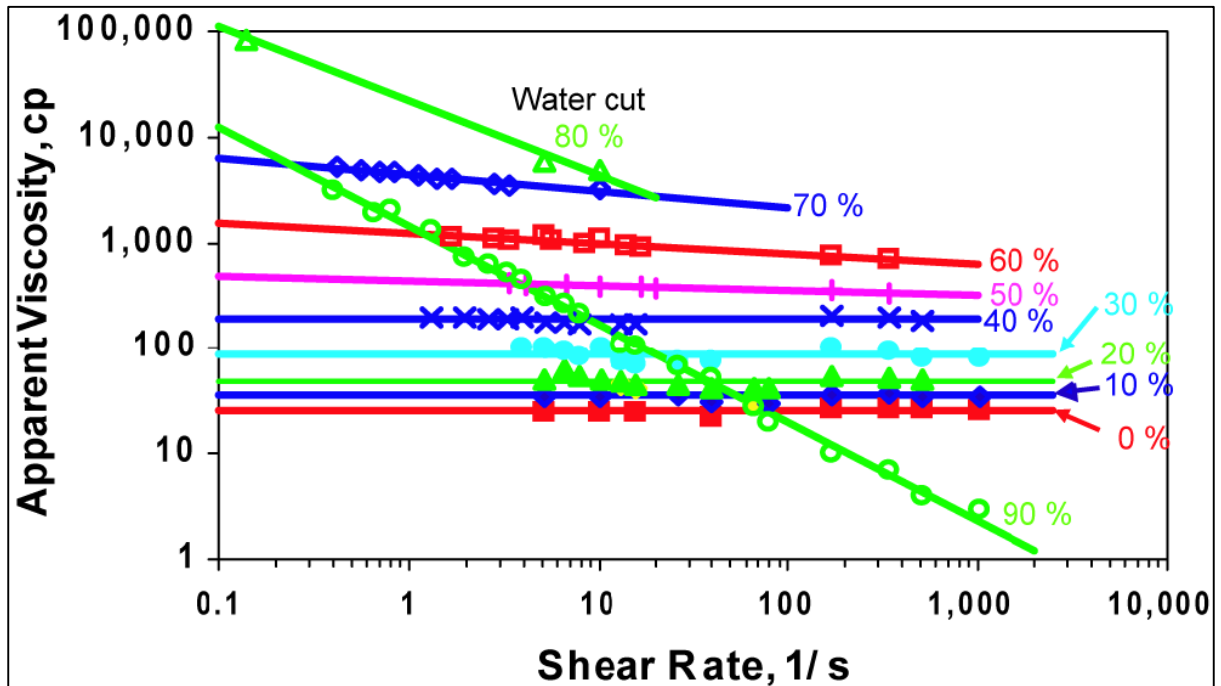


Figure 2.11 viscosities of tight emulsions at 125°F at different water cuts (Petrowiki, 2015).

CHAPTER 3

EXPERIMENTS

This chapter describes the properties of fluids used during the experiment. The chapter also focuses on the experimental procedure and setup of equipment's used to obtain results.

3.1 Materials

Two types of mineral oil, Bayol 35 and Exxsol D60, were examined in this study. They were used as the oil phase and tap water is used as the water phase. Since both phases are transparent, Sudan Blue was added to dye the oil phase blue to be able to easily distinguish between phases and to investigate if this dye has any effect on the emulsion. The measured properties of mineral oils and water are tabulated in Table 3.1 and the reference data for the two mineral oil are mentioned in Table 3.2:

Table 3.1 Physical Properties of materials measured at 20 °C.

Name of material	Density, g/cm³	Specific gravity	Viscosity, mPa.s
Water	0.9981	0.9999	1.0000
Water+0.25ml diluted Uranine	0.9933	0.9951	0.9700
Oil Exxsol D60	0.7889	0.7903	1.5200
Oil Exxsol D60+Sudan blue	0.7888	0.7903	1.4000
Oil Bayol 35	0.7830	0.7844	2.4000
Oil Bayol 35+Sudan blue	0.7829	0.7843	2.10

Table 3.2 Properties of mineral oils.

	Bayol 35	Exxsol D60
Physical State	Liquid	Liquid
Colour	Colourless	Colourless
Odour	Odourless	Mild petroleum/solvent
Relative Density	0.791(at 15.6°C)	0.789 (at 15.6°C)
Density [kg/m ³], [15 °C]	788	789
Viscosity, [cSt]	3.57 [at 25 °C], 2.57 [at 40 °C]	1.69 [at 25 °C], 1.45 [at 40 °C]
Flash Point Method	>81 °C [ASTM D-93]	>62 °C [ASTM D-56]
Flammable Limits (Approx. volume % in air)	LEL: 0.6 UEL: 4.9	LEL: 0.7 UEL: 5.4
Boiling point/Range	218 °C - 257 °C	190 °C - 211 °C
Autoignition Temperature	>200 °C	250 °C
pH	N/A	N/A
Vapour Pressure [kPa] [20°C]	0.012	0.06
Evaporation Rate (N-butyl Acetate =1)	< 0.01	0.06
Solubility in water	Negligible	Negligible

(Chemical, 2013, Limited, 2007)

Oil viscosity was measured using Anton Paar MCR 302 rheometer and C-LTD 70/PIV rheometer. The density and specific gravity was measured using densitometer. The mineral oil used in this study was considered as a Newtonian fluid because the viscosity of the mineral oils remains almost constant while being measured with a rheometer at different speed of rotation.

3.2 Preparation of Oil-Water Mixture

The oil-water mixtures were prepared by mixing oil and water in seven different proportions as shown in the Table 3.3.

The experiments were performed in two types of containers; first with 200 ml bottles and second with 200 ml beakers. In both cases, 100% correspond to 200 ml. The mineral oil phase was coloured using Sudan blue in all samples. Consequently, the samples were mixed either

by hand shaking or using a mechanical mixer and the resulted oil-water mixtures were examined visually or under microscope.

The two modes of mixing are:

- Hand shaking of the sample containing bottles for 1 minute.
- Mixing with Silverson LART-A mixer (see Figure 3.1), at different rotational speeds and for different times periods to better characterize its effect on emulsion formation. The samples (tap water + mineral oil) were mixed for 1 minute and 5 minutes with different stirring speed of 400 RPM, 1000 RPM and 1600 RPM. All the measurements were made under room temperature (20°C) unless otherwise specified. The oil to water volume ratio of each sample is shown in Table 3.3.

3.3 Evaluation of the separation of oil-water mixtures

The prepared oil-water mixtures were examined for their stability. The readings for degree of separation were recorded at t=0 min, t=5mins, t=1 hour and t=20 hours at room temperature, and microscopic or camera images were taken to evaluate the separation phenomena.

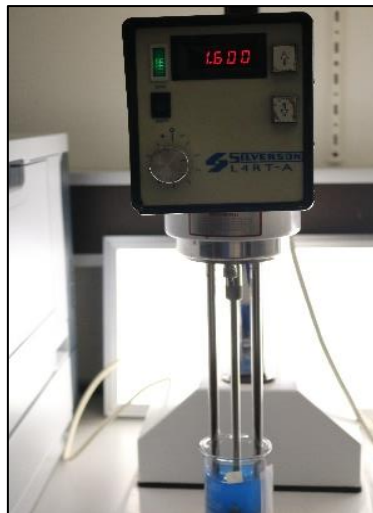


Figure 3.1 Silverson LART-A mixer

Table 3.3 Compositions of water-oil samples.

No.	RPM	Mixing times
1	400	a = 1 minute
2	1000	b = 5 minutes
3	1600	

Sample code	Water : Oil Proportion (%)	Water volume (ml)	Oil volume (ml)
S1 1a 1b 2a 2b 3a 3b	95 : 5	190	10
S2 1a 1b 2a 2b 3a 3b	80 : 20	160	40
S3 1a 1b 2a 2b 3a 3b	60 : 40	120	80
S4 1a 1b	50 : 50	100	100

2a			
2b			
3a			
3b			
S5	40 : 60	80	120
1a			
1b			
2a			
2b			
3a			
3b			
S6	20 : 80	40	160
1a			
1b			
2a			
2b			
3a			
3b			
S7	5 : 95	10	190
1a			
1b			
2a			
2b			
3a			
3b			

3.3 Microscopy Analysis of water-oil mixtures/emulsions

The droplet arrangement size distribution and their separation within the water-oil mixtures/emulsions was observed through an optical microscope Ziess Stemi DV4 connected with digital camera and determined by AxioVission AC software. The separation phenomena were observed at time intervals ranging from 0 min to 5 mins, 30 mins, 1hour and 2 hours.



Figure 3.2 Light microscope Zeiss Stemi DV4



Figure 3.3 Silverson LART-A mixer and the Light microscope Zeiss Stemi DV4

3.4 Rheology

The rheological measurements for all the oil-water mixtures were determined using two methods:

1. Rotational Digital Rheometer Model Anton Paar MCR 302 (Concentric cylinder type arrangement, see Figure 3.4) to measure viscosity, shear rate vs shear stress. The viscosity of the oil-water mixtures was measured, at different temperatures of 20 and 40 °C. The representative samples of oil-water mixtures which has the size of 20 ml each were used for the rheological analysis. The tests were run at shear rate ranging from 1 s^{-1} to 100 s^{-1} and then back again. The viscosity tests were run to see how the viscosity of the fluid act at different shear rates, and to characterize their rheological behaviour. There had been some challenges due to phase separation that occurred during some of measurements, which can be the reason for non-reproducibility of the forward and backward measurements. Hence careful observation was required to identify these problems.

2. Rotational Digital Rheometer Model C-LTD 70/PIV (see Figure 3.5) to measure viscosity, shear rate vs shear stress of water without dyeing, pure oil Exxol D60 and Bayol 35 with dyeing and Marcol 82 without dyeing at the room temperature (20 °C). The sample size of 15 ml each were used for analysis. In this method, the fluid is kept in a translucent glass container and thus this method was used to observe the interface of oil-water through naked eye, which is not possible using the first method. However, the results obtained in both the methods were mostly similar.

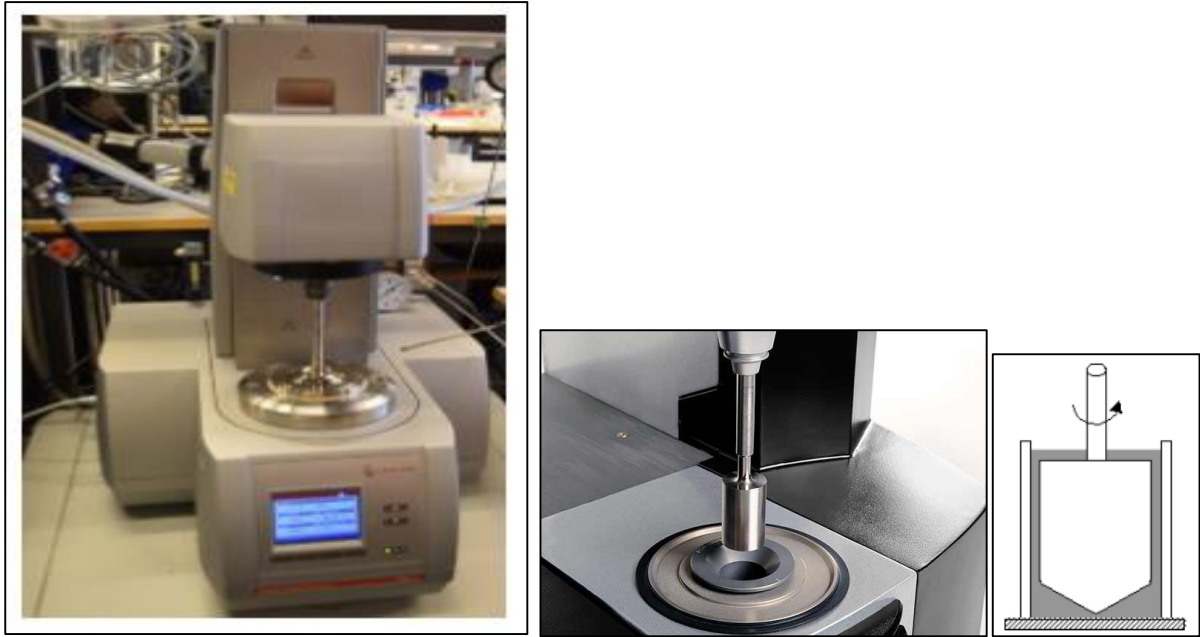


Figure 3.4 Anton Paar MCR 302 rheometer (Concentric cylinder systems)

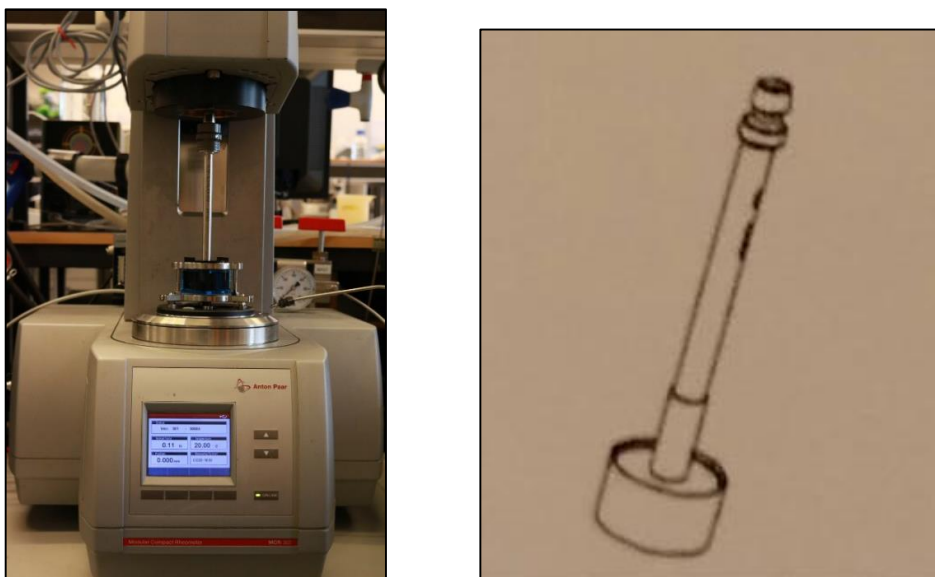


Figure 3.5 C-LTD 70/PIV rheometer (Measuring cylinder D:32mm; L:16.5mm, black anodized)

3.5 Surface and interfacial tension

The surface tension of the pure water and the mineral oils as well as the interfacial tension of the oil-water samples with varied oil-water ratios were measured using tensiometer (Type 8451, KRUSS). The measurement method used was Du Noüy Ring Method. It is explained in the section 3.5.1 as described by (Xu, 2005).

3.5.1 Du Noüy Ring Method

In this method, the interfacial tension relates to the force required to pull a wire ring off the interface. The ring is usually made up of platinum or a platinum-iridium alloy. The platinum rings need to be handled carefully. The radius (r) of the wire ranges from 1/30 to 1/60 of that of the ring. The measurement simply requires the ring to be wetted by the liquid and then pulled through the interface while measuring the force exerted on the ring. The ring must sit square and parallel to the interface and failure to do so will result in errors in the measurements. The maximum force of the vertical constituent is directly proportional to the surface tension. The surface or interfacial tension was seen on the white wheel, and the unit is mN/m.

The major error in this technique is caused by deformation of the ring, which is a very delicate probe and subject to inadvertent deformation during handling and cleaning. It is also important that perfect wettability of the ring surface by the denser fluid be maintained. If perfect wetting is not achieved, additional correction of the instrument reading is needed as shown in equation 3.1. And also the value needs to be corrected by using equation 3.2 and 3.3. The temperature during this experiment was 20°C.

$$\sigma = \sigma \cdot kF \quad (3.1)$$

where

σ = surface or interfacial tension

σ^* = surface or interfacial tension, non-calibrated value (read directly from the tensiometer)

k = calibration factor

F = correction factor for ring and fluid that is lifted.

$$k = \frac{\text{Surface tension of distilled water at } 20^\circ\text{C}}{\text{Measured surface tension distilled water}} = \frac{72.75}{71.10} = 1.0232 \quad (3.2)$$

Note: Surface tension of distilled water is found in table in (Fateev, 2014).

$$F = \left\{ 0.725 + \sqrt{\frac{0.01452 \cdot \sigma^*}{\frac{U^2}{4}(\rho_2 - \rho_1)} + 0.04534 - \frac{1.679}{R/r}} \right\} * 1.07 \quad (3.3)$$

Where

$$U = 2\pi (R_i + R_y) = 2\pi (R + R) = 4\pi \cdot R = 11.9996 \text{ cm}$$

R = mean radius of platinum ring = 0.9549 cm

r = platinum string cross-section = 0.0185 cm

ρ_1 = Density of the lightest liquid phase

ρ_2 = Density of the heaviest liquid phase

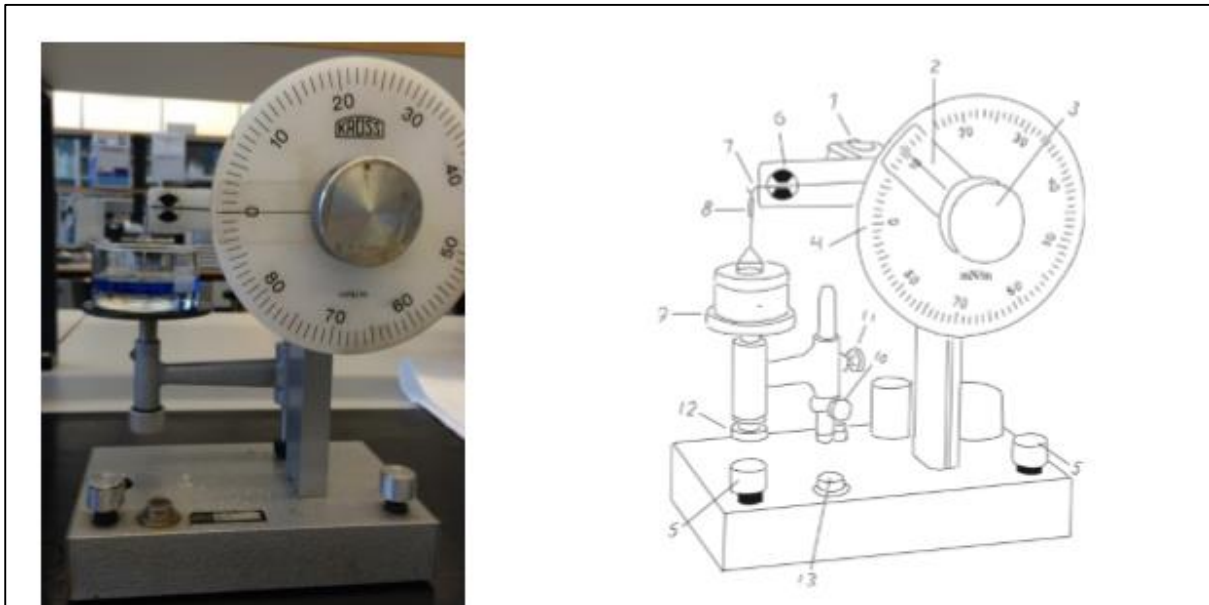


Figure 3.6 a) Picture of the tensiometer type 8451, KRÜSS b) Sketch of tensiometer

3.6 Density

The density of the tap water, mineral oil and water-oil mixtures were measured using Anton Paar DMA 4500 densitometer, see Figure 3.7. The temperature was set to 20°C, a representative sample of 2 ml was used, and it took approximately 1 minute before the density results could be displayed on the screen.



Figure 3.7 Anton Paar DMA 4500 densitometer

3.7 Selecting the better phase identification agent

The effect of adding a colouring agent for phase identification was tested on sample 3 (60-40% w-o). Uranine and Sudan blue were the selected colouring agents. The procedure used to select the better phase identifier is as follows:

1. Select the sample, in this case, sample 3 (60-40% w-o) was chosen for the experiment.
2. Conduct the experiment with both oils, Exxsol D60 and Bayol 35.
3. Colour the water phase with Uranine or oil phase with Sudan blue.
4. Mix the samples with the Silverson L4RT-A mixer at a speed of 1600 RPM for 5 mins.
5. Check the physical properties and the separation phenomena of the oil-water mixtures.

CHAPTER 4

RESULTS AND DISCUSSION

This chapter contains the results of the experiments and the obtained results are discussed in detail.

4.1 Physical properties of materials measured at 20 °C

Table 4.1 shows the physical properties of the samples measured in the laboratory. It can be observed that the samples with dyeing has slightly lower density and viscosity compared to those prepared without dyeing. The density measurement deviations are so little and can be neglected, but the viscosity variations are quite considerable and clearly has an influence of adding colouring agents.

Table 4.1 Physical properties of materials measured at 20 °C

Name of material	Density, g/cm³	Specific gravity	Viscosity, mPa.s
Water	0.9981	0.9999	1.0000
Water+0.25ml diluted Uranine	0.9933	0.9951	0.9700
Oil Exxsol D60	0.7889	0.7903	1.5200
Oil Exxsol D60+Sudan blue	0.7888	0.7903	1.4000

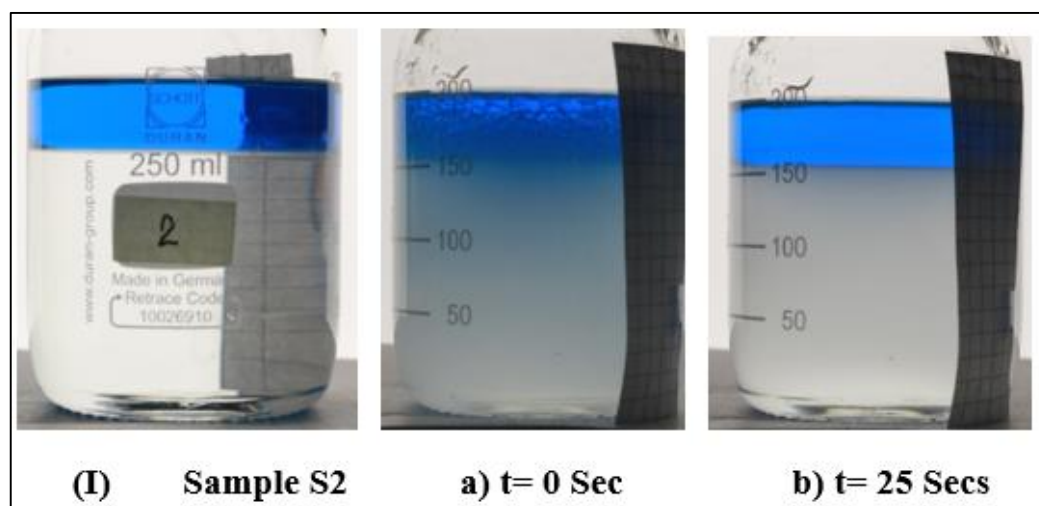
Oil Bayol 35	0.7830	0.7844	2.4000
Oil Bayol 35+Sudan blue	0.7829	0.7843	2.1000

4.2 Oil-water mixtures

As mentioned in section 3.3, the prepared oil-water mixtures were tested for emulsion stability. The results were recorded at $t=0$ min, 5 mins, 1 hour and 20 hours at room temperature. These oil water mixtures prepared at different conditions (mixing speed and mixing time) were examined using visual observations, microscopic/camera images and measuring their physical properties.

4.2.1 Mixing by manual shaking

The samples were prepared with different water-oil volume ratios as mentioned in the Table 4.2 and they were mixed by manual shaking for 1 min. The resultant oil-water mixtures for sample S2 and S6 are shown in Figure 4.1 & Figure 4.2. Sub figure (I) shows the experiments with added Sudan blue to the oil phase and sub figure (II) shows the experiments without any colouring agent.



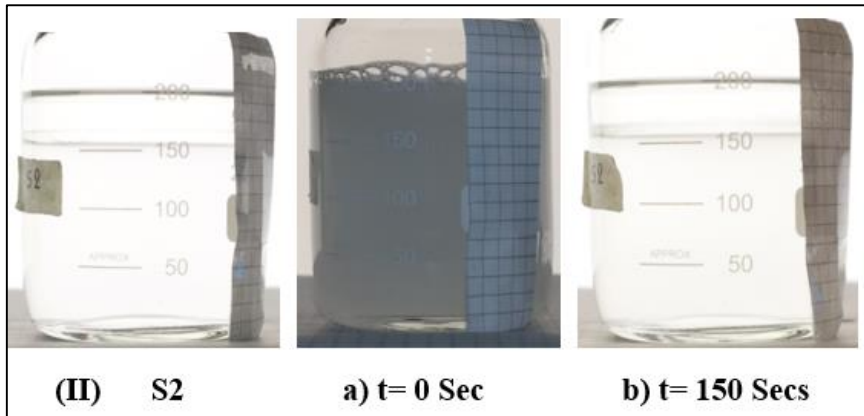


Figure 4.1 (I) Bayol 35_S2 (80-20 % water-oil mixture) with Sudan blue and (II) without Sudan blue

After rigorous mixing, initially we can observe water droplets in oil and oil droplets in water phase. However, within couple of tens of seconds oil and water phase separated out for the samples coloured with Sudan blue. Separation time was much longer when the sample was not coloured.

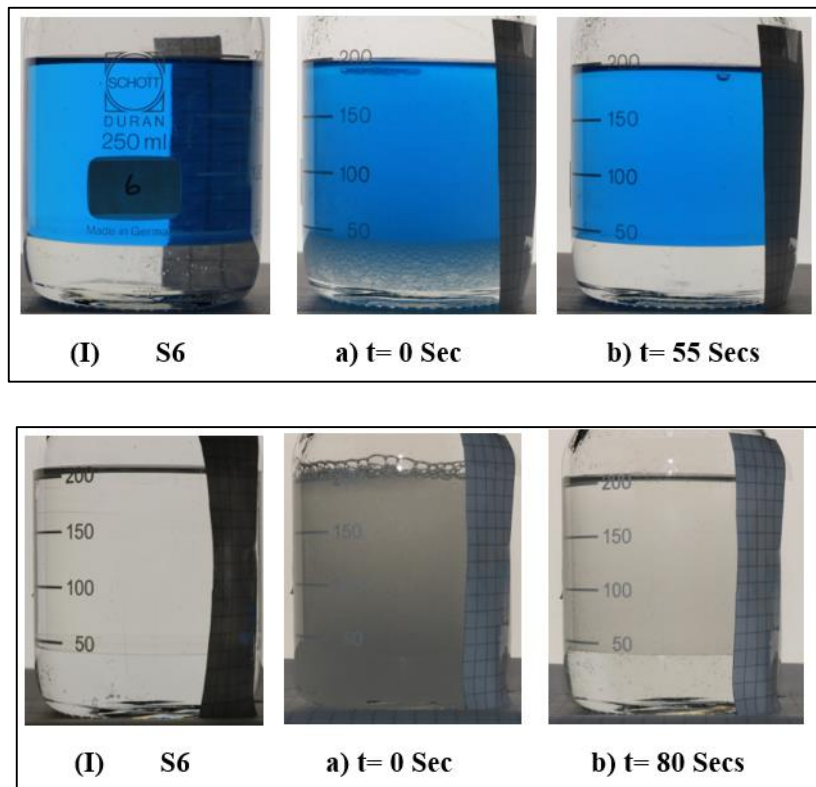


Figure 4.2 (I) Bayol 35_S6 (20-80 % water-oil mixture) with Sudan blue and (II) without Sudan blue

Similar trend of results for 80-20 % oil-water ratio was observed as in case of 20-80 % oil-water. Presence of dye in the samples reduced the separation time.

Table 4.2 contains the separation times for the oil-water mixtures with and without dyeing. Figure 4.3 depicts how the separation time has been decreased for each sample with the addition of Sudan blue. This means that adding Sudan blue has decreased the emulsion stability in some way.

Table 4.2 Illustrated separation times of w-o mixtures/emulsions (Bayol 35)

Sample code	% of Water : % of Oil proportion	Water volume (ml)	Oil volume (ml)	Mode of mixing	Interfacial mixing layer separation time (Seconds)	
					W-O with dyeing	W-O without dyeing
S1	95 : 5	190	10	Shaking by hands	50	110
S2	80 : 20	160	40	Shaking by hands	25	150
S3	60 : 40	120	80	Shaking by hands	53	130
S4	50 : 50	100	100	Shaking by hands	34	120
S5	40 : 60	80	120	Shaking by hands	60	87
S6	20 : 80	40	160	Shaking by hands	55	80
S7	5 : 95	10	190	Shaking by hands	40	67

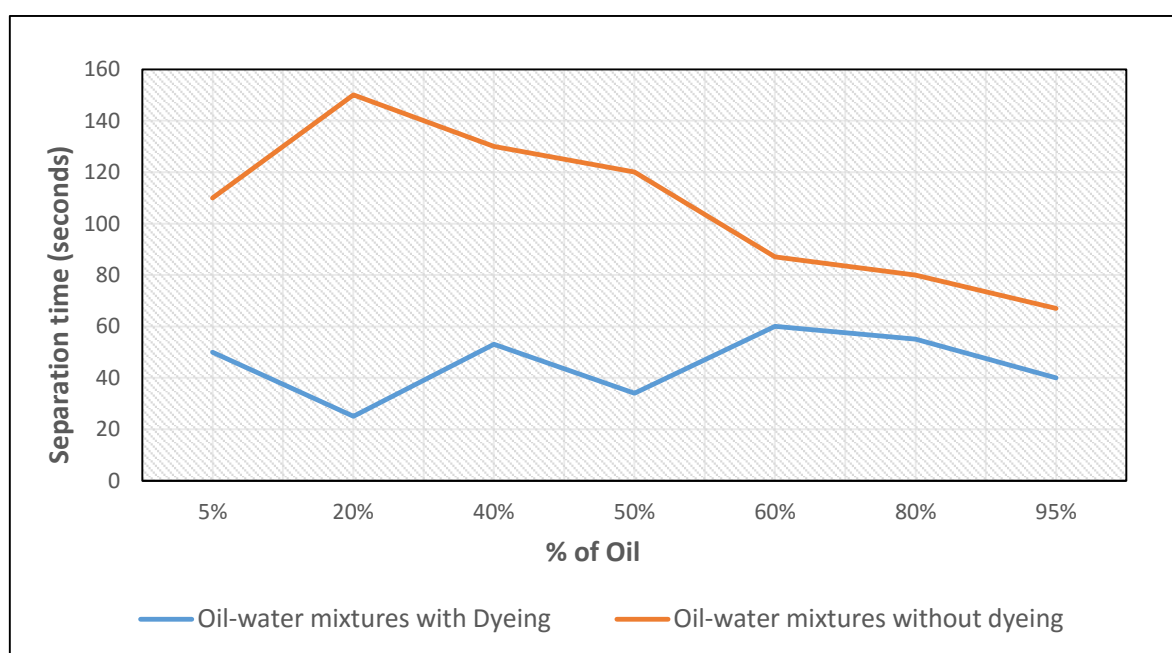


Figure 4.3 Illustrated separation times of w-o (Bayol 35) with mixing by hands shanking.

4.2.2 Mixing by Silverson L4RT-A mixer

As shown in Table 4.3 oil-water mixtures were prepared using the mechanical mixer and the resulted oil-water mixtures could be classified as ‘oil-in water emulsion’ for the least oil containing sample, ‘water in oil emulsion’ for the least water containing sample and ‘oil water mixtures with a clear interface’ for the intermediate water to oil proportions (see Figure 4.4)

Table 4.3 Oil-water mixtures/emulsions resulted by mixing with Silverson L4RT-A mixer.

Sample code	% Water : % Oil	Comment
	proportion	
S1	95 : 5	Oil-in-water emulsion.
S2	80 : 20	* Oil-water interface.
S3	60 : 40	* Intermediate mixing layer.
S4	50 : 50	* Leave oil droplets in water or water droplets
S5	40 : 60	in oil after the separation of intermediate
S6	20 : 80	mixing layer
S7	5 : 95	Water-in-oil emulsion.

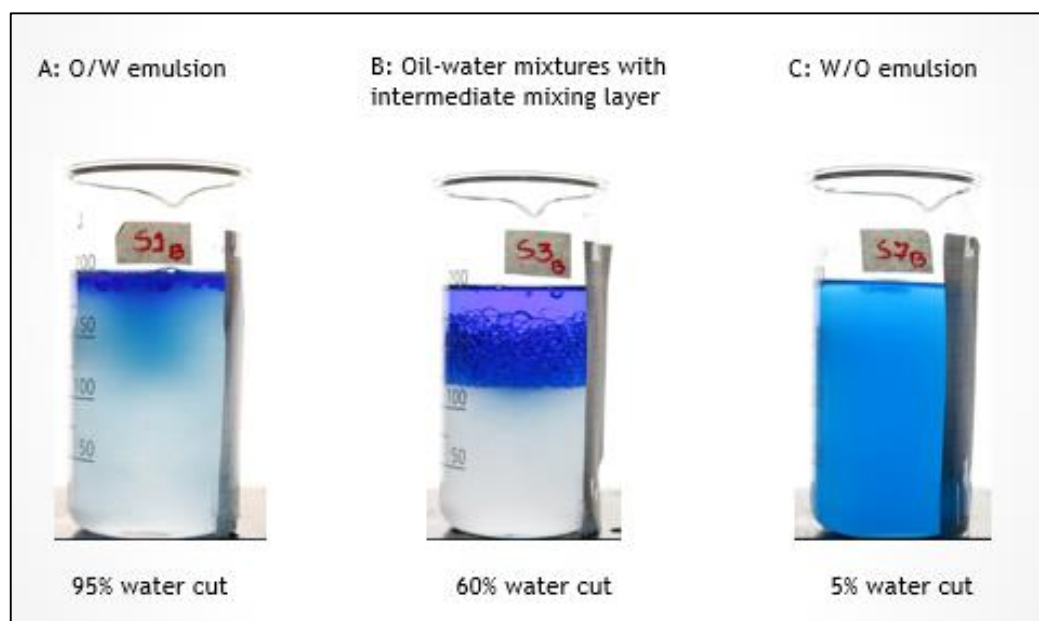


Figure 4.4 Oil-water mixture's pictures after mixing (Bayol 35 with Sudan blue)

Hence we could observe that emulsions were obtained in S1 and S7 which has higher percentage of either oil or water. For S2 to S6, we could see an oil-water interface with the presence of oil droplets in water and water droplets in oil.

4.2.2.1 Effect of type of the oil on separation

The oil-water samples were mixed for 1 minute and 5 minutes with different stirring speed of 400 RPM, 1000 RPM and 1600 RPM and the description for the samples are found in Table 4.4. For more pictures of the resulted oil water mixtures, see appendix A. Table 4.4 shows the separation times for oil water mixtures prepared using Bayol and Exxsol D60.

No.	RPM	Mixing times
1	400	a = 1 minute
2	1000	b = 5 minutes
3	1600	

Table 4.4 Interfacial mixing layer separation time for water-oil mixtures/emulsions.

Sample code	% of Water : % of Oil proportion	Water volume (ml)	Oil vol- ume (ml)	Mixer	Interfacial mixing layer sep- aration times (Second)	
					Bayol 35	Exxsol D60
S1	95 : 5	190	10	Silverson L4RT- A		
1a					15	18
1b					23	23
2a					17	20
2b					30	27
3a					20	24
3b					33	35
S2	80 : 20	160	40	Silverson L4RT- A		
1a					22	21
1b					30	29
2a					26	27
2b					34	30
3a					28	34
3b					39	36
S3	60 : 40	120	80	Silverson L4RT- A		
1a					27	27
1b					37	33

2a					33	30
2b					42	40
3a					44	40
3b					48	43
S4	50 : 50	100	100	Silverson L4RT- A		
1a					23	29
1b					43	35
2a					28	33
2b					45	47
3a					48	47
3b					54	49
S5	40 : 60	80	120	Silverson L4RT- A		
1a					25	31
1b					46	38
2a					36	39
2b					69	41
3a					50	49
3b					72	51
S6	20 : 80	40	160	Silverson L4RT- A		
1a					23	18
1b					40	20
2a					34	25
2b					41	34
3a					48	29
3b					62	44
S7	5 : 95	10	190	Silverson L4RT- A		
1a					34	20
1b					60	30
2a					50	45
2b					63	53
3a					56	54
3b					69	60

Observing the tabulated data in Table 4.4 and as it is depicted by Figure 4.5, it reveals that the oil-water mixtures those contain Exxsol D60 separates faster than that of Bayol 35.

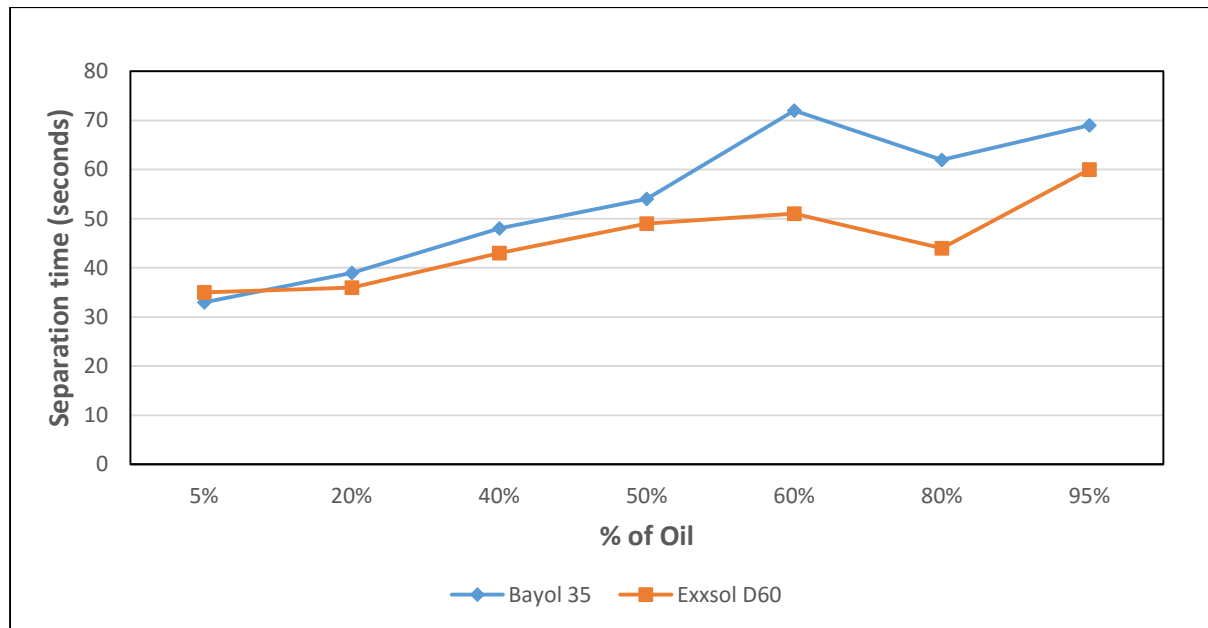


Figure 4.5 Comparison of separation time between mineral oil samples prepared at mixing speed 1600 rpm and mixing time 5 mins.

4.2.2.2 Effect of mixing time on separation

Figure 4.6 and Figure 4.7 shows the effect of mixing times for Bayol 35 and Exxsol D60 at the mixing speed of 400 rpm. It can be seen that longer the mixing time, more stable the oil-water mixtures/emulsions and thus longer separation time. Similar trend was shown for the other mixing speeds of 1000 rpm and 1600 rpm. Exxsol D60 behaved in the same way as Bayol 35 as shown in the appendix A. Mixing for longer time transfers more energy to the oil-water break up process and this can lead to further breakup of bigger droplets in to tiny droplets. When the droplet size gets smaller, the Laplace pressure drop of the droplets ΔP is higher. Laplace pressure is the pressure difference in and out of the droplet and this is shown by equation 4.1 (Tadros, 2013). Here, γ is interfacial tension and r is the radius of the droplet.

$$\Delta P = \frac{\gamma}{2r} \quad (4.1)$$

Interfacial tension does not change unless the droplet sizes are in few microns. Therefore, higher Laplace pressure drop means, higher stress or inertia is required to deform the droplets. Therefore, we can say that the higher energy transferring leads to much smaller droplets and much smaller droplets leads to more stable emulsions, thus longer the separation time.

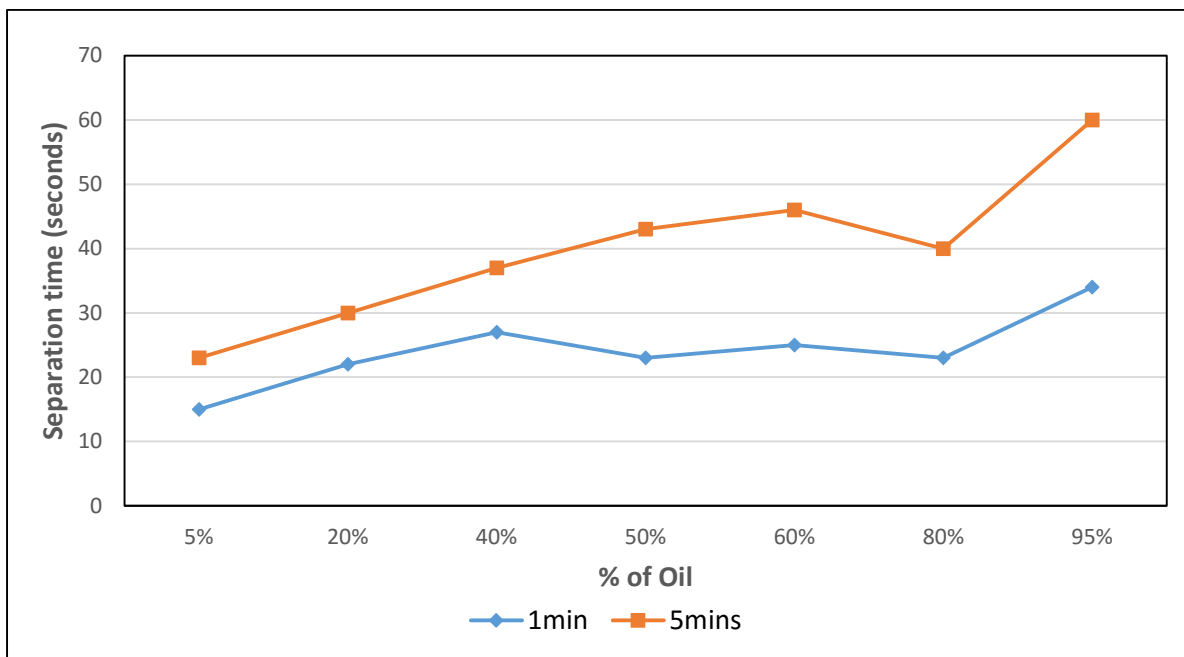


Figure 4.6 Comparison of oil-water mixtures prepared of Bayol 35 with stirring speed at 400 rpm.

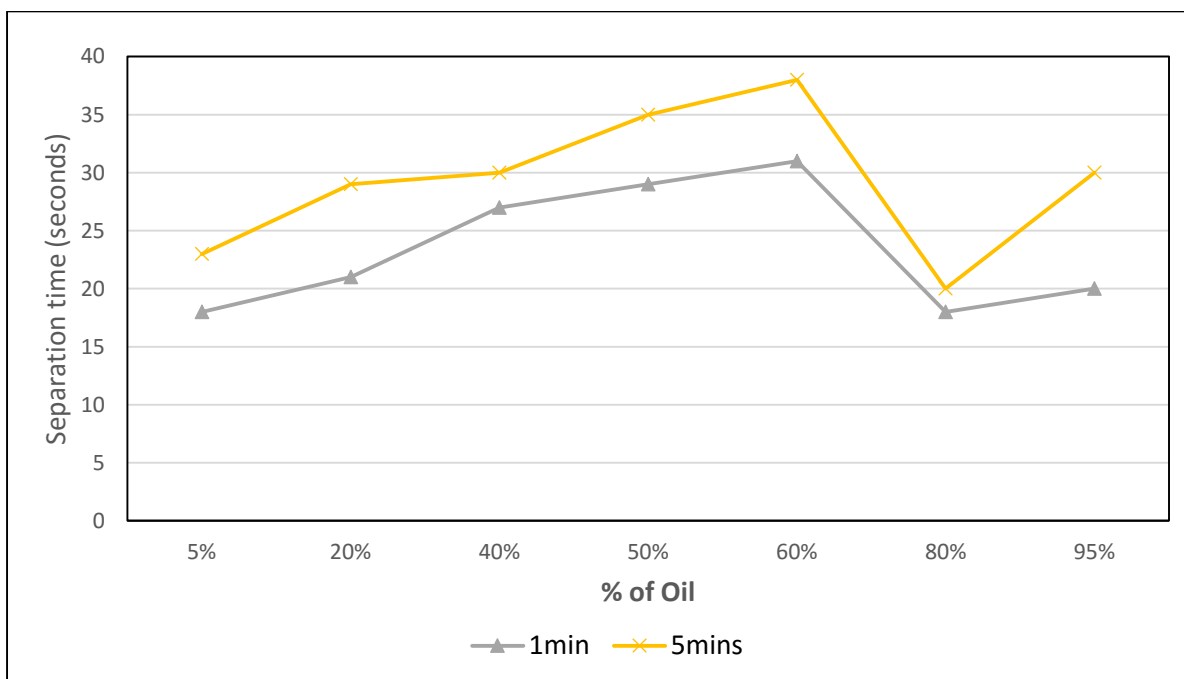


Figure 4.7 Comparison of oil-water mixtures prepared of Exxsol D60 with stirring speed at 400 rpm.

4.2.2.3 Effect of stirring speeds on separation

Figure 4.8 and Figure 4.9 shows the effect of three different stirring speeds for Bayol 35 and Exxsol D60 with the mixing time of 1 minute. It has seen that higher the mixing rate, higher

the separation time which means much stable oil-water mixtures/emulsions. Similar trend was shown for mixing duration of 5 mins as well. Exxsol D60 behaved in the same way as Bayol 35 as shown in the appendix A. Again this phenomenon can be explained with increased energy transferred to the breakup process that can lead to break the droplets in too much tiny droplets which leads to more stable emulsions.

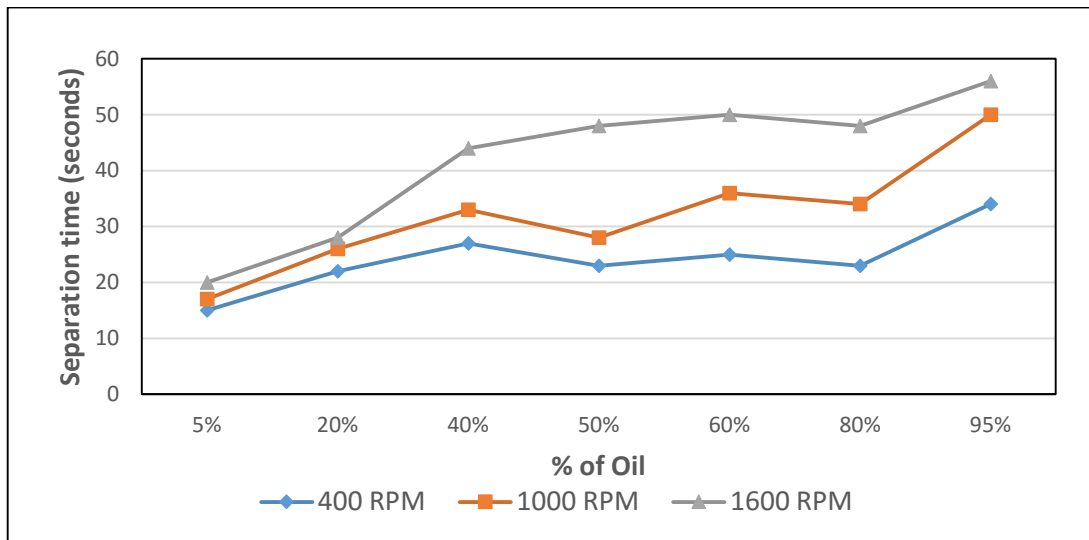


Figure 4.8 Comparison of three different stirring speeds of Bayol 35 with mixing time for 1 minute.

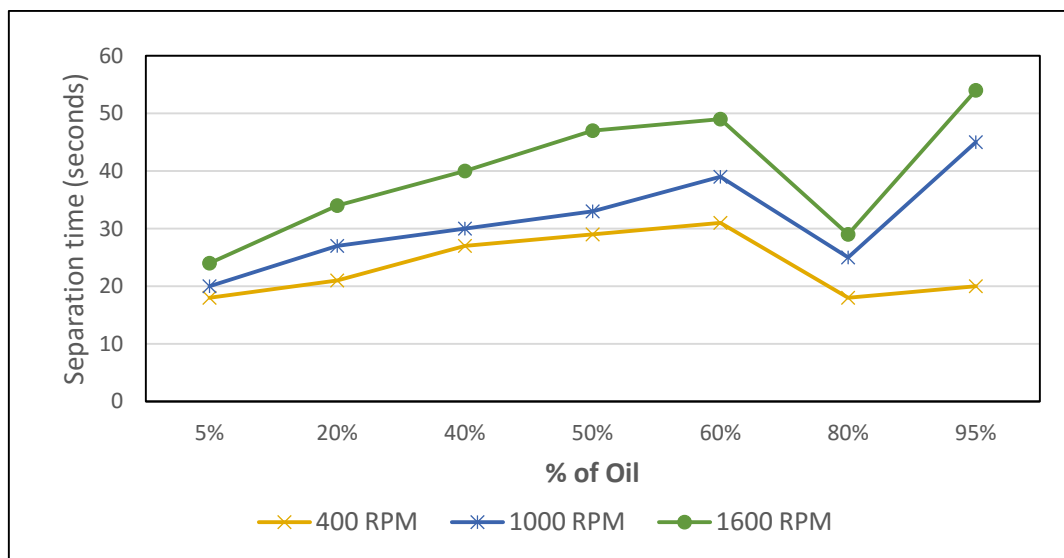


Figure 4.9 Comparison of three different stirring speeds of exxsol D60 with mixing time for 1 minute.

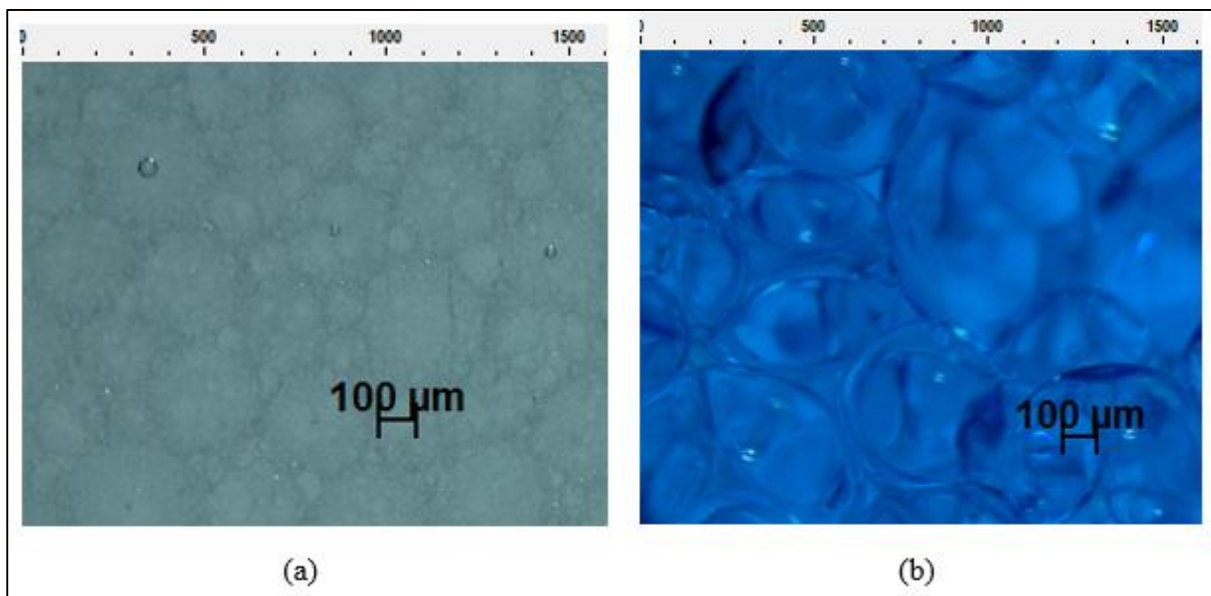
4.3 Microscopy

Microscopic studies were conducted on some chosen samples, S1, S2, S3, S4 and S5, using the optical microscope described in section 3.4. According to general description of emulsion

preparation by mechanical mixers, dispersed phase present as circular droplets. In our experiments the dispersed phase was present as droplets with a range of droplet sizes rather than droplets of a certain size. It was sometimes challenging to measure these droplet sizes due to coalesce or breaking of droplets during sampling limited image resolution of the microscope (Some of the droplets in samples mixed such as S6 and S7 is difficult to see in a regular microscope.) and difficulties arises in phase identification. On the other hand, the water droplets in oil phase can be seen through the microscope first, and there was a waiting time to image the oil droplets in water until all the water droplets present in oil get disappear.

The sizes of droplets were measured using Axio Vision software. The results indicate the broad range of droplet size distribution rather than a particular size of droplets.

From Figure 4.10 shows the distribution of droplet size for S1-S5 water-oil mixtures/emulsions for Bayol 35 with stirring speed 1600 rpm and mixing for 5 minutes. Sub Figure 4.10 (a) shows the oil in water emulsion which contains much tiny oil droplets. Rest of the sub figures show the water droplets in oil phase which can be first seen through the microscope, since S2-S5 samples always resulted with water droplets in oil phase and oil droplets in water phase separated with a clear interface. The range of droplet sizes is vast; it varies from 380 μm to 2400 μm . S5 (40% of water) has biggest droplet sizes (2400 μm) and faster separation times the rest of the samples. Exxsol D60 behaved in the same way, as show in appendix B.



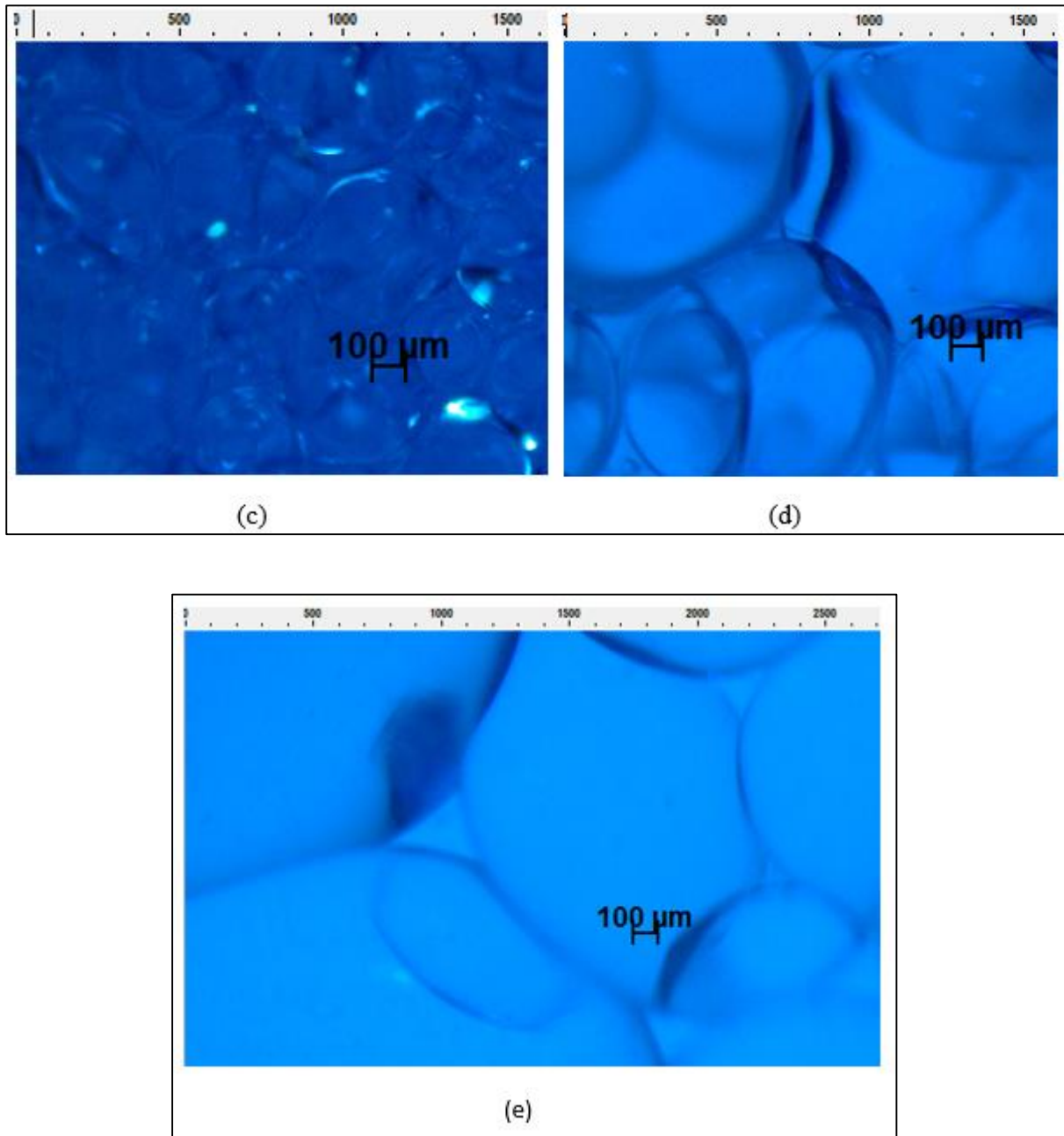


Figure 4.10 Microscope images for water-Bayol 35 mixtures with stirring speed 1600 rpm, mixing for 5 minutes. (a) S1,95% of water cut (b) S2,80% of water cut (c) S3,60% of water cut (d)S4,50% of water cut (e) S5,40% of water cut.

4.3.1 Droplet sizes

In chapter 2, it was reported that the phase ratio persuaded the droplet size distribution. As the ratio changes, the viscosity is also altered and affects the stability, thus effects the droplet size distribution. Table 4.5 shows the distribution of maximum of droplet sizes for S1-S5 w-o mixtures with stirring speed 400 rpm and mixing for 1 minute. All these droplet sizes

mentioned in the table are water droplets in oil phase which can be seen through microscope at first except for sample S1. It can be seen that highest percentage of water containing sample S1, which eventually forms an oil in water emulsion has smaller droplets size. Exxsol D60 oil-water mixtures resulted with smaller droplet sizes and less number of droplets and separated faster compared to Bayol 35. But according to the logic, Bayol 35 oil-water mixtures should separate faster since it gave much bigger droplets in the oil water mixture. But the reason for the observation can be due to the effect of surrounding oil viscosity over the effect of droplet size. Exxsol D60 has lower viscosity than the Bayol 35 and when the viscosity of the continuous phase increased the emulsion stability is higher. On the other hand, the droplet sizes don't change significantly between the two oil containing mixtures, so that the effect of droplet sizes becomes negligible when it comes to the effect of viscosity of the continuous phase.

Table 4.5 The droplet size distribution for S1-S5 w-o mixtures measurement.

Sample code	% of Water : % of Oil proportion	Bayol 35	Exxsol D60
		Max Droplet size (μm)	Max Droplet size (μm)
S1	95 : 5	75	68
S2	80 : 20	77	70
S3	60 : 40	82	77
S4	50 : 50	88	82
S5	40 : 60	145	91

All measures of droplet size are based on taken picture of emulsion structure with dimensions 2560*1920 pixels. Scale factor X: 1.69 micrometer/pixel and scale factor Y: 1.69 micrometer /pixel and the scale factor Z: 1 pixel/pixel. The maximum sizes were measured by AxioVission AC software with that approximation.

4.3.2 Separation Phenomena

Figure 4.11 shows the microscopic image of intermediate mixing layer which contains water droplets in oil phase.

Sample 3 (60-40% water-oil) at T= 0 min

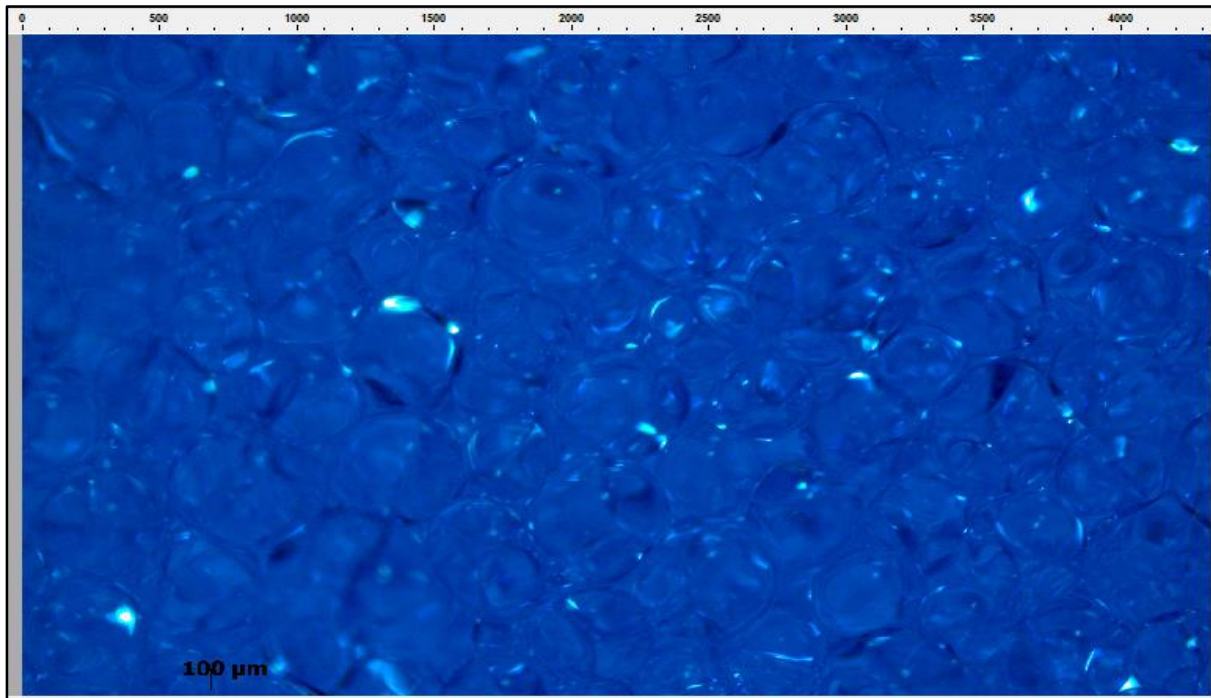


Figure 4.11 Microscope view of S3 (60-40 % w-o) at T = 0 minute.

Figure 4.12 show that droplet size becomes bigger in time due to droplet flocculation and coalescence.

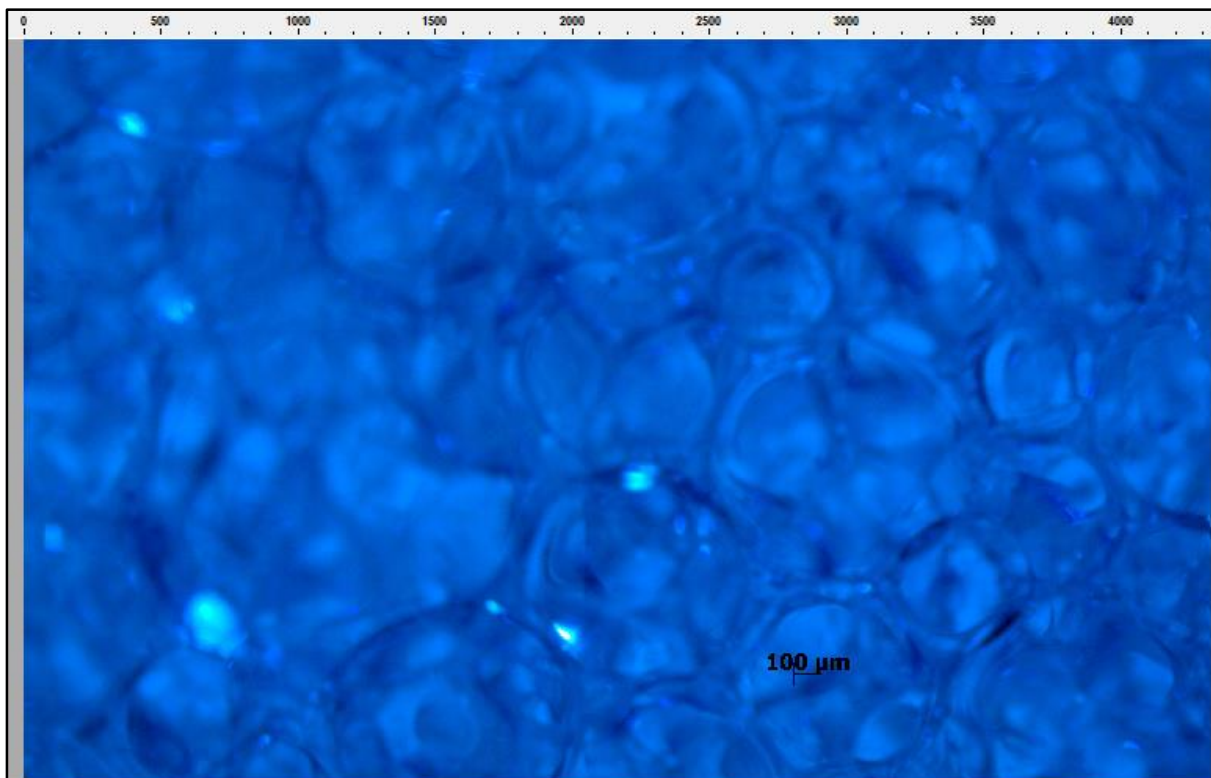


Figure 4.12 Microscope view of S3 (60-40 % w-o) at T = 1 minute.

Figure 4.13 shows that droplets become even bigger & the entrapped tiny oil droplets within the larger droplets.

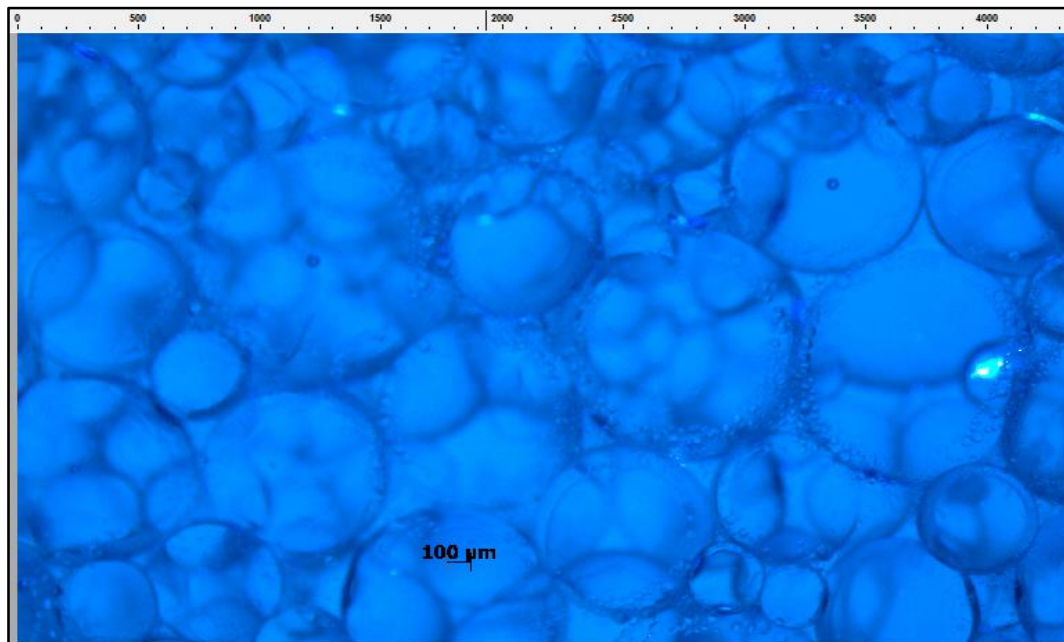


Figure 4.13 Microscope view of S3 (60-40 % w-o) at T = 2 minutes.

When the droplet size is bigger than a certain size, they can no longer maintain their round shape & break-off, this phenomenon can be seen in Figure 4.14.

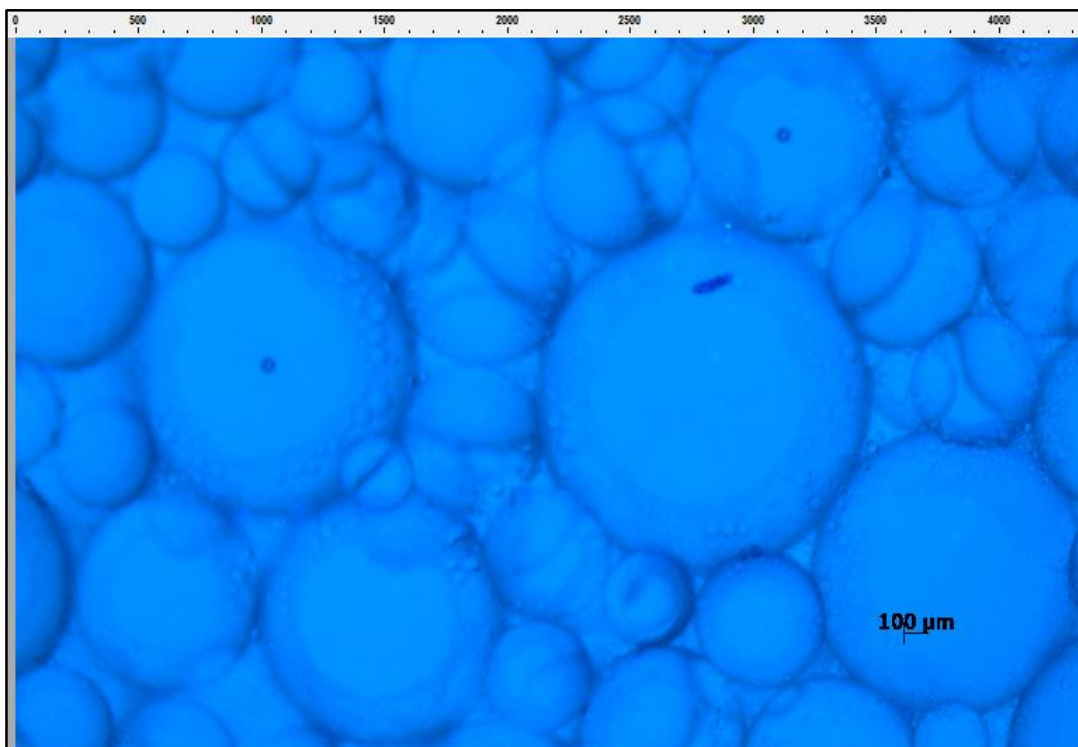


Figure 4.14 Microscope view of S3 (60-40 % w-o) at T = 5 minutes.

Figure 4.15 shows that after 30 minutes most of the water droplet separation is completed and the oil droplets in the water phase can be seen through. They follow the same method of separation until the complete separation occurs.

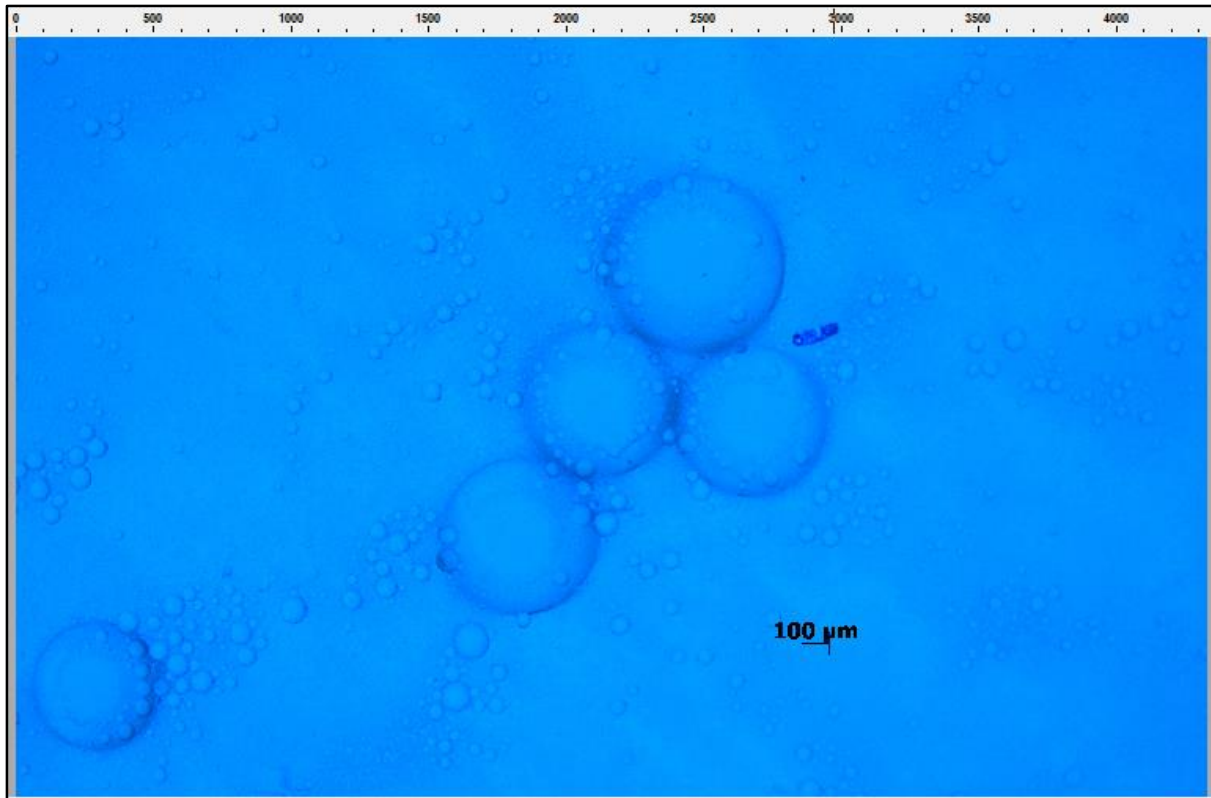
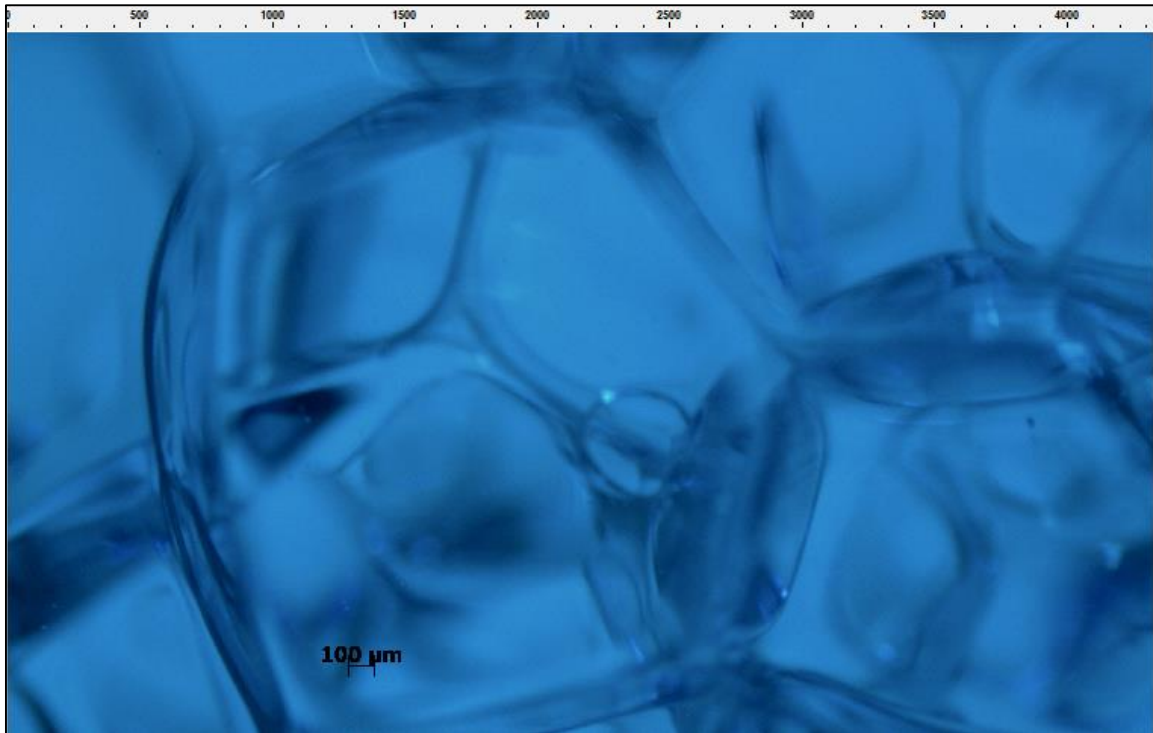


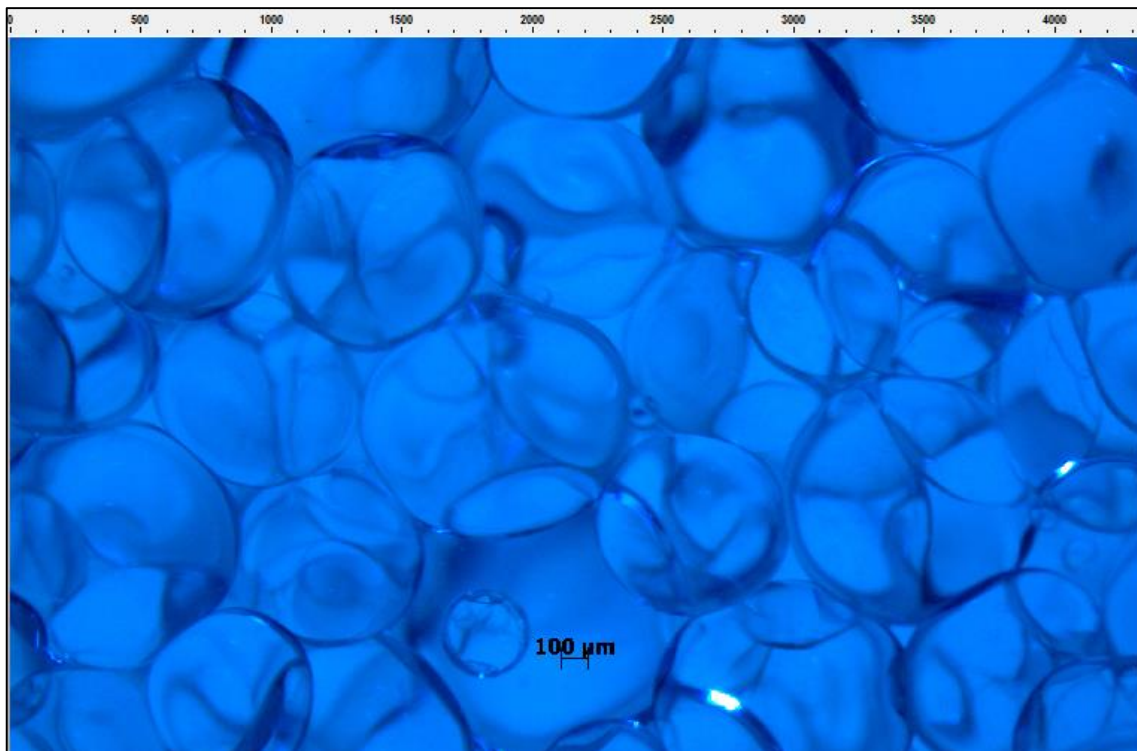
Figure 4.15 Microscope view of S3 (60-40 % w-o) at T = 30 minutes.

4.3.3 Effect of stirring speed

The oil and water phases of sample S4 (50-50 % water-oil Bayol 35) were mixed at two different speeds of 1000 and 1600 RPM. Figure 4.16 (a) and (b) below, shows the microscopic image of droplets sizes for the water droplets in oil for oil- water mixtures prepared at these two speeds. It can be observed and confirm that at 1600 RPM the droplet size is smaller than that of at 1000 RPM for both oil types, Exxsol D60 and Bayol 35. It is well seen that the increase in agitation speed leads to decrease in droplet sizes. The fall in sizes of droplets from 550 μm to droplet size smaller than 80 μm is observed. Exxsol D60 behaved in the same way, see in appendix B.



a) 1000 rpm after mixing at $t= 0$ min

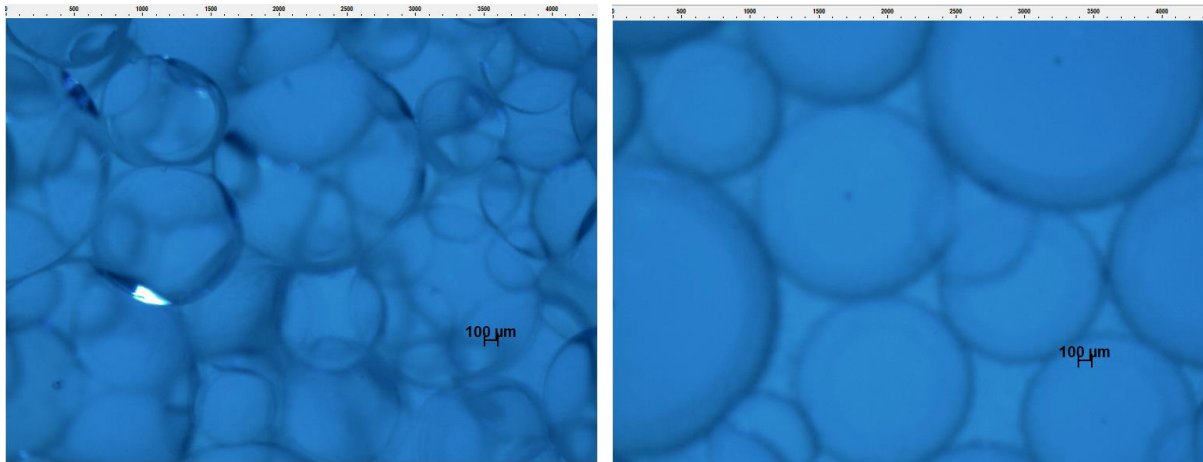


b) 1600 rpm after mixing at $t= 0$ min

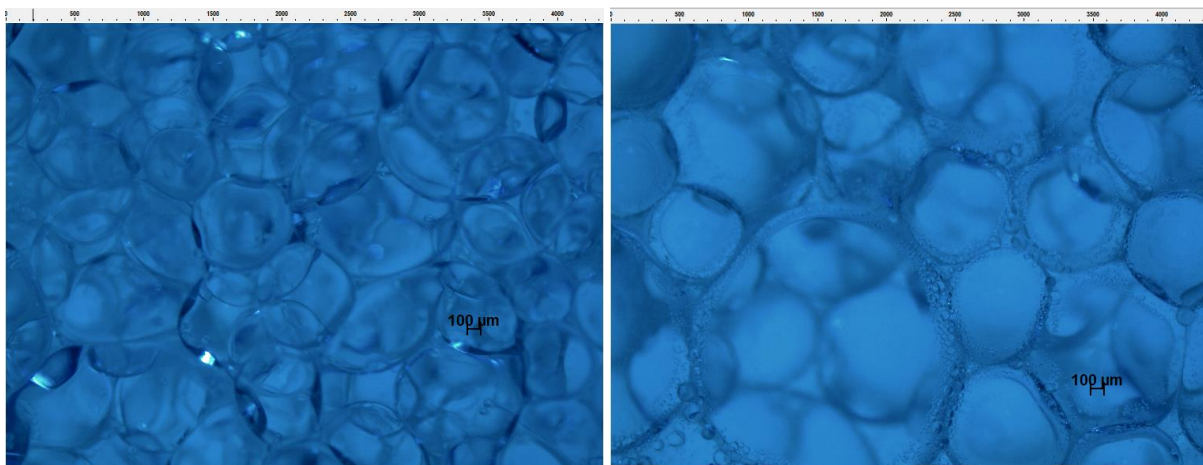
Figure 4.16 Droplet size distribution at (a) and (b) 50-50 % water-oil mixture of Bayol 35 mixing for 5 mins.

4.3.4 Effect of mixing times

Figure 4.17 shows the distribution of S3 (60-40% w-o mixtures/emulsions) of Bayol 35. After examining the mixture under microscopy, we can observe that longer the mixing time, smaller will be the size of droplets. Exxsol D60 behaved in the same way.



a) 1000 rpm, mixing for 1 minute after mixing at t=0 (Left) and t=1 min (Right)



a) 1000 rpm, mixing 5 minutes after mixing at t=0 (Left) and t=1 min (Right)

Figure 4.17 Droplet size distribution at (a) and (b) 60-40 % w-o mixture of Bayol 35

4.4 Rheology

4.4.1 Viscosity test

Viscosity measurements were done using two methods as described in section 3.4 in chapter 3.

Note: Mixing of oil and water samples is done in Silverson L4RT-A mixer. Representative samples from the oil-water mixture were fed in to the viscosity meter measuring cell as 20 ml for method 1 and 15 ml for method 2. The measured quantity of the sample is the amount transferred to the Rheometer. This process can cause some delay and separation of the oil-water mixtures which might induce an error into the final results of viscosity measurements.

Method 1

The following results show the measurement done in the laboratory using Rotational Digital Rheometer Model Anton Paar MCR 302.

Figure 4.18 shows that the viscosity is a constant, so water showed Newtonian behaviour. Adding uranine did not effect on viscosity (viscosity is approximately equal to 1mPa.s).

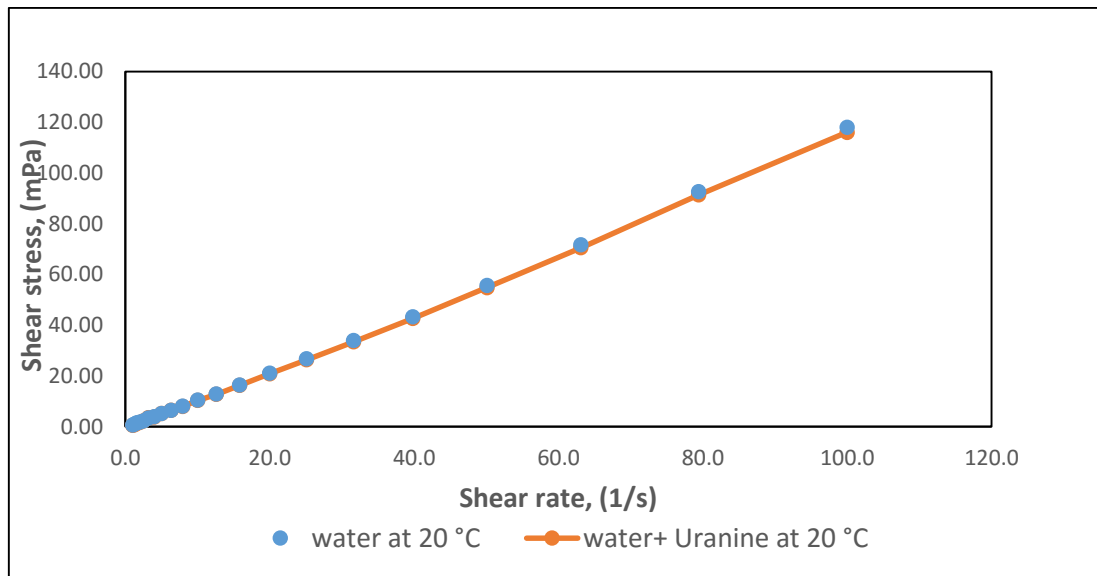
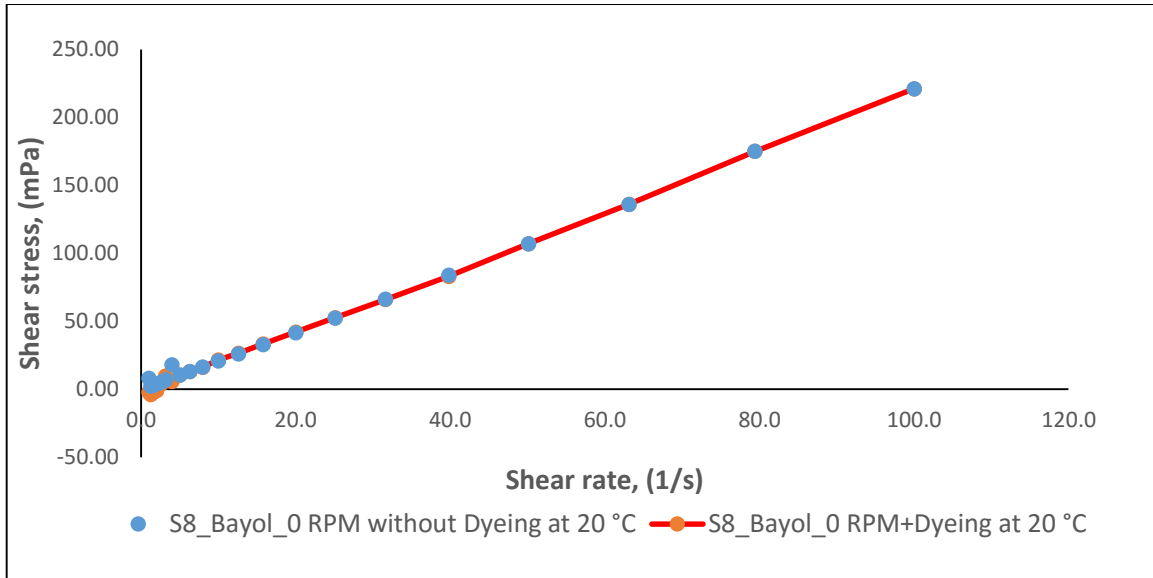


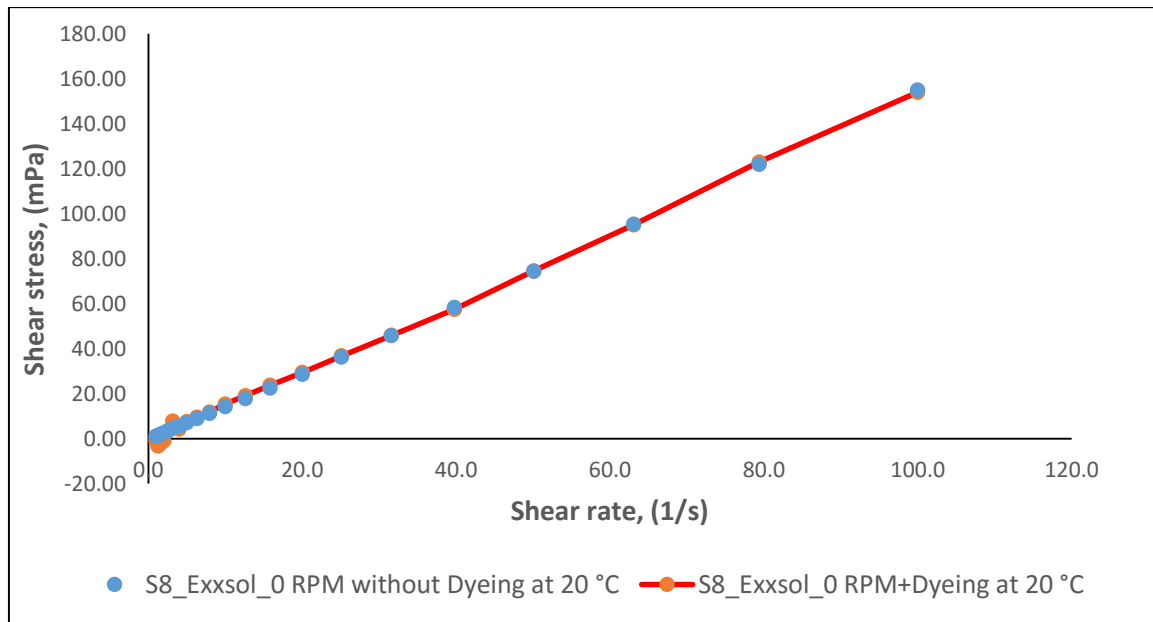
Figure 4.18 Viscosity measurement of water.

Figure 4.19 (a) and 4.20(b) show that viscosity is a constant, for both Bayol 35 & Exxsol D60 and they show Newtonian behaviour. Adding Sudan blue to the oil phase did not affect the viscosity.

Average viscosity of Bayol 35 = 2.40 mPa.s and Exxsol D60 = 1.52 mPa.s.



(a)



(b)

Figure 4.19 Viscosity measurement of Bayol 35 (a) and Exxsol D60 (b).

Figure 4.20 & Figure 4.21 show viscosity measurement of oil-water mixtures with different phase ratio under mixing conditions as below:

- Oil - Bayol 35 (Figure 4.20) and Exxsol D60 (Figure 4.21)
- Speed = 1600 rpm for 5 mins.
- T = 20 °C.

- Oil phase coloured with Sudan blue.

Figure 4.20 & Figure 4.21 show that oil-water mixtures are Non-Newtonian and do not have fixed viscosity. From Figure 4.20, sample S1, S3, S5, S6 and S7 show shear thickening behaviour and Figure 4.21 show that sample S1, S5 and S7 indicate shear thickening behaviour.

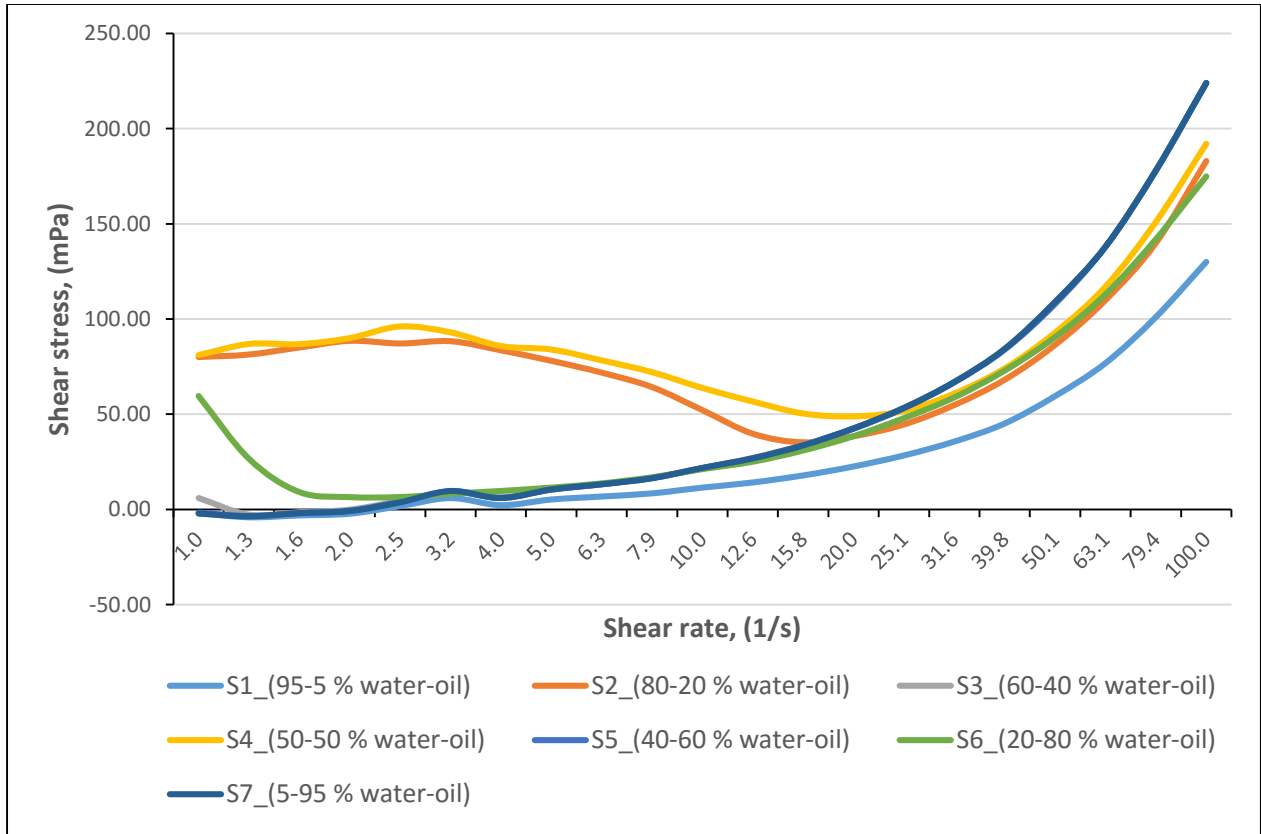


Figure 4.20 The behavior of oil-water mixtures for Bayol 35 at different phase ratio.

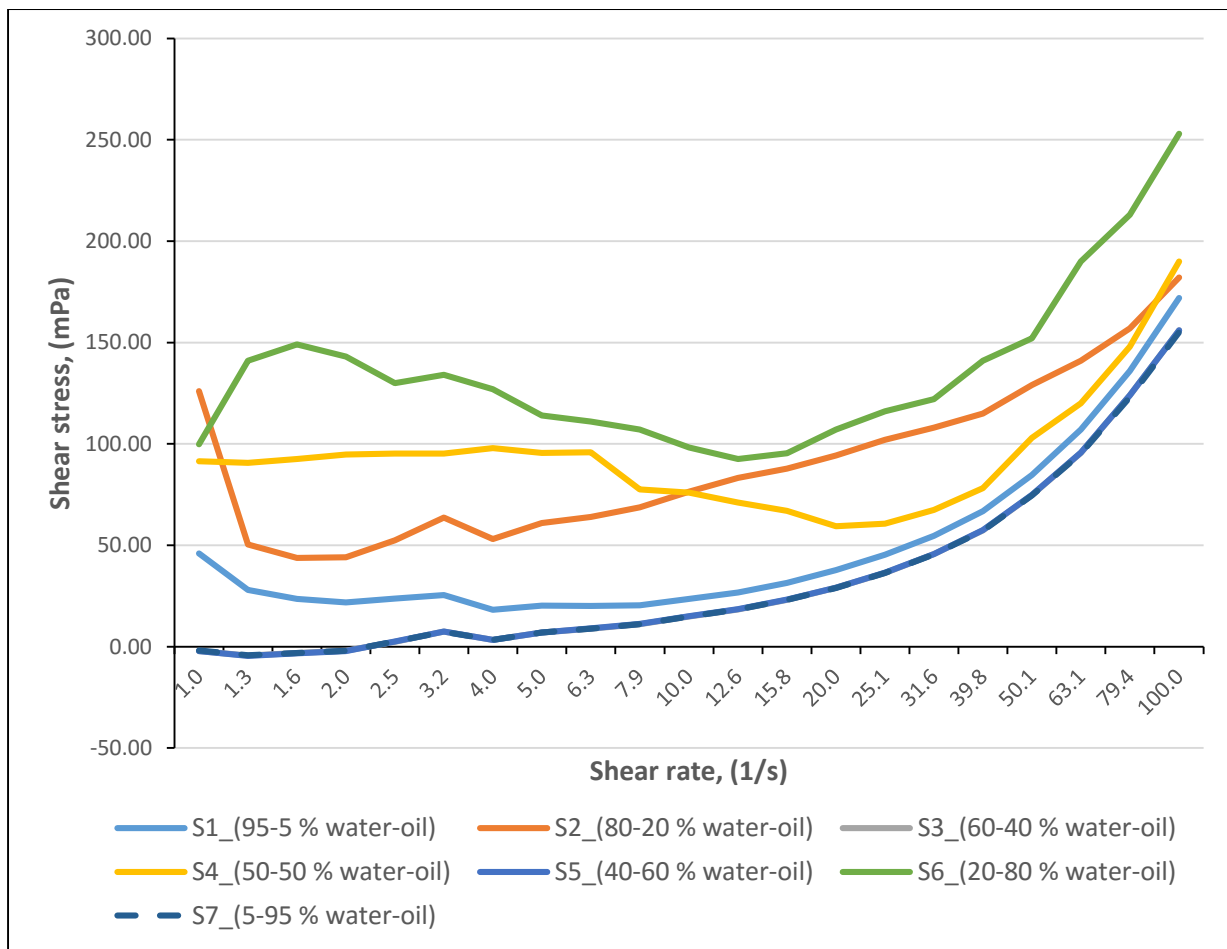


Figure 4.21 The behavior of oil-water mixtures for Exxsol D60 at different phase ratio.

4.4.3 Effects of stirring speed on viscosity

The effects of stirring speed were examined through plot graph of viscosity versus varied stirring process from 1000 and 1600 rpm under mixing conditions $T = 20\text{ }^{\circ}\text{C}$ and oil phase coloured with Sudan blue. For each stirring speed condition, the droplet size distribution is determined by microscope associated to an image analysis. From Figure 4.22 (a) and (b) show that higher the stirring speed, higher the viscosity. And similar trend was shown for Bayol 35 as show in the appendix C.

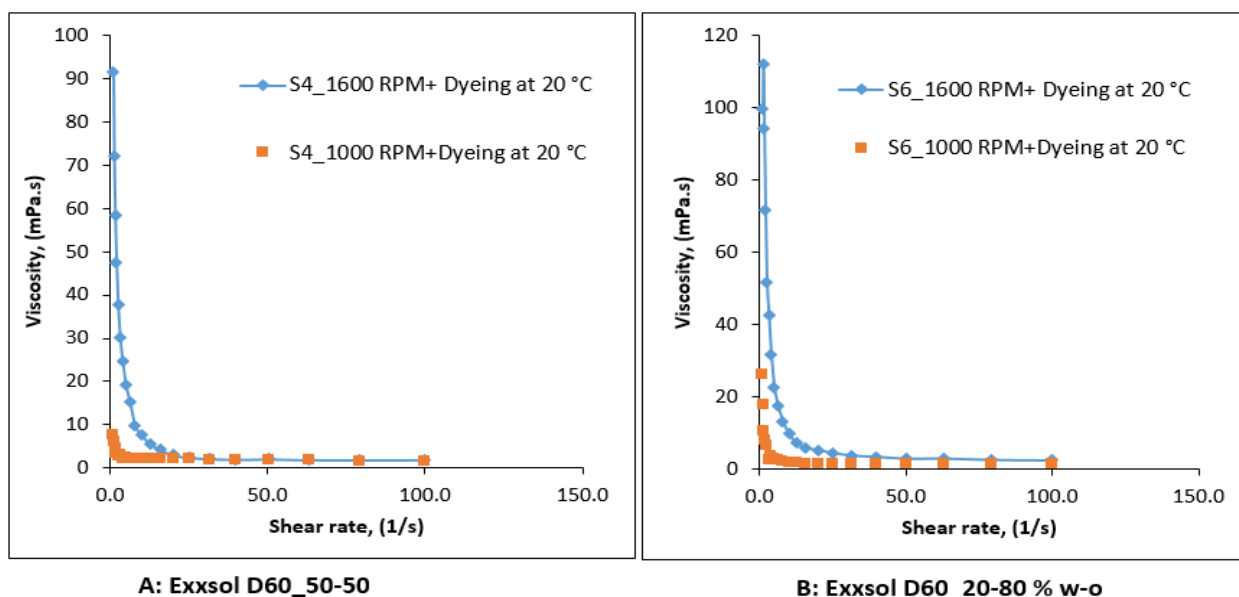


Figure 4.22 Comparison of viscosity for samples containing Exxsol D60 with different stirring speeds, (a) Exxsol D60 (50-50% w-o) and (b) Exxsol D60 (20-80% w-o).

4.4.4 Effects of Temperature on viscosity

The effects of temperature for oil-water mixtures/emulsions also had been studied. Temperature changes usually cause changes in the emulsion stability whether invert the emulsion or may break the emulsion.

When temperature was increased, the flow molecules through the interfaces also increased resulting in a decrease in emulsion stability. The flow molecules correlated with viscosity. The increasing temperature results in decreasing the viscosity. The viscosity is very sensitive to temperature hence; the increment temperature caused reduction of emulsion viscosity. Figure 4.23 (a) and (b) demonstrated that both phase ratios show the decreasing of viscosity as increasing temperature. Similar trend was shown for Exxsol D60.

- **Mixing conditions:**
 - Speed = 1600 rpm,
 - Water-oil (Bayol 35) = 50-50 % and 20-80 %.
 - Oil phase coloured with Sudan blue.

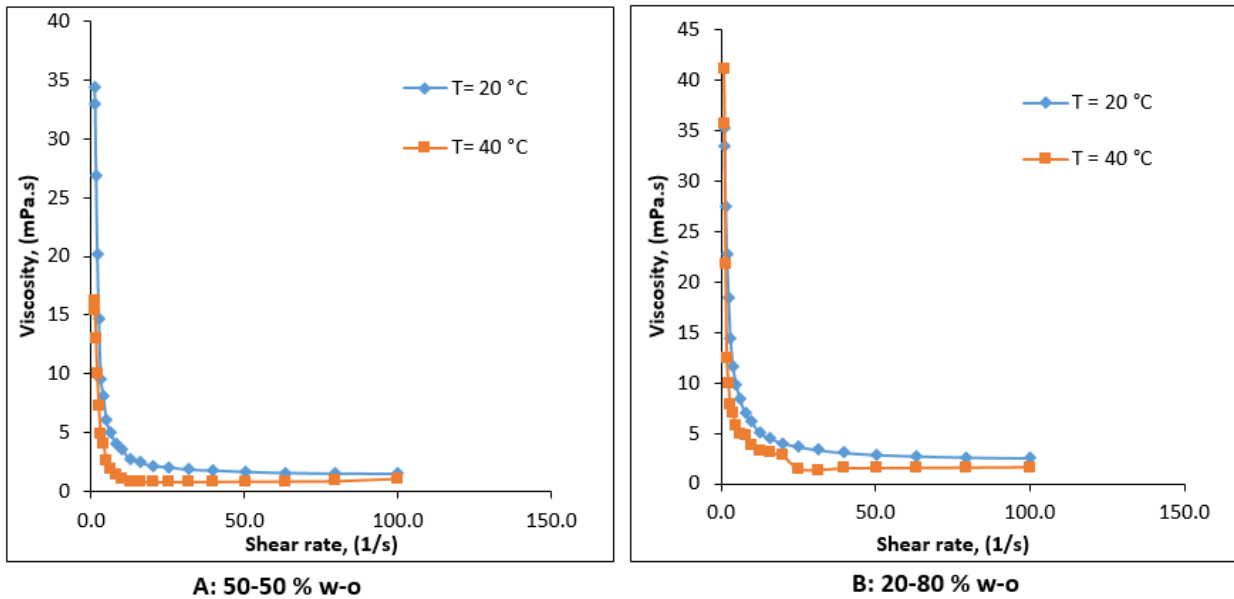


Figure 4.23 (a) Effects of viscosity at varied temperature in 50-50 % w-o and (b) 20-80 % w-o

Method 2

This method uses Rotational Digital Rheometer Model C-LTD 70/PIV for shear stress vs shear rate and viscosity measurements. As mentioned earlier in section 3.4, this method is used to compare the results with method 1 as it is more convenient to observe the fluid phases through naked eye.

Figure 4.24 compares the shear rate vs shear stress profile for two oil samples Bayol 35 and Exxsol D60 in the presence of dye. It can be seen from the plot that both the samples have fairly straight/linear profile and thus, Newtonian type fluid behaviour.

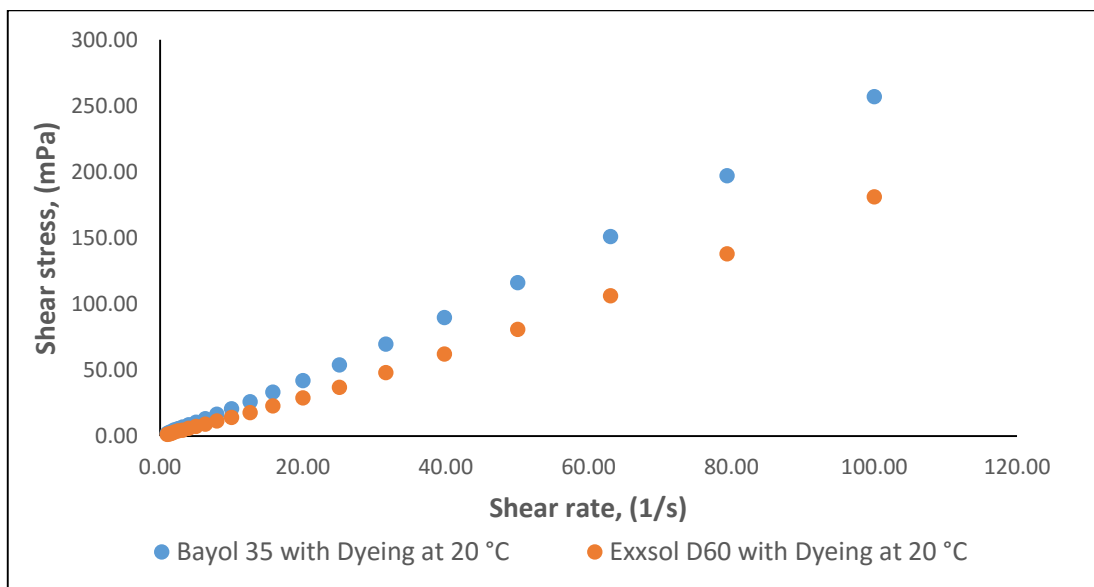


Figure 4.24 Shear rate vs shear stress for oil samples with dye at room temperature.

Figure 4.25 shows a similar behaviour (linear profile) for high viscous Marcol 82 oil sample as in case of Bayol 35 and Exxsol D60 and hence we can say that this fluid sample exhibit Newtonian behaviour.

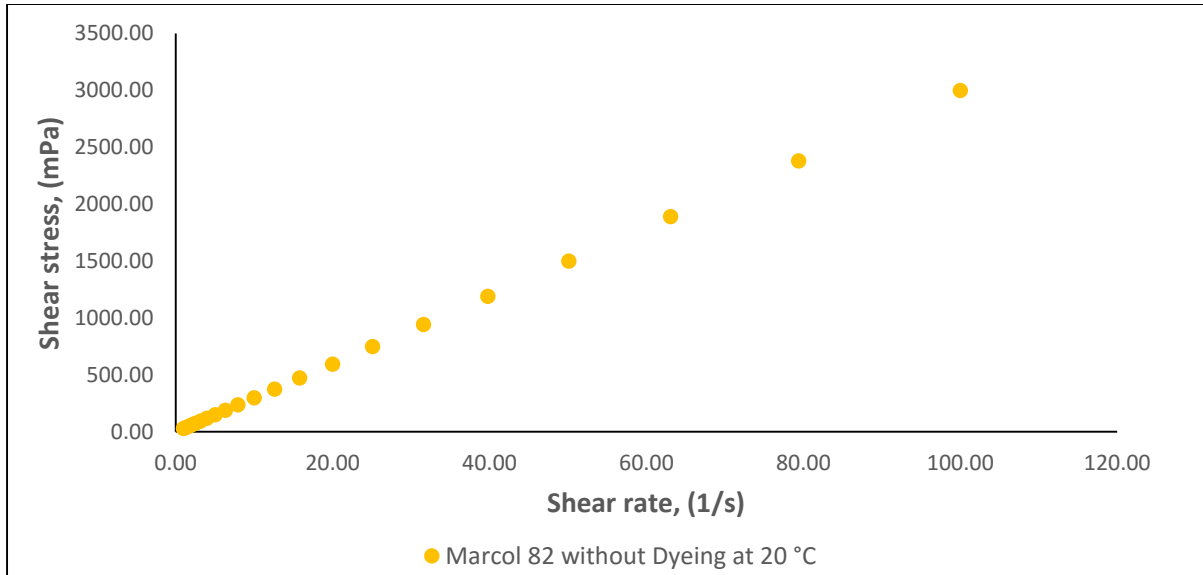


Figure 4.25 Shear rate vs shear stress for high viscous Marcol 82 at room temperature.

4.5 Surface and interfacial tension

Surface tension is a measure of the force acting at a boundary between two phases. If these forces are between two immiscible liquids, like oil and water, they are referred to as interfacial tension. The surface and interfacial tensions are important because they are indicative of the ease of formation and stability of emulsions and foams, that is, they indicate the relative interfacial properties of a crude oil sample. Interfacial tension provides information pertaining to the presence and concentration of surface-active agents. These compounds play an important role in the performance of emulsion systems.

The results and the calculated corrected values from the tensiometer are presented in Table 4.6 and Table 4.7. The surface tension for both Bayol 35 and Exxsol D60 solutions are lower than water. However, the interfacial tension between oil-water mixtures is higher than pure oil Bayol 35 and pure oil Exxsol D60.

Table 4.6 Preparation of oil-water mixtures.

Liquids	% of Water	% of Oil	Volume of Water	Volume of Oil
	(%)	(%)	(ml)	(ml)
Water	100	-	100	-
Oil (B)/W	60	40	60	40
Oil (E)/W	60	40	60	40
W/Oil (B) + Dyeing	60	40	60	40
W/Oil (E) + Dyeing	60	40	60	40
Oil (Bayol 35), O(B)	-	100	-	100
Oil (Exxsol D60), O(E)	-	100	-	100

Table 4.7 Typical surface and interface tensions of liquids at 20 °C.

Details	Water	Oil	Oil	Oil (B)	Oil (E)	W/Oil (B)	W/Oil (E)	W/Oil (B)	W/Oil (E)
		Bayol 35 ,O(B)	Exxsol D60, O(E)	+ Dyeing	+ Dyeing			+ Dyeing	+ Dyeing
	(mN/m)	(mN/m)	(mN/m)	(mN/m)	(mN/m)	(mN/m)	(mN/m)	(mN/m)	(mN/m)
Correction Factor, F	0.9939	0.9467	0.9466	0.9467	0.9467	0.9480	0.9647	0.9516	0.9649
Calibration Factor, K	1.0232	1.0232	1.0232	1.0232	1.0232	1.0232	1.0232	1.0232	1.0232
Read Value	71.10	24.70	24.80	24.70	24.90	31.60	43.10	34.20	43.30
Correction value	72.31	23.93	24.02	23.93	24.12	30.65	42.54	33.30	42.75

4.5.1 Effect of phase Ratios

The effect of varied phase ratio on surface and interface tensions is shown Table 4.9 and Figure 4.26 of W/O of oil Bayol 35 and w-o of oil Exxsol D60. As examined the results, mixtures prepared with Exxsol D60 have higher interfacial tension in comparison to Bayol 35 mixtures. Pure Exxsol D60 and Bayol 35 have same surface tension. Higher the percentage of oil, lower the interfacial tension.

Table 4.8 Preparation of oil-water mixtures.

Liquids	% of Water	% of Oil	Volume of Water	Volume of Oil
	(%)	(%)	(ml)	(ml)
Water	100	-	100	-
S1	95	5	95	5
S2	80	20	80	20
S3	60	40	60	40
S4	50	50	50	50
Oil (Bayol 35), O(B)	-	100	-	100
Oil (Exxsol D60), O(E)	-	100	-	100

Table 4.9 Typical surface and interface tensions of various liquid mixtures at 20 °C.

Details	Water	O(B)	O(E)	S1		S2		S3		S4	
				W-O(B)	W-O(E)	W-O(B)	W-O(E)	W-O(B)	W-O(E)	W-O(B)	W-O(E)
				(mN/m)	(mN/m)	(mN/m)	(mN/m)	(mN/m)	(mN/m)	(mN/m)	(mN/m)
Correction Factor, F	0.9939	0.9467	0.9466	0.9818	0.9893	0.9620	0.9835	0.9480	0.9647	0.9433	0.9646
Calibration Factor, K	1.0232	1.0232	1.0232	1.0232	1.0232	1.0232	1.0232	1.0232	1.0232	1.0232	1.0232
Read Value	71.1	24.7	24.8	59.9	66.8	42.5	59.6	31.6	43.1	25.8	40.4
Correction value	72.31	23.93	24.02	60.17	67.62	41.83	59.98	30.65	42.54	24.90	39.87

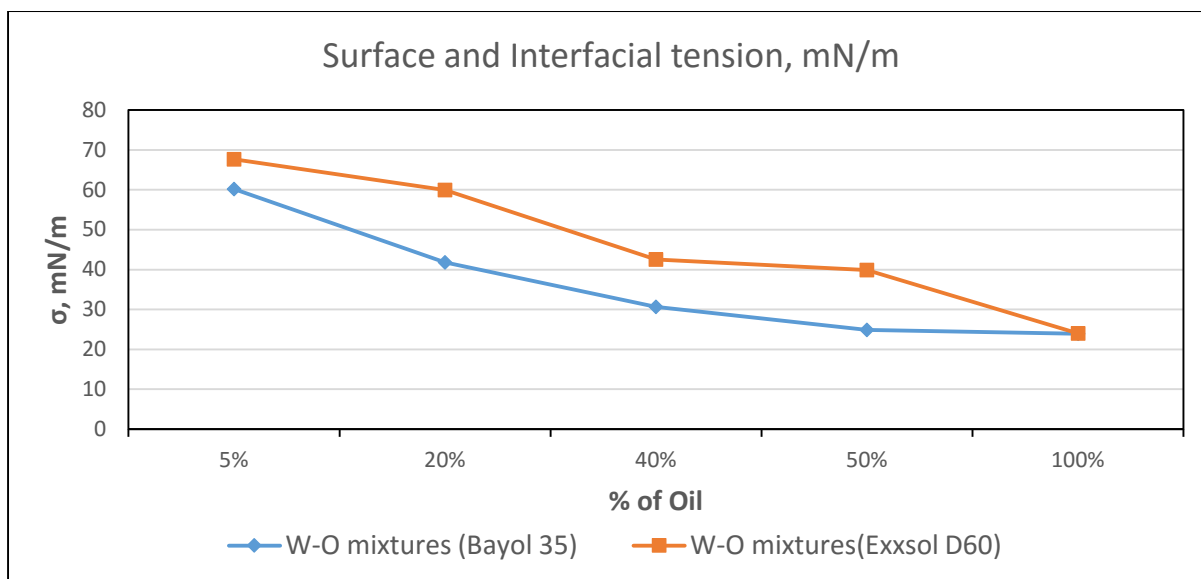


Figure 4.26 Surface and interface tensions measurements for varying volume fraction of oil at 20 °C.

4.6 Density

From Table 4.10, Table 4.11 and Figure 4.27 it shows that the density of oil-water mixtures prepared with Bayol 35 & Exxsol D60 has not varied considerably. But higher the % of oil, lower the mixture density.

Note: Mixing of oil and water samples was done using in Silversan L4RT-A mixer. Then the representative samples 2 ml were collected from the resulted oil-water mixtures and transferred to the densitometer. Possibilities can be that these samples might not accurately represent the oil-water mixture composition due to ongoing separation or errors occur due to sampling procedure. These errors might be the reason for why we do not see the expected straight line for the mixture density vs phase fraction in Figure 4.27.

Table 4.10 Preparation of oil-water mixtures.

Liquids	% of Water	% of Oil	Volume of Water	Volume of Oil	Dyeing
	(%)	(%)	(ml)	(ml)	
Water	100	-	200	-	
Water+Dyeing	100	-	200	-	mix with 0.25ml dilute Uranine
S1	95	5	190	10	Sudan blue
S2	80	20	160	40	Sudan blue
S3	60	40	120	80	Sudan blue
S4	50	50	100	100	Sudan blue
S5	40	60	80	120	Sudan blue
S6	20	80	40	160	Sudan blue
S7	5	95	10	190	Sudan blue
Pure Oil	-	100	-	200	Sudan blue

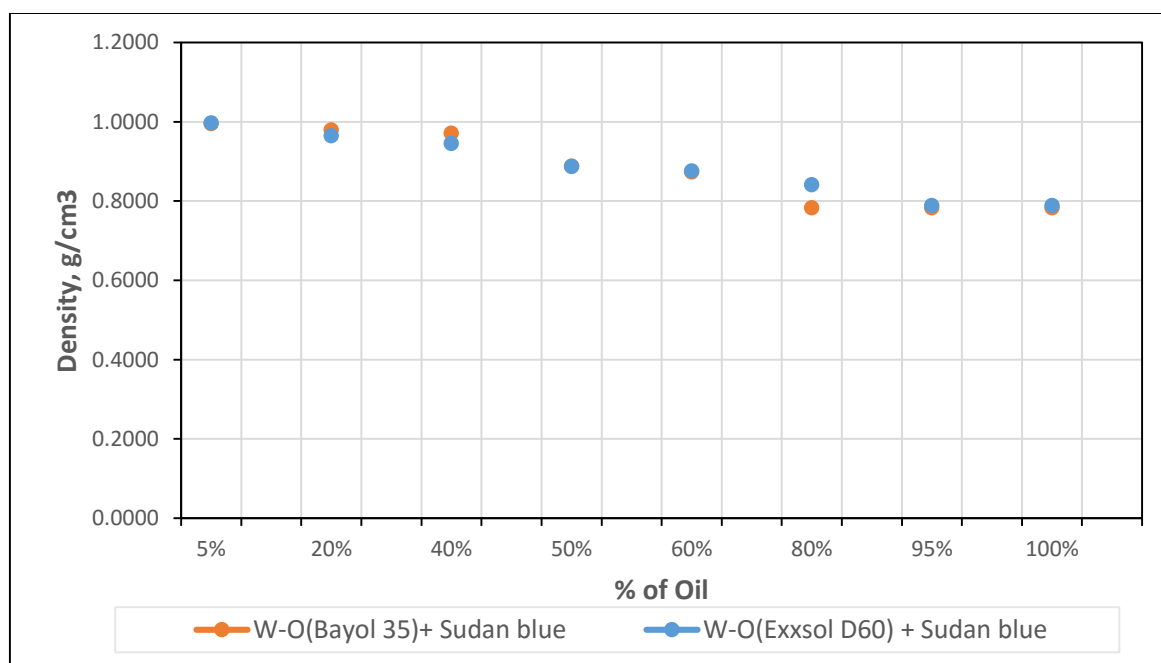


Figure 4.27 Density measurements of two oils.

Table 4.11 The results from the density test.

Liquids	Density (g/cm3)	Specific gravity (SG)	Oil			
			W-O(Bayol 35)+ Sudan blue		W-O(Exxsol D60) + Sudan blue	
			Density (g/cm3)	Specific gravity (SG)	Density (g/cm3)	Specific gravity (SG)
Pure Water	0.9981	0.9999	-	-	-	-
Water+Uranine	0.9933	0.9951	-	-	-	-
S1 ($\lambda_w=95\%$)	-	-	0.9952	0.9970	0.9969	0.9987
S2 ($\lambda_w=80\%$)	-	-	0.9795	0.9813	0.9652	0.9670
S3 ($\lambda_w=60\%$)	-	-	0.9710	0.9728	0.9459	0.9476
S4 ($\lambda_w=50\%$)	-	-	0.8884	0.8899	0.8876	0.8892
S5 ($\lambda_w=40\%$)	-	-	0.8736	0.8751	0.8763	0.8779
S6 ($\lambda_w=20\%$)	-	-	0.7828	0.7842	0.8414	0.8429
S7 ($\lambda_w=5\%$)	-	-	0.7830	0.7844	0.7891	0.7905
Oil Bayol 35+Sudan blue	0.7829	0.7843	-	-	-	-
Oil Exxsol D60+Sudan blue	0.7888	0.7903	-	-	-	-
Pure Bayol 35	0.7829	0.7843	-	-	-	-
Pure Exxsol D60	0.7888	0.7903	-	-	-	-

4.7 Selecting the better phase identification additive

This section presents the results obtained through the procedure described in section 3.7 to select the better additive for phase identification.

Two sets of samples S3 were used, one with Bayol 35 and second with Exxsol D60. Two types of dyeing agents, Sudan Blue and Uranine, were used for both the samples S3. The oil phase was coloured using Sudan Blue for the first set of oil-water samples and the water phase was coloured with Uranine for the second set of oil-water samples. Figure 4.28 shows the Bayol 35 and water mixture where oil phase is coloured with Sudan blue and water phase is coloured with Uranine. Figure 4.29 shows the Exxsol D60 and water mixture where oil phase is coloured

with Sudan blue and water phase is coloured with Uranine. We could observe bigger oil and water droplets in case of Sudan blue added samples compared to Uranine added sample. Also, the separation for Sudan blue added sample was much quicker as couple of tens of seconds while it took longer time (around 1 hour) for the oil and water droplets to separate out when the colouring agent was Uranine. This implies that the colouring agents have had a surfactant effect on the oil water droplets. After doing the interfacial tension calculations it was found that the Sudan blue has increased the interfacial tension and Uranine has decreased the interfacial tension. As a result, the droplets sizes in Uranine added samples were smaller in comparison to the Sudan blue added sample.

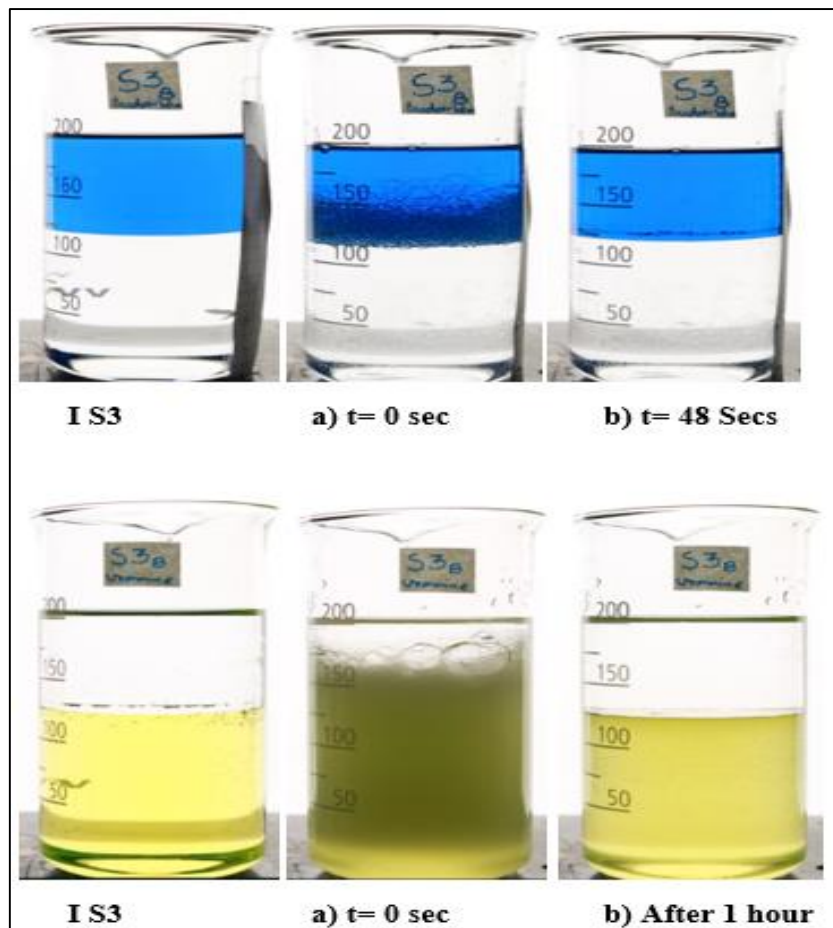


Figure 4.28 Comparing the effect of Sudan blue and Uranine dye in Bayol 35 sample.

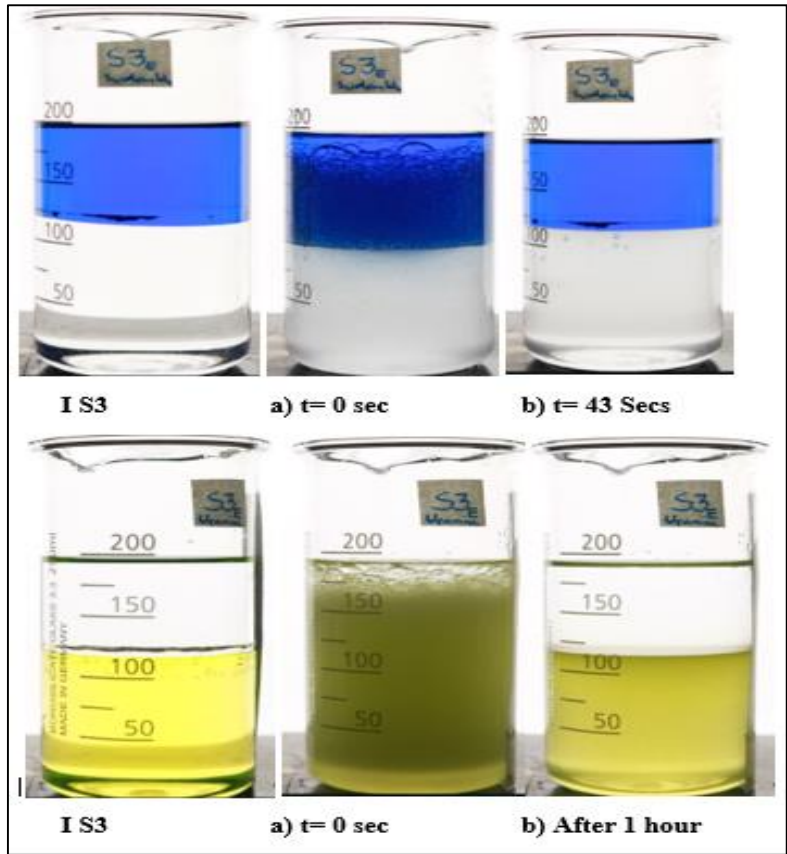


Figure 4.29 Comparing the effect of Sudan blue and Uranine dye in Exxsol D60 sample.

Table 4.12 gives the measured interfacial tension data for sample S3(60-40% w-o) with Sudan blue and Uranine. Both oil samples with Sudan blue gave higher value of interfacial tension than that of oil samples with Uranine as shown in Table 4.12. The formula used to calculate the values is described in chapter 3 section 3.5.1 equation 3.1 and 3.2.

Table 4.12 Surface and interfacial tension for sample 3 with Sudan blue and Uranine

Details	Water	Water + Dyeing	O(B)	O(E)	S3							
					Without Dyeing		With Sudanblue		With 0.5ml Uranine		With 0.25ml Uranine	
					W-O(B)	W-O(E)	W-O(B)	W-O(E)	W-O(B)	W-O(E)	W-O(B)	W-O(E)
					(mN/m)	(mN/m)	(mN/m)	(mN/m)	(mN/m)	(mN/m)	(mN/m)	(mN/m)
Correction Factor, F	0.9939	0.9907	0.9467	0.9466	0.9480	0.9647	0.9516	0.9649	0.9429	0.9552	0.9433	0.9494
Calibration Factor, K	1.0232	1.0232	1.0232	1.0232	1.0232	1.0232	1.0232	1.0232	1.0232	1.0232	1.0232	1.0232
Read Value	71.1	68.1	24.7	24.8	31.60	43.10	34.20	43.30	27.93	35.97	28.23	31.75
Correction value	72.31	69.03	23.93	24.02	30.65	42.54	33.30	42.75	26.95	35.16	27.25	30.84

Figure 4.30 and Figure 4.31 gives the shear stress vs shear rate and viscosity profile for sample S3 with Bayol 35 and Exxsol D60 respectively. In Figure 4.30, the shear rate vs shear stress profile gives us non-Newtonian fluid behaviour. The average viscosity measured for Exxsol D60 with Sudan blue dye is 1.45 mPa.S.

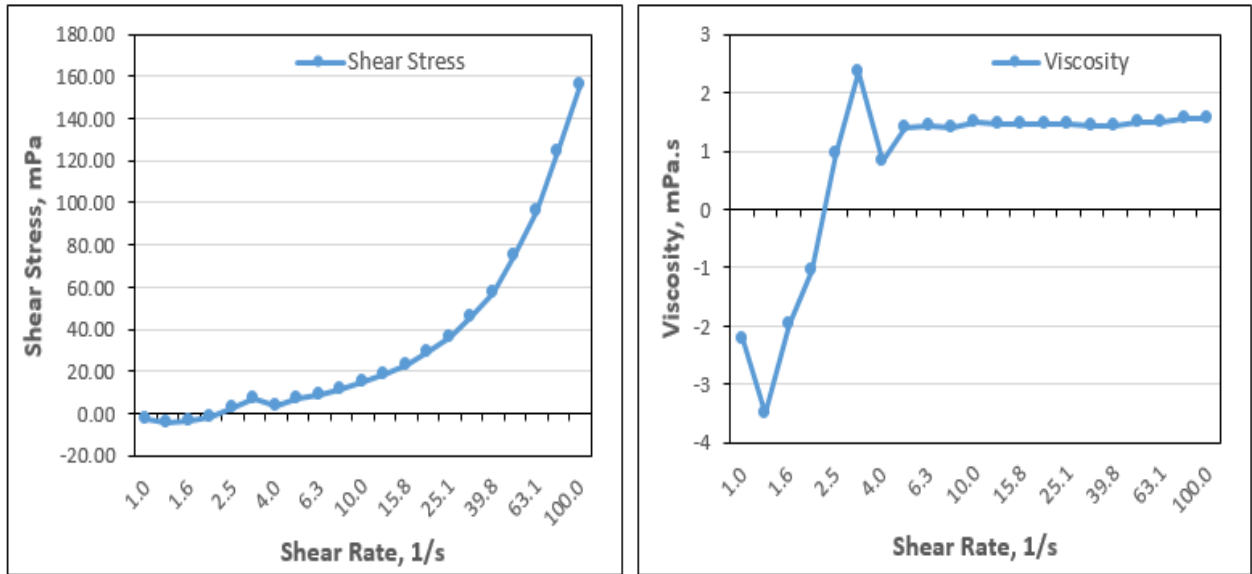


Figure 4.30 Sample 3 (60-40% w-o) with Sudan blue (Exxsol D60)

For Bayol 35 also, we get non-Newtonian fluid behaviour which can be observed in Figure 4.31. The average viscosity for Bayol 35 with Sudan Blue dye is 2.13 mPa.S.

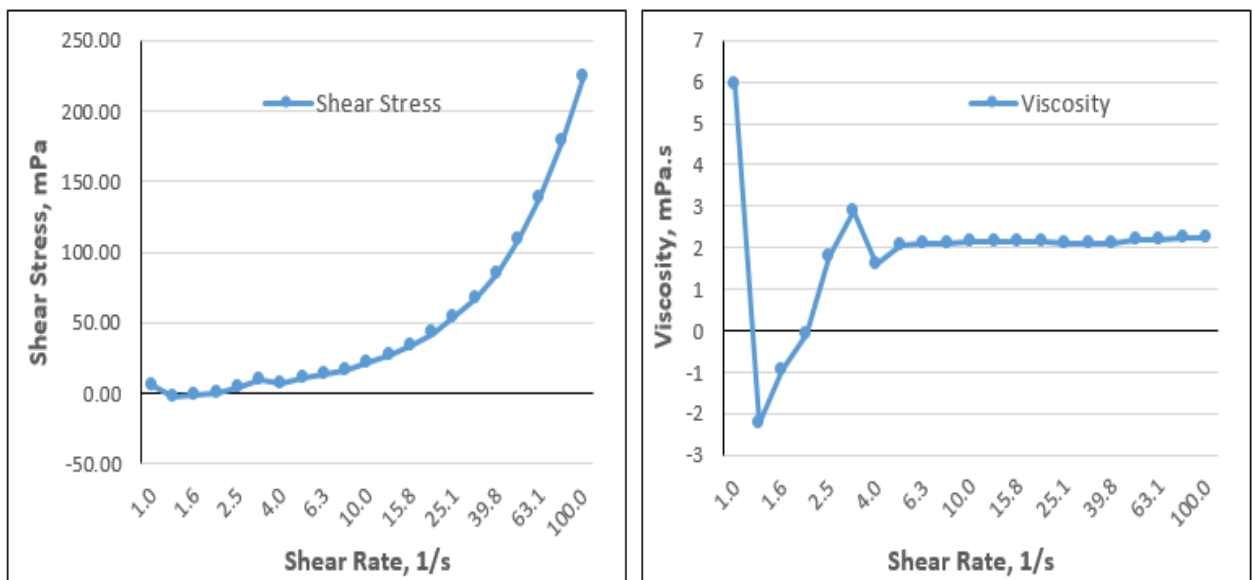


Figure 4.31 Sample 3 (60-40% w-o) with Sudan blue (Bayol 35)

Following observation can be drawn based on above mentioned figures and table for selecting the better phase identification additive:

1. Adding Uranine to water phase reduced oil-water interfacial tension by 11%.
2. Adding Sudan blue increased oil-water interfacial tension by 8%.
3. Normally when you lower the interfacial tension it reduces the droplet size. This is why we get finer droplets with Uranine & coarser droplets with Sudan blue.
4. So, these colouring agents have surfactant effect since they modify the interfacial tension.

4.8 Important observations

1. Water droplets in the oil phase were usually bigger than oil droplets in the water phase
2. In almost all the samples; water droplets separated faster than oil droplets.

This observation can be explained with respect to Stoke's Law which is defined mathematically as:

$$v_s = \frac{2gr^2(\rho_d - \rho_c)}{9\eta_c}$$

Where r is the particle radius.

ρ_d and ρ_c are density of the dispersed and the continuous phases.

η_c is the viscosity of continuous phase.

g is the acceleration either due to gravity ($g = 9.81 \text{ m/s}^2$).

- Concerning the size of water droplet is $319.8 \mu\text{m}$ & oil droplet is $69.37 \mu\text{m}$, as resulted in an experiment for sample 3.

- Calculated:

Sink velocity of water droplets in oil = $5.7 \times 10^{-3} \text{ m/s}$.

Rise velocity of oil droplets in water = $5.6 \times 10^{-4} \text{ m/s}$.

- Water droplets sink x10 times higher velocity than the oil droplets rise.
- Higher the velocity, higher the kinetic energy it has. Also this makes the frequency of the collisions between water droplets. So it causes fast coalescence and might lead to faster separation.
- Also bigger the droplet size, much unstable they are.

- Also phase separation is viscosity dependent for example;
- when the water droplets are in the Bayol 35 continuous phase ($\mu=2.1$ mPa.s) it took longer the separation than in Exxsol D60 medium ($\mu=1.4$ mPa.s)

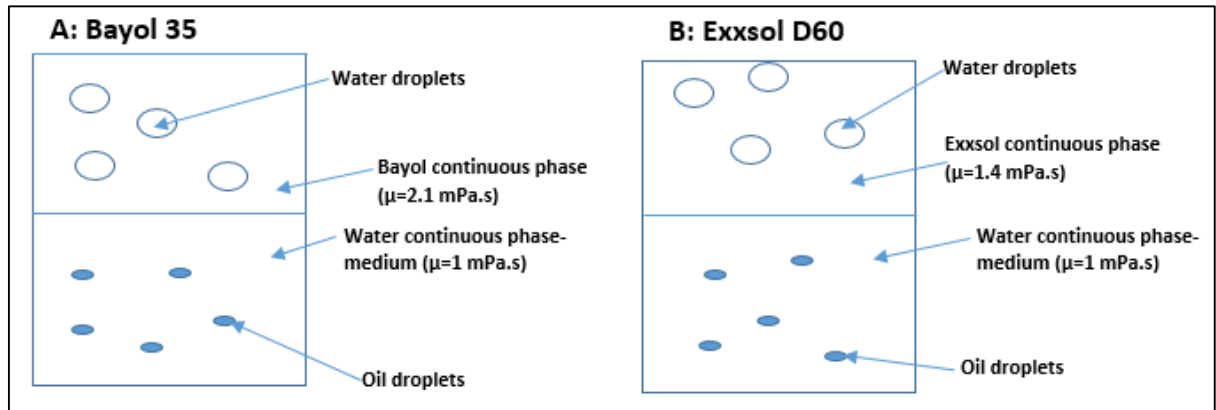


Figure 4.32 Illustrated water/oil droplets in different phases for two oils.

3. Adding the colour Sudan blue to the oil phase much bigger droplets in the samples adding Uranine to the water phase produced much tinier droplets in the samples.
 - Adding Uranine to water phase reduced oil-water interfacial tension by 11%.
 - Adding Sudan blue increased oil-water interfacial tension by 8%.
 - Normally when you lower the interfacial tension it reduces the droplet size. This is why we get finer droplets with Uranine & coarser droplets with Sudan blue.
 - So, these colouring agent have surfactant effect since they modify the interfacial tension.
4. Adding the colour Uranine to the water phase lead to longer separation time in comparison to adding Sudan blue.

CHAPTER 5

CONCLUSIONS

This thesis explores the oil-water mixture/emulsion characteristics and its separation. The thesis describes in detail the theoretical concepts of fundamentals and characteristics of an emulsion, stability of emulsion, types of mixtures/emulsions, demulsification process and mechanisms, droplet size and its distribution, etc. Several laboratory experiments were carried out to better understand the characteristics of mixture of an oil and water phase mixed in different proportions. Bayol 35 and Exxsol D60 were used for the oil phase while tap water was used as water phase. These phases were mixed by manual shaking or using Silversan mixer and the resultant mixtures were observed both through naked eyes and under microscope. The effect of type of the oil and their physical properties, mixing speed, mixing time and phase ratio on separation phenomena was studied in detail. The droplet sizes of water and oil in oil-water mixtures were observed and analysed.

Furthermore, such experiments were repeated in the presence of a dyeing agent Sudan Blue or Uranine added to the mixture to investigate how these colouring agents affect the oil-water mixture properties and find out how good they are as phase identification agents.

Following are the conclusions that can be derived out of this piece of work.

1. In the oil-water mixtures, water droplets are usually bigger than oil droplets irrespective of proportion of oil and water.

2. Samples with dyeing agent Sudan blue separated faster in comparison to the samples without dyeing.
3. Bayol 35, which has lower density and higher viscosity than Exxsol D60, has longer separation time when mixed with tap water compared to Exxsol D60-water mixtures.
4. Longer the mixing time of oil and water phases, higher the separation time due to much stable oil-water mixture/emulsion.
5. Higher the mixing rate, higher the separation time which means more stable oil-water mixture/emulsion.
6. Microscopic images of intermediate mixing layer confirm the bigger water droplet sizes in oil phase.
7. After certain residence time, droplet size becomes bigger due to droplet flocculation and coalescence. With time, droplet size increases and becomes even bigger until it can no longer maintain its spherical shape and separated out.
8. Tap water, Bayol 35 and Exxsol D60 exhibit Newtonian fluid behaviour individually. However, when oil and water phases are mixed, non-Newtonian behaviour is seen for the mixture.
9. Higher the stirring speed, higher the viscosity of oil-water mixture.
10. The viscosity of mixture decreases with increase in temperature.
11. Higher the percentage of oil, lower the mixture density.
12. Mixture prepared with Exxsol D60 and water have higher interfacial tension in comparison to Bayol 35 mixture.
13. In almost all the samples, water droplets separated faster than oil droplets.
14. Adding Uranine to water phase reduced oil-water interfacial tension while adding Sudan blue increased oil-water interfacial tension
15. Adding the colour Sudan blue to the oil phase gives much bigger droplets in the samples and adding Uranine to the water phase produced much tinier droplets in the samples.
16. Adding the colour Uranine to the water phase lead to longer separation time in comparison to adding Sudan blue.

REFERENCES

- ABDEL-RAOUF, M. 2012. Factors affecting the stability of crude oil emulsions. *Crude oil emulsions—composition, stability and characterization. Croatia: Intech*, 183-204.
- ALWADANI, M. S. 2010. *Characterization and rheology of water-in-oil emulsion from deepwater fields*. Rice University.
- ANISA, A. I. & NOUR, A. H. 2010. Affect of Viscosity and Droplet Diameter on water-in-oil (w/o) Emulsions: An Experimental Study. *J World Academy of Science Engineering and Technology*, 38, 692-4.
- AUSTRHEIM, T. 2006. Experimental characterization of high-pressure natural gas scrubbers.
- BRAUNER, N. & ULLMANN, A. 2002. Modeling of phase inversion phenomenon in two-phase pipe flows. *International Journal of Multiphase Flow*, 28, 1177-1204.
- CABANILLAS, J. L. P. 2013. Experimental study on two phase oil-water dispersed flow.
- CHEMICAL, E. 2013. MSDS Exxsol D60.
- CHHABRA, R. P. 2010. Non-Newtonian fluids: an introduction. *Rheology of Complex Fluids*. Springer.
- DATTA, A. 2013. *Process Engineering and Design Using Visual Basic®*, CRC Press.
- DUAN, L., JING, J., WANG, J., HUANG, X., QIN, X. & QIU, Y. Study on Phase Inversion Characteristics of Heavy Oil Emulsions. The Twentieth International Offshore and Polar Engineering Conference, 2010. International Society of Offshore and Polar Engineers.
- ELSETH, G. 2001. An experimental study of oil/water flow in horizontal pipes.
- FATEEV, G. 2014. Effect of small amounts of surfactants on oil-water dispersion.
- HENRÍQUEZ, C. J. M. 2009. *W/O Emulsions: formulation, characterization and destabilization*.
- KHATIBI, M. 2013. Experimental study on droplet size of dispersed oil-water flow.
- KOKAL, S. L. 2005. Crude oil emulsions: A state-of-the-art review. *SPE Production & facilities*, 20, 5-13.

- LANGEVIN, D., POTEAU, S., HÉNAUT, I. & ARGILLIER, J. 2004. Crude oil emulsion properties and their application to heavy oil transportation. *Oil & gas science and technology*, 59, 511-521.
- LIMITED, I. O. 2007. MSDS Bayol 35.
- MANDAL, A. & BERA, A. 2015. Modeling of flow of oil-in-water emulsions through porous media. *Petroleum Science*, 12, 273-281.
- MEHTA, S. D. 2006. *Making and breaking of water in crude oil emulsions*. Texas A&M University.
- MEZGER, T. G. 2006. *The rheology handbook: for users of rotational and oscillatory rheometers*, Vincentz Network GmbH & Co KG.
- PAL, R., BHATTACHARYA, S. & RHODES, E. 1986. Flow behaviour of oil-in-water emulsions. *The Canadian Journal of Chemical Engineering*, 64, 3-10.
- PETROWIKI. 2015. *Oil Emulsions* [Online]. Society of Petroleum Engineers. Available: http://petrowiki.org/Oil_emulsions [Accessed 5th June 2016].
- RØNNINGSEN, H. P. 2012. Rheology of petroleum fluids. *Ann. Trans. Nord. Rheo. Soc*, 20.
- SCHRAMM, G. 2004. *A practical approach to rheology and rheometry*, Thermo Electron (Karlsruhe) GmbH.
- SCHRAMM, L. L. 2006. *Emulsions, foams, and suspensions: fundamentals and applications*, John Wiley & Sons.
- SJÖBLOM, J. 2012. *Emulsions: a fundamental and practical approach*, Springer Science & Business Media.
- TADROS, T. F. 2009. Emulsion science and technology: a general introduction. *Emulsion science and technology*, 1-56.
- TADROS, T. F. 2013. *Emulsion formation and stability*, John Wiley & Sons.
- TROPEA, C., YARIN, A. L. & FOSS, J. F. 2007. *Springer handbook of experimental fluid mechanics*, Springer Science & Business Media.
- VAN DER TUUK OPEDAL, N., SØRLAND, G. & SJÖBLOM, J. 2009. Methods for droplet size distribution determination of water-in-oil emulsions using low-field NMR. *Diffusion fundamentals*, 7, 1-29.
- VIJAYAMOHAN, P., MAJID, A., CHAUDHARI, P., SLOAN, E. D., SUM, A. K., KOH, C. A., DELLACASE, E. & VOLK, M. Hydrate Modeling & Flow Loop Experiments for

Water Continuous & Partially Dispersed Systems. Offshore Technology Conference, 2014. Offshore Technology Conference.

WEBB, E. B. 2007. Rheology of methane hydrate slurries formed from water-in-oil emulsions.

XU, W. 2005. *Experimental investigation of dynamic interfacial interactions at reservoir conditions*. Citeseer.

APPENDIX A

Pictures

Mixing by Silverson L4RT-A mixer

Case 3b: Stirring speed 1600 rpm, mixing for 5 minutes.

Sample: S1 (95-5 % w-o)

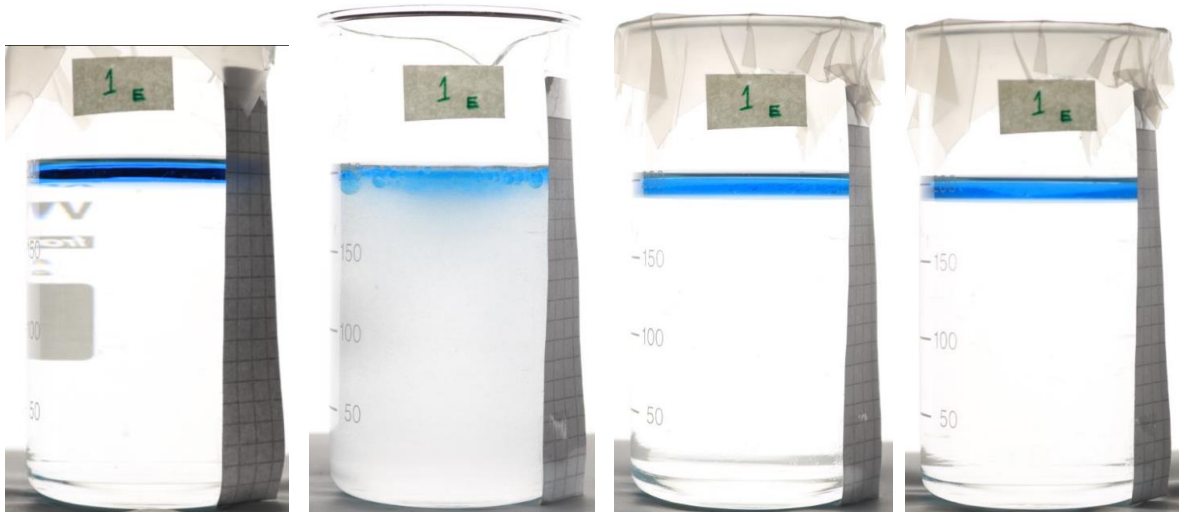


S1_3b_Bayol 35

a) t= 0 minute

b) t= 1 hour

c) t= 20 hours



S1_3b_Exxsol D60

a) t= 0 minute

b) t= 1 hour

c) t= 20 hours

Sample: S3 (60-40 % w-o)

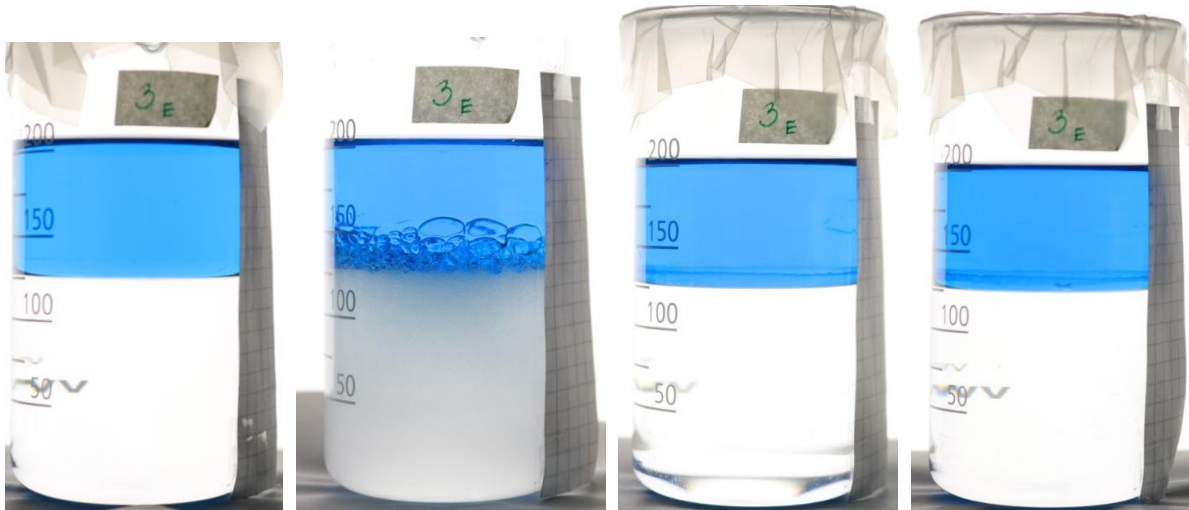


S3_3b_Bayol 35

a) t= 0 minute

b) t= 1 hour

c) t= 20 hours



S3_3b_Exxsol D60

a) t= 0 minute

b) t= 1 hour

c) t= 20 hours

Sample: S7 (5-95 % w-o)



S7_3b_Bayol 35

a) t= 0 minute

b) t= 1 hour

c) t= 20 hours



S7_3b_Exxsol D60

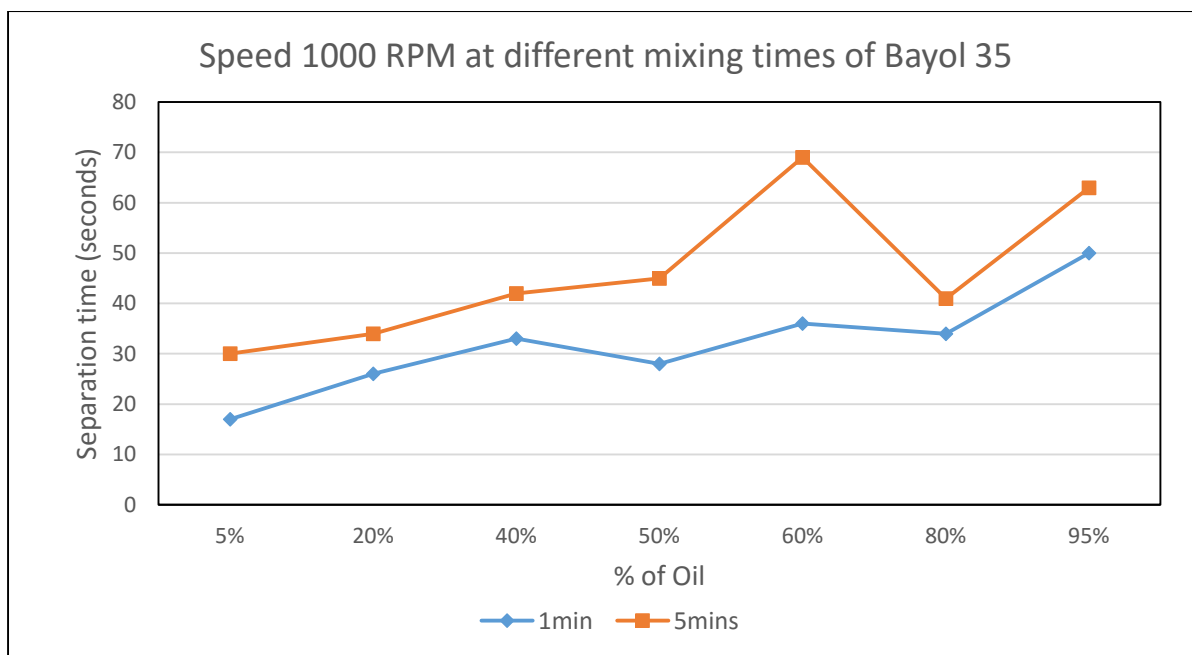
a) t= 0 minute

b) t= 1 hour

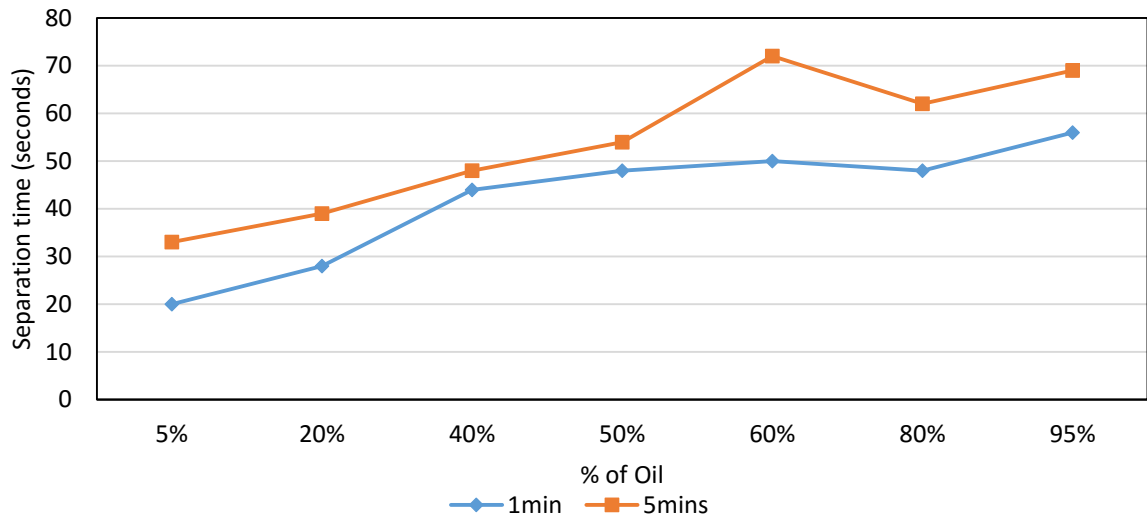
c) t= 20 hours

I) Mixing by Silverson L4RT-A mixer

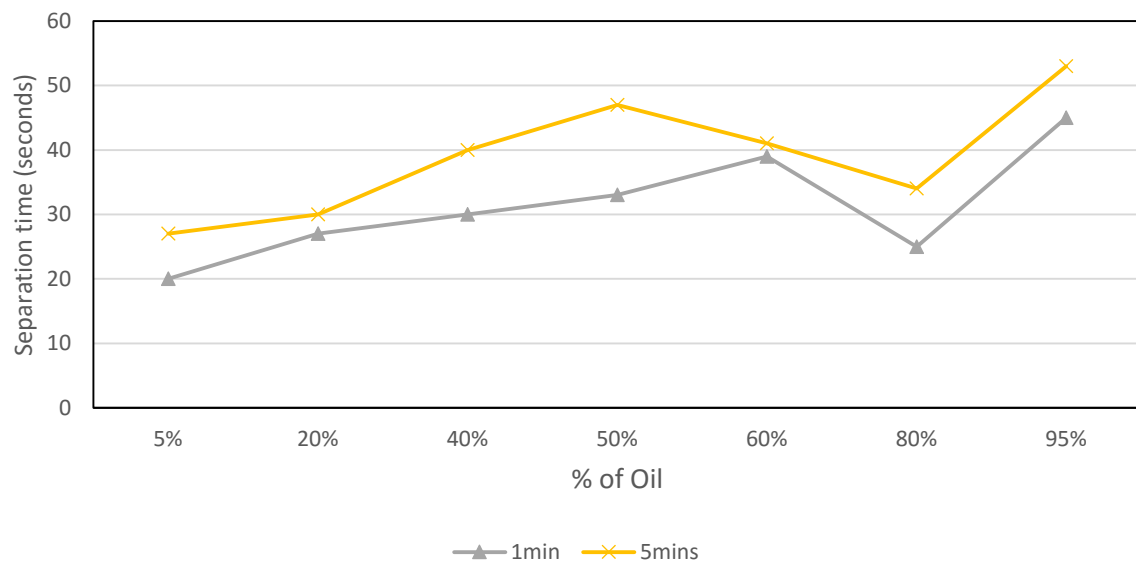
1. Effect of mixing times:

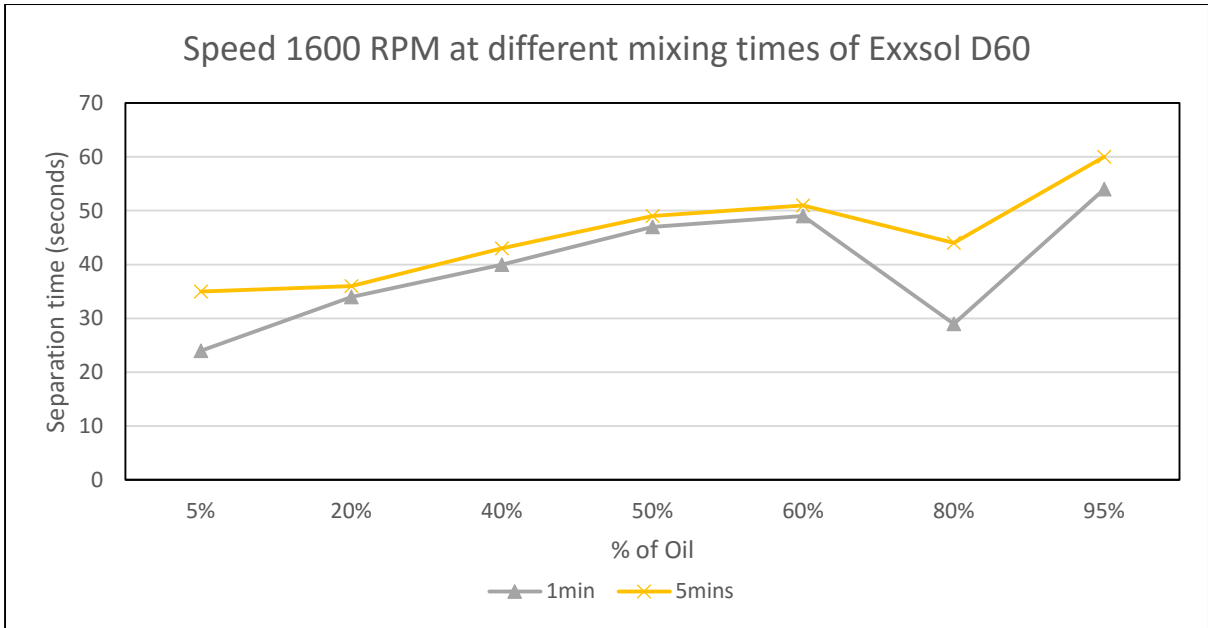


Speed 1600 RPM at different mixing times of Bayol 35

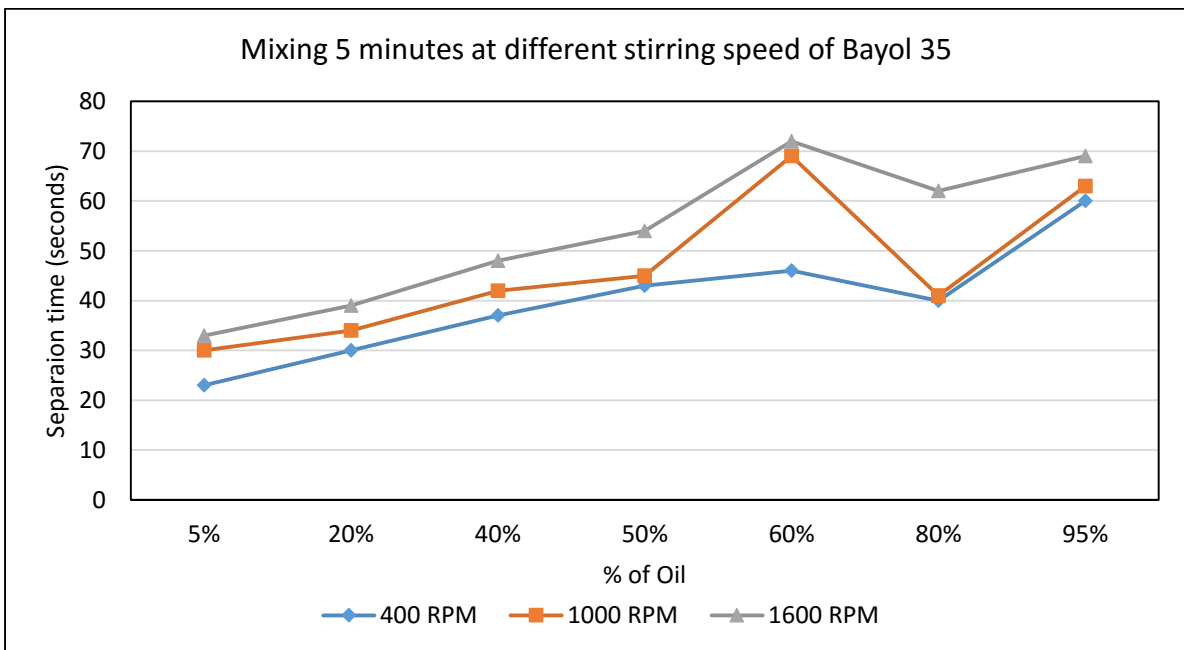


Speed 1000 RPM at different mixing times of Exxsol D60

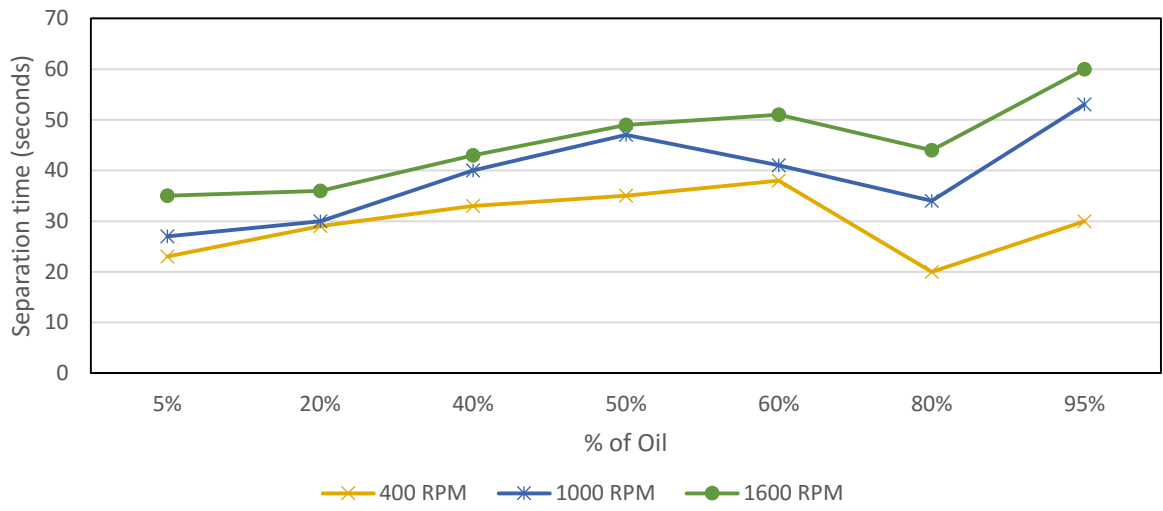




2. Effect of stirring speeds:



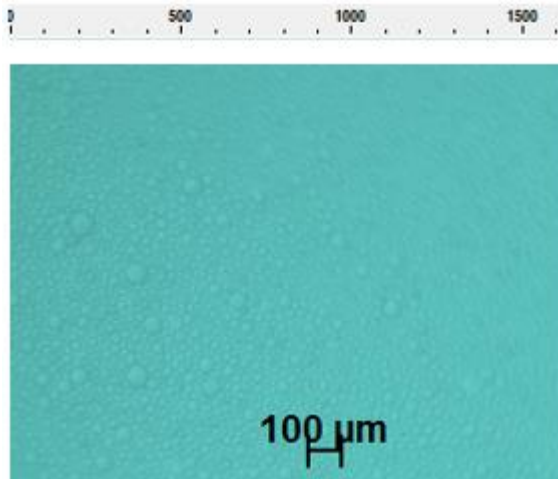
Mixing 5 minutes at different stirring speed of Exxol D60



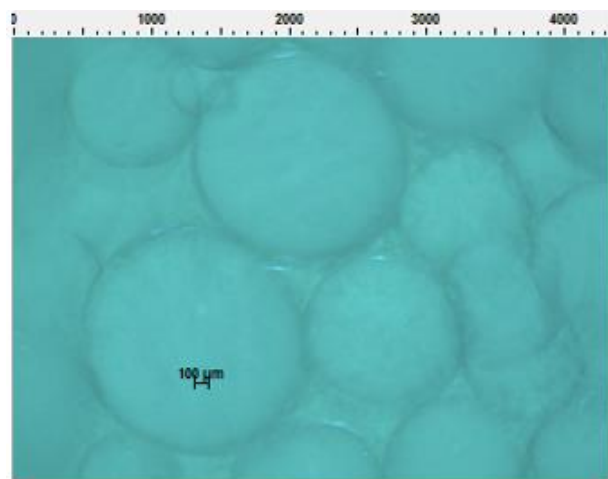
APPENDIX B

Microscope images

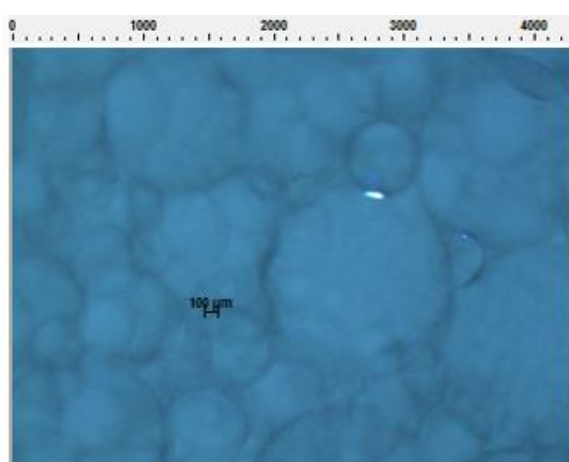
From fig B.1 shows the distribution of droplet size for S1-S5 water-oil mixtures/emulsions for Exxsol D60 with stirring speed 1600 rpm and mixing for 5 minutes.



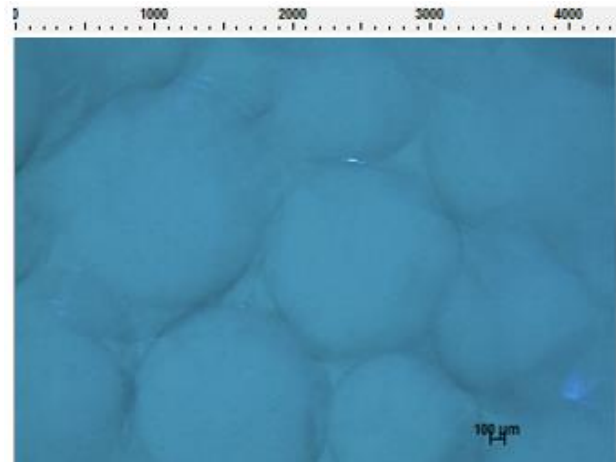
(a)



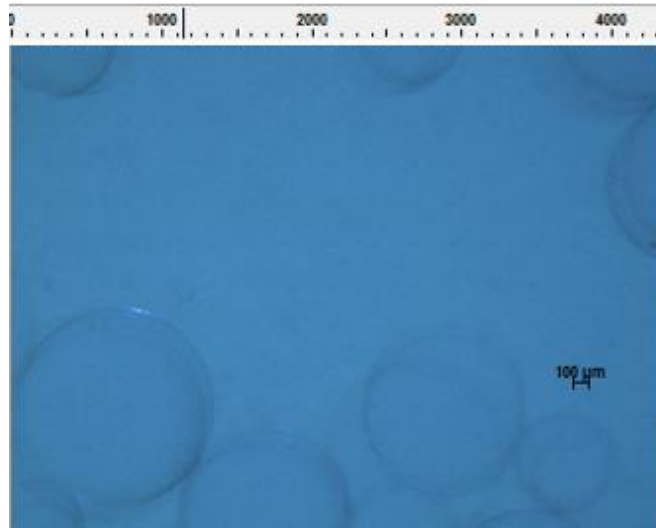
(b)



(c)



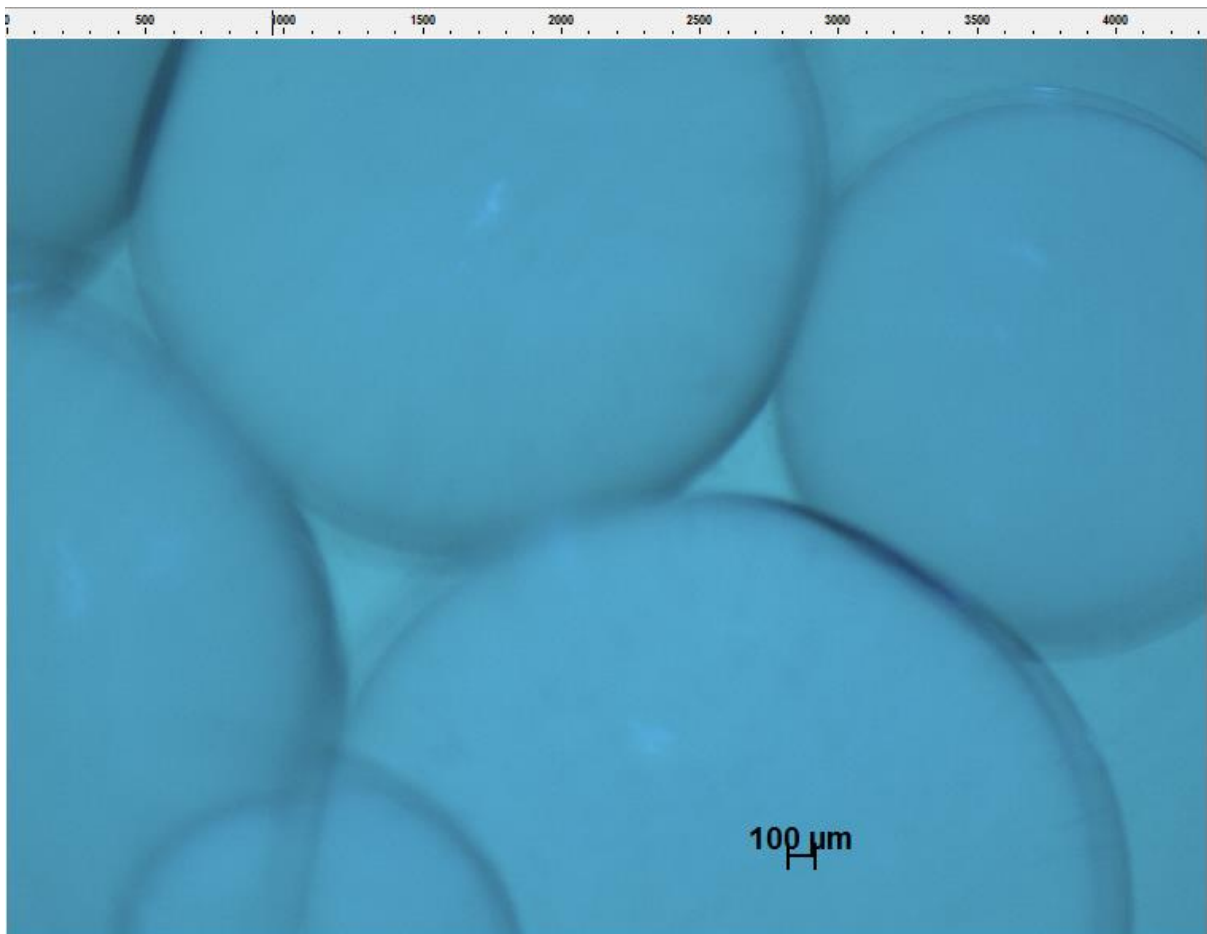
(d)



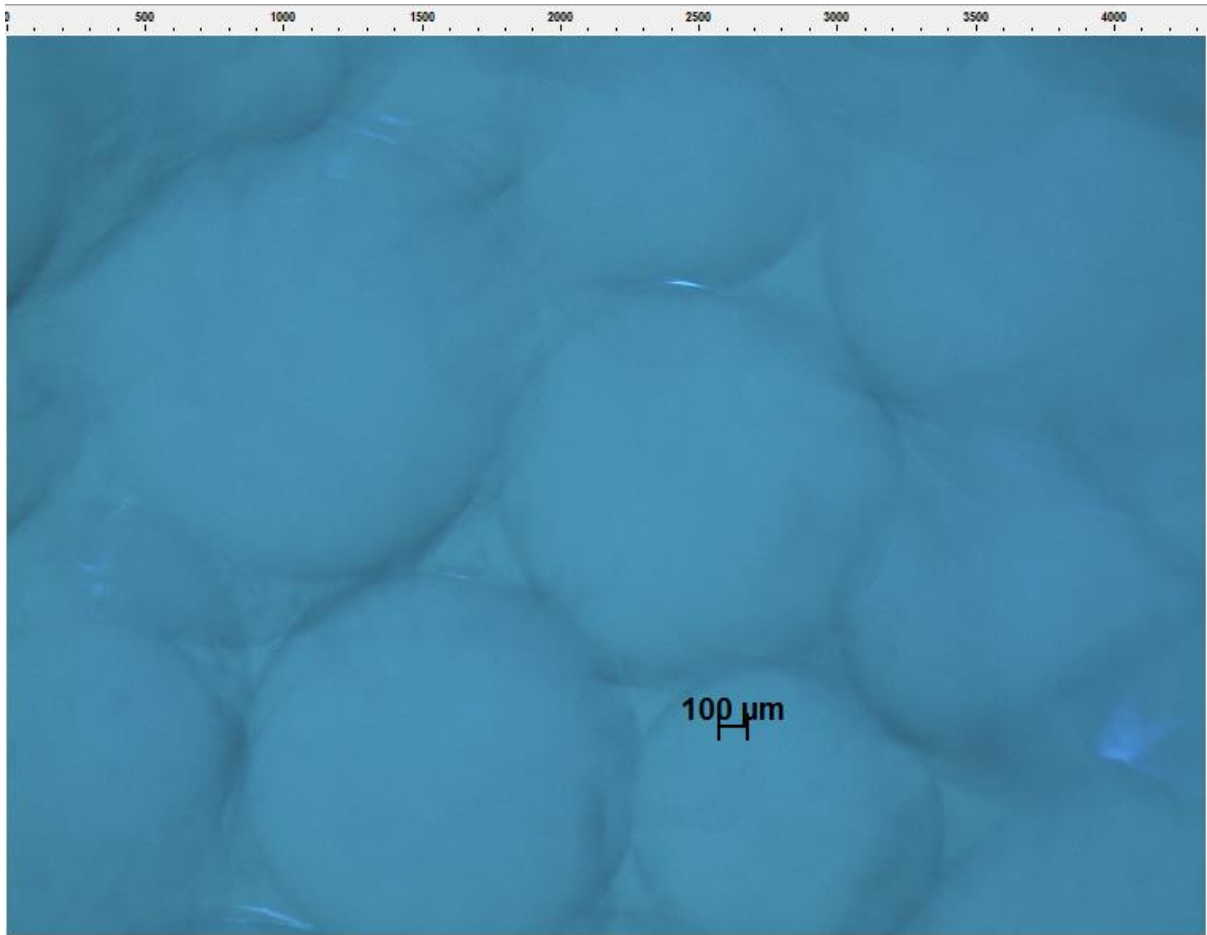
(e)

Figure B.1: Microscope images after mixing for Exxsol D60 with stirring speed 1600 rpm, mixing for 5 minutes. (a) S1, 95% of water cut (b) S2, 80% of water cut (c) S3, 60% of water cut (d) S4, 50% of water cut (e) S5, 40% of water cut

Effect of stirring speed



a) 1000 rpm after mixing at t= 0 min



b) 1600 rpm after mixing at $t=0$ min

Figure B.2 Droplet size distribution at (a), (b) and (c) 50-50 % water-oil mixture of Exxsol D60 mixing for 5 mins.

APPENDIX C

Rheometer

Data Series Information					Data Series Information				
Name:	Pure water at 20 °C				Name:	Water+Dyeing at 20 °C			
Sample:	Pure water at 20 °C				Sample:	water+Uranine at 20 °C			
Operator:	Kan				Operator:	Kan			
Meas. Pts.	Shear Rate	Shear Stress	Viscosity	Zero Shear Viscosity	Meas. Pts.	Shear Rate	Shear Stress	Viscosity	Zero Shear Viscosity
	[1/s]	[mPa]	[mPa·s]	[Pa·s]		[1/s]	[mPa]	[mPa·s]	[Pa·s]
1	1.0	0.57	0.569	*****	1	1.0	0.43	0.427	*****
2	1.3	0.95	0.758	*****	2	1.3	0.73	0.581	*****
3	1.6	1.44	0.909	*****	3	1.6	1.26	0.794	*****
4	2.0	1.79	0.896	*****	4	2.0	1.60	0.802	*****
5	2.5	2.28	0.907	*****	5	2.5	2.20	0.876	*****
6	3.2	3.42	1.08	*****	6	3.2	3.50	1.11	*****
7	4.0	3.91	0.982	*****	7	4.0	3.78	0.95	*****
8	5.0	5.14	1.03	*****	8	5.0	5.10	1.02	*****
9	6.3	6.45	1.02	*****	9	6.3	6.37	1.01	*****
10	7.9	8.07	1.02	*****	10	7.9	7.95	1	*****
11	10.0	10.40	1.04	*****	11	10.0	10.30	1.03	*****
12	12.6	12.90	1.03	*****	12	12.6	12.70	1.01	*****
13	15.8	16.40	1.04	*****	13	15.8	16.20	1.02	*****
14	20.0	21.10	1.06	*****	14	20.0	20.80	1.04	*****
15	25.1	26.70	1.06	*****	15	25.1	26.30	1.05	*****
16	31.6	33.90	1.07	*****	16	31.6	33.40	1.06	*****
17	39.8	43.30	1.09	*****	17	39.8	42.60	1.07	*****
18	50.1	55.60	1.11	*****	18	50.1	54.80	1.09	*****
19	63.1	71.60	1.13	*****	19	63.1	70.50	1.12	*****
20	79.4	92.60	1.17	*****	20	79.4	91.30	1.15	*****
21	100.0	118.00	1.18	*****	21	100.0	116.00	1.16	*****
Meas. Pts.	Shear Rate	Shear Stress	Viscosity	Zero Shear Viscosity	Meas. Pts.	Shear Rate	Shear Stress	Viscosity	Zero Shear Viscosity
	[1/s]	[mPa]	[mPa·s]	[Pa·s]		[1/s]	[mPa]	[mPa·s]	[Pa·s]
1	1.00E+02	1.18E+02	1.18	*****	1	1.00E+02	1.17E+02	1.17	*****
2	7.94E+01	9.16E+01	1.15	*****	2	7.94E+01	9.02E+01	1.14	*****
3	6.31E+01	7.09E+01	1.12	*****	3	6.31E+01	6.98E+01	1.11	*****
4	5.01E+01	5.53E+01	1.1	*****	4	5.01E+01	5.45E+01	1.09	*****
5	3.98E+01	4.33E+01	1.09	*****	5	3.98E+01	4.27E+01	1.07	*****
6	3.16E+01	3.39E+01	1.07	*****	6	3.16E+01	3.33E+01	1.05	*****
7	2.51E+01	2.66E+01	1.06	*****	7	2.51E+01	2.62E+01	1.04	*****
8	2.00E+01	2.08E+01	1.04	*****	8	2.00E+01	2.04E+01	1.02	*****
9	1.58E+01	1.63E+01	1.03	*****	9	1.58E+01	1.60E+01	1.01	*****
10	1.26E+01	1.29E+01	1.02	*****	10	1.26E+01	1.26E+01	1	*****
11	1.00E+01	1.04E+01	1.04	*****	11	1.00E+01	1.02E+01	1.02	*****
12	7.94E+00	8.18E+00	1.03	*****	12	7.94E+00	8.04E+00	1.01	*****
13	6.31E+00	6.43E+00	1.02	*****	13	6.31E+00	6.30E+00	0.999	*****
14	5.01E+00	5.03E+00	1	*****	14	5.01E+00	4.90E+00	0.977	*****
15	3.98E+00	4.22E+00	1.06	*****	15	3.98E+00	4.20E+00	1.05	*****
16	3.16E+00	3.05E+00	0.965	*****	16	3.16E+00	2.88E+00	0.912	*****
17	2.51E+00	2.50E+00	0.993	*****	17	2.51E+00	2.47E+00	0.985	*****
18	2.00E+00	2.21E+00	1.11	*****	18	2.00E+00	2.30E+00	1.15	*****
19	1.58E+00	1.82E+00	1.15	*****	19	1.58E+00	1.95E+00	1.23	*****
20	1.26E+00	1.21E+00	0.965	*****	20	1.26E+00	1.29E+00	1.02	*****
21	1.00E+00	5.96E-01	0.596	*****	21	1.00E+00	4.35E-01	0.435	*****

Data Series Information
 Sample: Exxsol D60 without Dyeing at 20 °C
 Operator: Kan

Meas. Pts.	Shear Rate [1/s]	Shear Stress [mPa]	Viscosity [mPa·s]	Zero Shear Viscosity [Pa·s]
1	1.0	1.15	1.15	*****
2	1.3	1.46	1.16	*****
3	1.6	2.00	1.26	*****
4	2.0	2.57	1.29	*****
5	2.5	3.39	1.35	*****
6	3.2	4.66	1.47	*****
7	4.0	5.48	1.38	*****
8	5.0	7.08	1.41	*****
9	6.3	8.90	1.41	*****
10	7.9	11.20	1.41	*****
11	10.0	14.20	1.42	*****
12	12.6	17.80	1.41	*****
13	15.8	22.50	1.42	*****
14	20.0	28.60	1.43	*****
15	25.1	36.20	1.44	*****
16	31.6	45.80	1.45	*****
17	39.8	58.30	1.46	*****
18	50.1	74.40	1.48	*****
19	63.1	95.30	1.51	*****
20	79.4	122.00	1.54	*****
21	100.0	155.00	1.55	*****

Meas. Pts.	Shear Rate [1/s]	Shear Stress [mPa]	Viscosity [mPa·s]	Zero Shear Viscosity [Pa·s]
1	1.00E+02	1.56E+02	1.56	*****
2	7.94E+01	1.22E+02	1.53	*****
3	6.31E+01	9.48E+01	1.5	*****
4	5.01E+01	7.44E+01	1.48	*****
5	3.98E+01	5.84E+01	1.47	*****
6	3.16E+01	4.58E+01	1.45	*****
7	2.51E+01	3.61E+01	1.44	*****
8	2.00E+01	2.84E+01	1.42	*****
9	1.58E+01	2.24E+01	1.41	*****
10	1.26E+01	1.77E+01	1.4	*****
11	1.00E+01	1.42E+01	1.42	*****
12	7.94E+00	1.12E+01	1.41	*****
13	6.31E+00	8.86E+00	1.4	*****
14	5.01E+00	6.96E+00	1.39	*****
15	3.98E+00	5.72E+00	1.44	*****
16	3.16E+00	4.28E+00	1.35	*****
17	2.51E+00	3.59E+00	1.43	*****
18	2.00E+00	3.06E+00	1.53	*****
19	1.58E+00	2.52E+00	1.59	*****
20	1.26E+00	1.88E+00	1.5	*****
21	1.00E+00	1.12E+00	1.12	*****

Data Series Information
 Sample: Exxsol D60+Dyeing at 20 °C
 Operator: Kan

Meas. Pts.	Shear Rate [1/s]	Shear Stress [mPa]	Viscosity [mPa·s]	Zero Shear Viscosity [Pa·s]
1	1.0	-0.89	-0.886	*****
2	1.3	-3.28	-2.6	*****
3	1.6	-2.23	-1.4	*****
4	2.0	-1.09	-0.547	*****
5	2.5	3.46	1.38	*****
6	3.2	7.84	2.48	*****
7	4.0	4.18	1.05	*****
8	5.0	7.57	1.51	*****
9	6.3	9.57	1.52	*****
10	7.9	11.80	1.48	*****
11	10.0	15.40	1.54	*****
12	12.6	19.10	1.52	*****
13	15.8	23.70	1.5	*****
14	20.0	29.40	1.47	*****
15	25.1	36.80	1.46	*****
16	31.6	45.90	1.45	*****
17	39.8	57.50	1.44	*****
18	50.1	74.60	1.49	*****
19	63.1	95.10	1.51	*****
20	79.4	123.00	1.55	*****
21	100.0	154.00	1.54	*****

Meas. Pts.	Shear Rate [1/s]	Shear Stress [mPa]	Viscosity [mPa·s]	Zero Shear Viscosity [Pa·s]
1	1.00E+02	1.55E+02	1.55	*****
2	7.94E+01	1.21E+02	1.52	*****
3	6.31E+01	9.46E+01	1.5	*****
4	5.01E+01	7.49E+01	1.49	*****
5	3.98E+01	5.94E+01	1.49	*****
6	3.16E+01	4.55E+01	1.44	*****
7	2.51E+01	3.66E+01	1.46	*****
8	2.00E+01	2.76E+01	1.38	*****
9	1.58E+01	2.18E+01	1.38	*****
10	1.26E+01	1.65E+01	1.31	*****
11	1.00E+01	1.60E+01	1.6	*****
12	7.94E+00	1.16E+01	1.46	*****
13	6.31E+00	9.38E+00	1.49	*****
14	5.01E+00	6.38E+00	1.27	*****
15	3.98E+00	7.44E+00	1.87	*****
16	3.16E+00	2.12E+00	0.67	*****
17	2.51E+00	5.93E+00	2.36	*****
18	2.00E+00	7.77E+00	3.9	*****
19	1.58E+00	7.86E+00	4.96	*****
20	1.26E+00	5.91E+00	4.7	*****
21	1.00E+00	-1.50E+00	-1.5	*****

Data Series Information
 Sample: Bayol 35 without Dyeing at 20 °C
 Operator: Kan

Meas. Pts.	Shear Rate [1/s]	Shear Stress [mPa]	Viscosity [mPa·s]	Zero Shear Viscosity [Pa·s]
1	1.0	8.01	8.01	*****
2	1.3	2.12	1.68	*****
3	1.6	2.94	1.85	*****
4	2.0	3.75	1.88	*****
5	2.5	5.00	1.99	*****
6	3.2	6.96	2.2	*****
7	4.0	17.90	4.5	*****
8	5.0	10.40	2.07	*****
9	6.3	13.00	2.06	*****
10	7.9	16.30	2.06	*****
11	10.0	20.70	2.07	*****
12	12.6	26.00	2.07	*****
13	15.8	32.80	2.07	*****
14	20.0	41.50	2.08	*****
15	25.1	52.40	2.09	*****
16	31.6	66.30	2.1	*****
17	39.8	84.00	2.11	*****
18	50.1	107.00	2.13	*****
19	63.1	136.00	2.16	*****
20	79.4	175.00	2.2	*****
21	100.0	221.00	2.21	*****

Meas. Pts.	Shear Rate [1/s]	Shear Stress [mPa]	Viscosity [mPa·s]	Zero Shear Viscosity [Pa·s]
1	1.00E+02	2.22E+02	2.22	*****
2	7.94E+01	1.74E+02	2.19	*****
3	6.31E+01	1.36E+02	2.16	*****
4	5.01E+01	1.07E+02	2.14	*****
5	3.98E+01	8.43E+01	2.12	*****
6	3.16E+01	6.63E+01	2.1	*****
7	2.51E+01	5.24E+01	2.09	*****
8	2.00E+01	4.13E+01	2.07	*****
9	1.58E+01	3.26E+01	2.06	*****
10	1.26E+01	2.58E+01	2.05	*****
11	1.00E+01	2.07E+01	2.07	*****
12	7.94E+00	1.64E+01	2.06	*****
13	6.31E+00	1.30E+01	2.06	*****
14	5.01E+00	1.02E+01	2.04	*****
15	3.98E+00	8.34E+00	2.1	*****
16	3.16E+00	6.29E+00	1.99	*****
17	2.51E+00	5.25E+00	2.09	*****
18	2.00E+00	4.44E+00	2.22	*****
19	1.58E+00	3.64E+00	2.3	*****
20	1.26E+00	2.75E+00	2.19	*****
21	1.00E+00	1.69E+00	1.69	*****

Data Series Information
 Sample: Bayol 35+Dyeing at 20 °C
 Operator: Kan

Meas. Pts.	Shear Rate [1/s]	Shear Stress [mPa]	Viscosity [mPa·s]	Zero Shear Viscosity [Pa·s]
1	1.0	-2.25	-2.25	*****
2	1.3	-3.99	-3.17	*****
3	1.6	-2.33	-1.47	*****
4	2.0	-1.17	-0.588	*****
5	2.5	3.69	1.47	*****
6	3.2	9.76	3.09	*****
7	4.0	5.74	1.44	*****
8	5.0	10.40	2.07	*****
9	6.3	13.10	2.07	*****
10	7.9	16.20	2.04	*****
11	10.0	21.60	2.16	*****
12	12.6	26.50	2.1	*****
13	15.8	33.30	2.1	*****
14	20.0	42.00	2.11	*****
15	25.1	52.60	2.09	*****
16	31.6	65.90	2.08	*****
17	39.8	83.00	2.08	*****
18	50.1	107.00	2.14	*****
19	63.1	136.00	2.16	*****
20	79.4	175.00	2.21	*****
21	100.0	221.00	2.21	*****

Meas. Pts.	Shear Rate [1/s]	Shear Stress [mPa]	Viscosity [mPa·s]	Zero Shear Viscosity [Pa·s]
1	1.00E+02	2.22E+02	2.22	*****
2	7.94E+01	1.73E+02	2.18	*****
3	6.31E+01	1.36E+02	2.16	*****
4	5.01E+01	1.07E+02	2.14	*****
5	3.98E+01	8.51E+01	2.14	*****
6	3.16E+01	6.57E+01	2.08	*****
7	2.51E+01	5.25E+01	2.09	*****
8	2.00E+01	4.01E+01	2.01	*****
9	1.58E+01	3.13E+01	1.98	*****
10	1.26E+01	2.40E+01	1.9	*****
11	1.00E+01	2.21E+01	2.21	*****
12	7.94E+00	1.63E+01	2.05	*****
13	6.31E+00	1.29E+01	2.04	*****
14	5.01E+00	8.86E+00	1.77	*****
15	3.98E+00	9.83E+00	2.47	*****
16	3.16E+00	3.06E+00	0.967	*****
17	2.51E+00	6.57E+00	2.62	*****
18	2.00E+00	8.73E+00	4.37	*****
19	1.58E+00	8.60E+00	5.42	*****
20	1.26E+00	5.75E+00	4.56	*****
21	1.00E+00	-2.73E+00	-2.73	*****

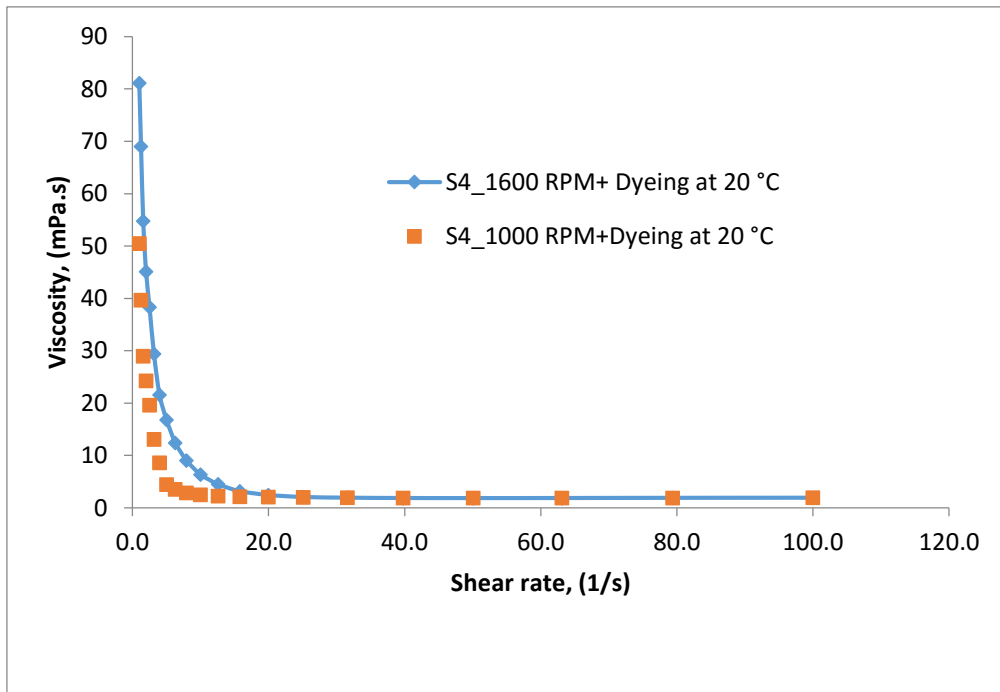
Data Series Information

Sample: Marcol 82 without Dyeing at 20 °C
 Operator: Kan

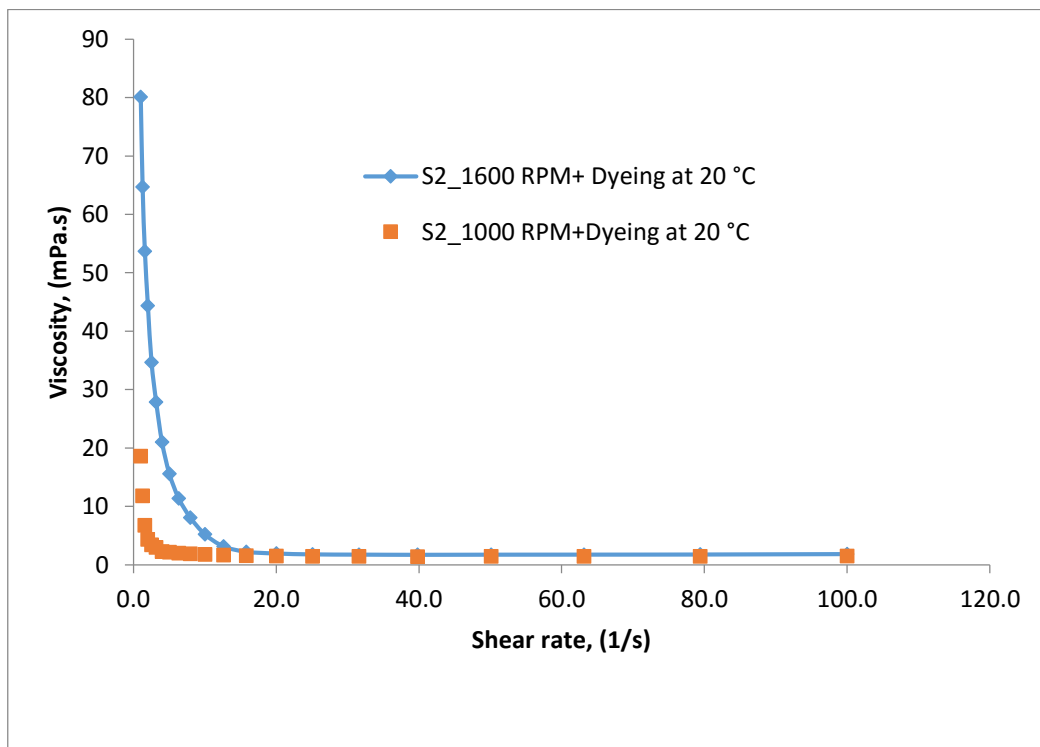
Meas. Pts.	Shear Rate [1/s]	Shear Stress [mPa]	Viscosity [mPa·s]	Zero Shear Viscosity [Pa·s]
1	1.00	29.40	29.4	*****
2	1.26	37.30	29.6	*****
3	1.58	46.90	29.6	*****
4	2.00	58.80	29.5	*****
5	2.51	74.60	29.7	*****
6	3.16	94.00	29.7	*****
7	3.98	119.00	29.8	*****
8	5.01	149.00	29.8	*****
9	6.31	188.00	29.8	*****
10	7.94	237.00	29.8	*****
11	10.00	298.00	29.8	*****
12	12.60	376.00	29.8	*****
13	15.80	473.00	29.8	*****
14	20.00	595.00	29.8	*****
15	25.10	749.00	29.8	*****
16	31.60	944.00	29.9	*****
17	39.80	1190.00	29.9	*****
18	50.10	1500.00	29.9	*****
19	63.10	1890.00	29.9	*****
20	79.40	2380.00	30	*****
21	100.00	3000.00	30	*****

Meas. Pts.	Shear Rate [1/s]	Shear Stress [mPa]	Viscosity [mPa·s]	Zero Shear Viscosity [Pa·s]
1	100.00	3010.00	30.1	*****
2	79.40	2380.00	30	*****
3	63.10	1890.00	29.9	*****
4	50.10	1500.00	29.9	*****
5	39.80	1190.00	29.9	*****
6	31.60	944.00	29.9	*****
7	25.10	750.00	29.9	*****
8	20.00	596.00	29.9	*****
9	15.80	473.00	29.9	*****
10	12.60	376.00	29.9	*****
11	10.00	299.00	29.9	*****
12	7.94	237.00	29.9	*****
13	6.31	188.00	29.9	*****
14	5.01	150.00	29.9	*****
15	3.98	119.00	29.9	*****
16	3.16	94.50	29.9	*****
17	2.51	74.90	29.8	*****
18	2.00	59.70	29.9	*****
19	1.58	47.50	30	*****
20	1.26	37.70	30	*****
21	1.00	29.90	29.9	*****

Effects of stirring speed on viscosity



(a)



(b)

Figure C.1 Comparison of viscosity for samples containing Bayol 35 with different stirring speeds, (a) Bayol 35 (50-50% w-o) and (b) Bayol 35 (80-20% w-o).